PRACTICAL ADAPTIVE HYBRIDS WITH NO BURSTING

Submitted by
LIWEN WANG

A thesis
submitted to the School of Graduate Studies and Research
in partial fulfillment of the requirements for the
Degree of Master of Applied Science
in Electrical Engineering.

Ottawa-Carleton Institute of Electrical Engineering
Department of Electrical Engineering
Faculty of Engineering
University of Ottawa
Ottawa, Ontario
Canada.

I hereby declare that I am the sole author of this document. I authorize the University of Ottawa to lend this document to other institutions or individuals for the purpose of schloarly research.

Liwen Wang

I further authorize the University of Ottawa to reproduce this document by photocopying or by other means, in total or in part, at the request of other institutions or individuals for the purpose of scholarly research.

Liwen Wang

Abstract

In this thesis, the bursting phenomenon in echo cancellation of telephone system is investigated. Bursting is characterized as long periods of successful echo attenuation alternating with short periods of wildly oscillating signals. The objective of this thesis is to propose means of modifying the echo cancellation algorithm to ensure bursting does not happen in practical hybrids. Several approaches are proposed first for the simple cases currently discussed in the literature , then for realistic hybrids. The advantages and disadvantages of these solutions are discussed , and extensive computer simulations are provided to illustrate the effectiveness of the proposed approaches for low-order hybrids as well as realistic ones.

Acknowledgement

I would like to express my sincere gratitude to my supervisor Dr.T.Aboulnasr for her generous encouragement, continued support and invaluable guidance throughout this work, without which this thesis would have not been possible.

I would also like to thank all my colleagues for the discussions we shared. I am also very thankful to the faculty and staff of the Department of Electrical Engineering, University of Ottawa.

Finally, I wish to acknowledge the special support from my family.

Publications

1. T.Aboulnasr and L.Wang "Elimation of Bursting in Adaptive Hybrids", 16th Biennial Symposium on Communications, Kingston, Ontario, May 27-29, 1992.

2. L.Wang and T.Aboulnasr "Practical Adaptive Hybrids with no Bursting ", ICASSP-93, Minneapolis, Minnesota, April 27-30, 1993.

3. T.Aboulnasr and L.Wang "Practical Adaptive Hybrids with no Bursting" to be submitted to IEEE Trans. on ASSP.

Contents

List of Figures

List of Symbols

EC	echo canceller
AF	adaptive filter
DTD	double talk detector
ACC	averaged cross correlation
LMS	least mean square
NLMS	normalized LMS
$\mathbf{X(k)}$	input vector to the echo canceller
v	near-end input
w	far-end input
$y(k)$	real echo
$\hat{y}(k)$	estimate echo
$e(k)$	error signal
N	number of taps for adaptive filter
M	order of the echo path
α	far-end feedback scalar
β	leakage factor
μ	step size for LMS algorithm
T	matrix and vector transposition operator
$E\{\}$	estimation operator
z^{-1}	unit sample delay operator
h_i	*ith* near-end echo channel impulse response
$\hat{h}_i$	*ith* echo canceller tap weight
h_0	optimum echo canceller tap weight vector

Chapter 1

Introduction

1.1 Use of Echo Cancellers in Telephony

In telephone system, the local link is set up by simply connecting the customer's telephone set to the central office using a 2-wire bidirectional loop, while the long-distance link uses two separate unidirectional channels for "4-wire" transmission. The typical long-distance telephone link setup is illustrated in Figure 1.1.

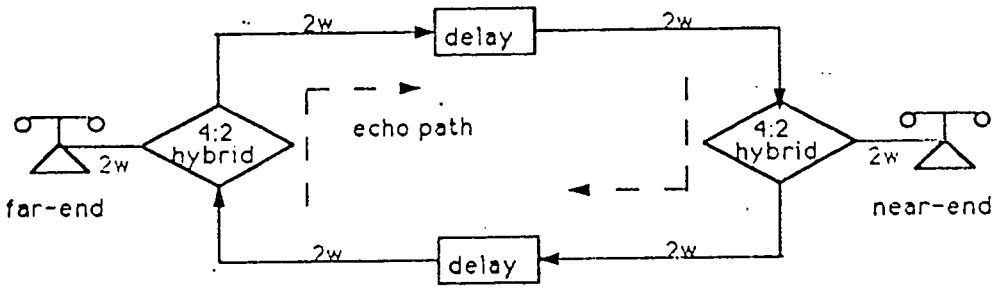

Figure 1.1: Simplified version of the typical long-distance telephone link

The use of the separate channels for the two directions of transmission is a necessary characteristic of long-distance transmission links. There are two reasons for this. First, long circuits require amplification, and amplifiers are one-way devices. Second, for reasons of economy, most long-distance calls are multiplexed, i.e.; a number of calls use portions of one wide-band transmission channel. Multiplexing requires that signals in the two directions be sent over different slots. Thus, provision of the connection between the

4-wire long-distance receive and transmit lines and the 2-wire local line must be made[6]. A device called "4:2 hybrid" is used to accomplish this work. An ideal hybrid would completely transfer the incoming signal from the 4-wire receive line to the 2-wire subscriber line, and simultaneously move all the outgoing signals from the 2-wire subscriber line to the 4-wire transmit loop. Practically, variations in component characteristics, loop length and impedance cause imperfect separations of the incoming and the outgoing signals at the hybrid. Thus, some energy on the incoming branch leaks into the outgoing branch and returns to the source as an echo. Typically, the hybrid reduces the amplitude of the "leakage" signal by about 10-15 dB relative to the incoming signal. The echoes caused by the leakage on each end of the long-distance circuit may be very apparent to some users even when the echo is as much as 40 dB below the incoming signal if the echo delay is long[3][6].

During the past decades, an echo suppressor was a principal method of controlling echo in telephony [1][2][6]. Fig.1.2 shows the installation of a rudimentary echo suppressor to control echo in a satellite circuit.

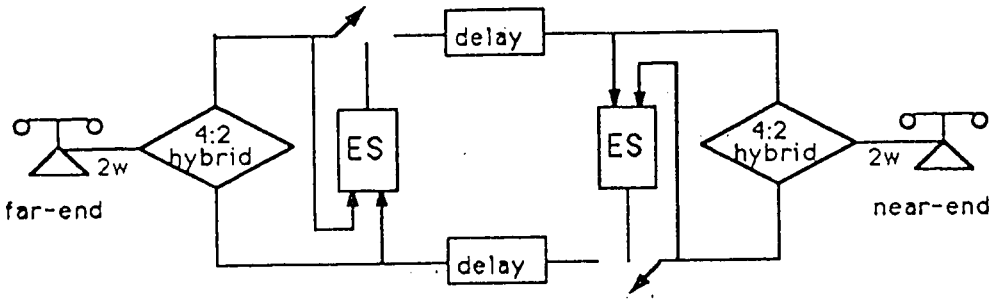

Figure 1.2: Echo suppressors in the telephone system

The near-end echo suppressor opens the lower transmission path to block the echo when it detects speech energy on the upper path. But this decision to open is overruled if it is decided that the returned signal from the near-end hybrid contains near-end speech along with echo since the near-end speech must be transmitted to the far-end. Thus,

the echo suppressor is naturally incapable of blocking the echo during double talk(both near-end and far-end speakers are talking). Another problem with echo suppressor is that it imparts a choppiness to the speech by the opening and closing of the transmission path. Both of these shortcomings have been found more annoying with the long echo delays of satellite circuits (approximately 540 ms)[13][21]. This has stimulated the development of the adaptive echo canceller(EC).

A model of a long-distance system with adaptive echo cancellation is diagrammed in Figure 1.3.

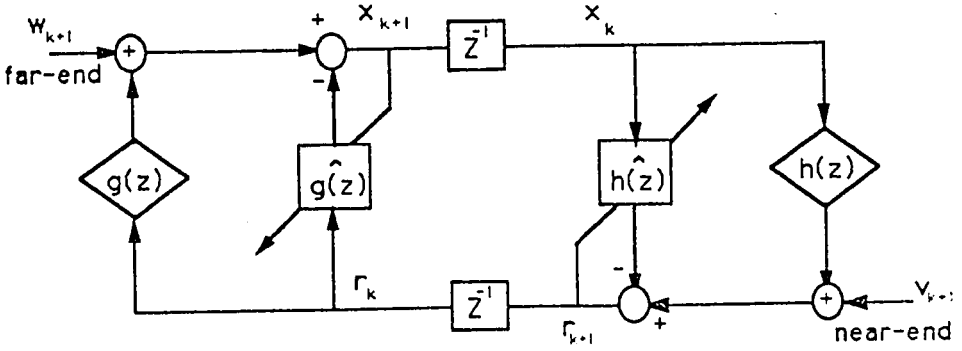

Figure 1.3: Simplified model of echo cancellers in the telephone system

At a given end of the long-distance line, the incoming signal is applied to both the hybrid and the adaptive filter(AF). The AF forms an estimate of the echo path impulse response and then estimates the echo. This estimated echo will be subtracted from the hybrid output to yield an echo-free received signal. The adaptive solution to the hybrid problem is well established and has been used satisfactorily in a wide variety of situations [12]-[15].

1.2 Problem Description

Adaptive echo cancellation has been successfully applied to attentuate echoes in long distance connections. Recently, with the increased ability to process signals cheaply, adaptive echo cancellation is being employed on shorter telephone circuits. Such short

connections will generate a problem of high correlation between x and v(only consider the near-end part) of Fig.1.3, especially when v is present and w(far-end input) is not. Given this possibility, in common practice, a double-talk detector(DTD) will be used to turn off(or on) adaptation when the ratio of the energy in v to the energy in x rises above(or falls below) a given threshold. However, there is a danger in the aggressive use of the DTD. Noting that the adaptive hybrid operates in a closed loop(with feedback). If an adaptive echo canceller is switched into a circuit with worst case hybrids and before the echo canceller can adapt, double talk is detected and the LMS algorithm is halted. If at this time the closed loop gain exceeds one, the system can become trapped in a sustained "singing" mode until the double talk condition ends and adaptation can resume. To avoid entrapment in a singing mode, DTD should be used conservatively.

If a DTD is not used in the circuit and an EC is implemented on a short line, a new but undesirable phenomenon called "bursting" arises. Figs.1.4 and 1.5 give the typical time series of an echo signal and one of the coefficients of the adaptive filter of a bursting system. Bursting can be characterized as long periods of good echo attentuation alternating with brief periods of rapid oscillation of signals throughout the system. This phenomenon was first noticed in the Tellab Laboratory Research[33]. They reported on real time tests utilizing a 20-tap adaptive hybrid at the near-end of the line and a nonadaptive hybrid at the far-end, giving 6-dB attenuation around the loop with independent narrow-band signal injected at each end. It is observed that after long periods of close match between the output of the adaptive hybrid and the echo path, the system would suddenly begin "bursting". Consequently, the signals degenerated into wild oscillation. These large errors then cause the system to quickly restabilize. When the transmission at the far-end is silent, the bursts appeared more frequently. Bursting was also observed in simulations of a variety of combinations of hybrid/EC setup in [23]-[25] which can be cataloged into two groups: single adaptive hybrid system and double adaptive hybrid system.

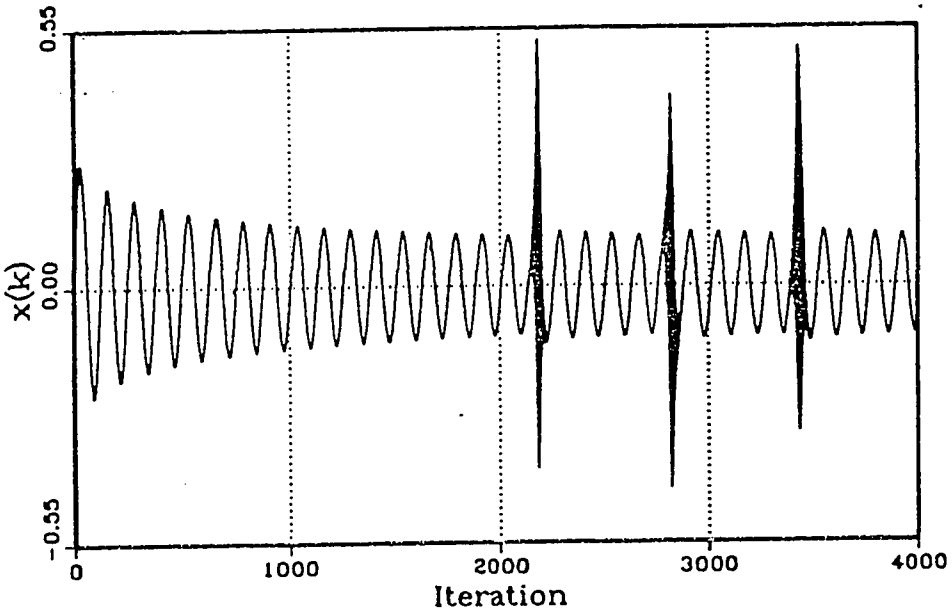

Fig.1.4 Bursting in an echo signal of the adaptive hybrid.

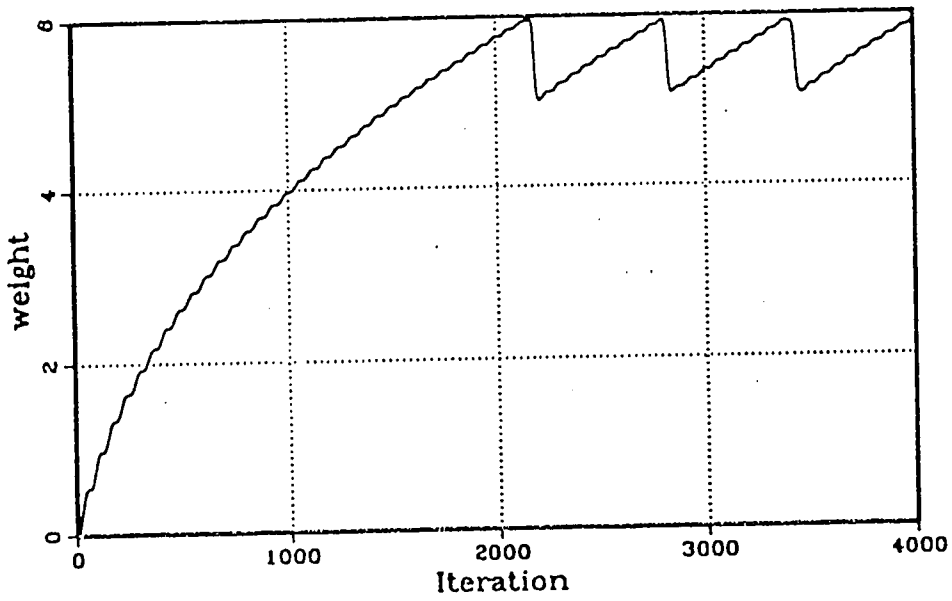

Fig.1.5 Bursting in one coefficient of the adaptive filter.

For a system with single adaptive hybrid as depicted in Fig.1.6, it is assumed the near-end has an adaptive hybrid and the far-end hybrid is only a single scalar. If a narrow-band signal(disturbance) is injected at the near-end and zero or very small input at the far-end, then bursting is guaranteed to occur. If the input conditions for the near-end and the far-end are exchanged(the normal configuration for training the EC), then echo cancellation is achieved at the frequencies included in the narrow-band signal , but there is no guarantee of the performance at the other frequencies[25]. However, there would not be bursting in the near-end adaptive filter.

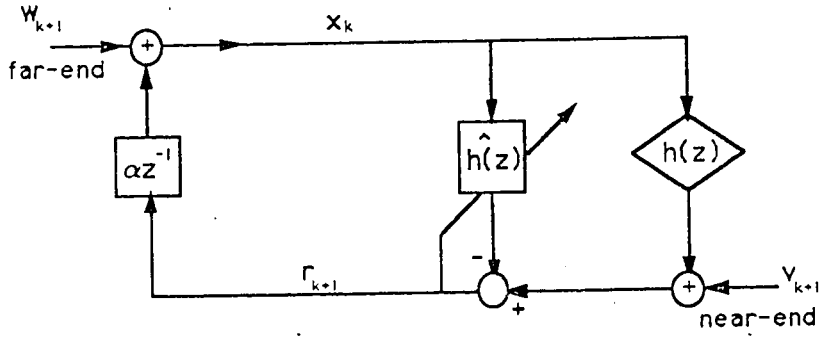

Figure 1.6: Single adaptive hybrid system

For double adaptive hybrid system(Fig.1.3), if a narrow-band signal is applied to one side of the circuits, e.g. near-end, then it is the adaptive hybrid on the near-end which may exhibit bursting, while the far-end hybrid will adapt normally to cancel this narrowband frequency. If the far-end EC exactly matches the far-end hybrid, the feedback path will be opened and bursting will not show up any more. However, this ideal match is unlikely in practical communications channels, so bursting can still happen, although it is likely to have very low magnitudes(depending on the match at the far-end).

It is worth noting that no bursting is observed if white gaussian noise is applied to any of the above situations.

From the above observations, it is clear that the essential driving force behind bursting is attributed to the correlation between the signal the near(far) end is to transmit and the

signal the near(far) end receives from the far(near) end. More specifically, suppose that at the near-end, v_{k+1} is the dominant component of r_{k+1}. r_{k+1} is then fed back through the far-end hybrid. If the far-end hybrid is only a scalar(nonadaptive hybrid)as in Fig.1.6, x_k will be a scaled version of r_{k+1}. Under the condition of no far-end input, this x_k is definitely highly correlated with r_{k+1} within the time-window of the AF if the length of delay is short. If the far-end has an adaptive hybrid as in Fig.1.3, this hybrid will work normally and try to cancel the input as the echo. Even in this case, there will still be a correlation between the leaked signal x_k and r_{k+1}, although x_k will likely be of very small magnitude. This correlation will lead the "normal" LMS algorithm to assume that the component in the r_{k+1} which is correlated with x_k is part of the leaked echo from the hybrid and $\hat{h}(z)$ will be adjusted to increase its magnitude in an effort to cancel it, which will eventually lead $\hat{h}(z)$ to drift away from $h(z)$ thus causing the poles of the overall system to cross to the outside of the unit circle. Simple observation of the error does not allow us to predict the occurrence of bursting ahead of time. However, the coefficients will consistly grow in magnitude to the point where the effective poles of the system become unstable . This will be discussed in more detail later in Chapter 3.

The occurrence of bursting is affected by various parameters including step size of the adaptive algorithm, matching between the filter order and the hybrid response, the quality of echo cancellation at the far-end, and the presence of the far-end signal(for single adaptive hybrid only).

In conclusion, bursting is such a detrimental phenomenon that it has to be avoided. In this thesis, several efficient solutions will be proposed concerning bursting control. Simulation results verifying the performance of these approaches are provided.

1.3 Thesis Organization

This thesis is organized in 5 chapters. In Chapter 2, several published solutions about avoidance of bursting are reviewed and their advantages and disadvantages are discussed. The concentration of Chapter 3 and Chapter 4 is on the work done in this thesis. In Chapter 3, several simple and effective approaches for bursting control such as the combination of monitoring pole positions with the usage of leaky LMS and restricting the dynamic range of the coefficients, etc. are described. However, these approaches are either applicable to low orders or require some knowledge of the hybrid response. In Chapter 4, two approaches based on cross-correlation of the input and the error of EC are proposed and their effectiveness are verified by computer simulations. Finally, conclusions and suggestions for further research are included in Chapter 5.

Chapter 2

Review of Current Methods For Bursting Control

The bursting problem is not unique to telephone systems. It is also observed in adaptive systems such as model reference adaptive control, autoregressive moving average(ARMA) whitener/predictor used in adaptive pulse code modulation(ADPCM)[30] , etc. It has been extensively studied in numerous recent papers proposing possible ways to avoid it. In this chapter, current approaches, e.g.: providing the persistent excitation to the input of the EC[28], adding proper leakage to LMS algorithm[30], usage of a new double-talk detector(DTD)[38], and usage of double adaptive filter systems[16][18], etc. are reviewed. The advantages and disadvantages of each method will be summarized. As a general rule, all methods proposed up to the present except the last one studied very simple cases of the first-order adaptive filters with scalar feedback. Bursting was also shown to happen in those "simple" cases. Most methods proposed are for these unrealistic cases and are not generalizable for the practical ones. However, due to the mathematical complexity of the problem, it was not possible to address the general case. The usage of double adaptive filters is the only one applicable to higher orders.

2.1 Persistence of Excitation

In [26], it was shown that regular LMS adaptive algorithm can generate parameter drift when driven by bounded sequences even if there is no feedback loop. For the persistently excited cases, parameter estimates are bounded. In [28], several adaptive problems in which bursting may happen are discussed, and it is concluded that the occurrence of bursting is attributed to a lack of persistence of excitation combined with the presence of disturbances inside a feedback loop. Thus, a sufficient condition for avoidance of bursting is persistency of excitation[28][27]. This solution is also applicable to the adaptive hybrid problem . Here, the excitation is the input to the EC, the input at the near(far) end acts as a disturbance to the algorithm at the near(far) end. Referring to Fig.1.6, when there is only narrow-band signal injected to the near-end, the excitation, x_k, to the EC is also narrow-band, i.e. nonpersistent. Combining the disturbance v_{k+1} within the feedback loop, bursting will definitely happen[23][24].

Following the above analysis, it is not hard to conclude that as long as we can provide persistent excitation(roughly frequency richness, e.g., speech or white noise) to the input of the EC, then proper performance of the EC is guaranteed. However, the excitation is not a design parameter. A tone or a whistle or some other narrow-band signals could be injected as near-end input. Thus, this sufficient condition is not practically enforcable . It can be applied by the addition of a signal correlator at the input of the EC. Adaptation is stopped upon the detection of an "unsufficiently persistent" input. However, the complexity of this correlator is significant.

2.2 Application of Leaky LMS

Nowadays, LMS is the most commonly used algorithm in the EC. There are numerous papers discussing its effectiveness [3][7][19][25]. The LMS algorithm[9]-[13] is considered as an approximation to the well known steepest descent(SD) algorithm, using instantaneous

estimate of the input optimization technique driven with a fixed step size. The basic operation of LMS in EC problem is illustrated in Figure 2.1.

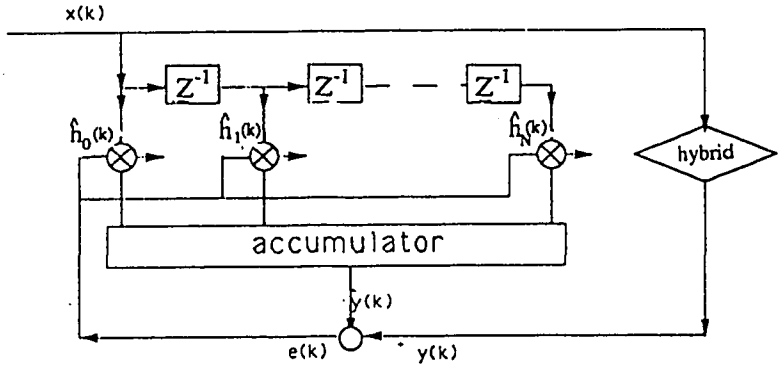

Figure 2.1: LMS algorithm used in the echo cancellation problem

The incoming signal at time k, $x(k)$, is applied to both the AF and the hybrid. The AF forms an estimate $\hat{y}(k)$ (echo estimate) of the echo path output $y(k)$. The difference between $y(k)$ and $\hat{y}(k)$ is the estimate error $e(k)$ to be used to adjust the filter parameter $h_i(k), i = 1, \ldots, N$ (N represents the number of the coefficients of the AF) so that the echo will be cancelled as best as possible in the least-square sense[4][5]. LMS reaches an unbiased optimum.

The updated equation for the ith weight can be expressed as:

$$\hat{h}_i(k+1) = \hat{h}_i(k) + \mu x(k-i+1)e(k) \tag{2.1}$$

where μ is the step size which determines the convergence speed and the steady state mean square error. To guarantee the convergence of coefficients to optimum, μ is bounded by $0 < \mu < \frac{2}{\lambda_{max}}$, where λ_{max} is the largest eigenvalue of the correlation matrix of the input vector. To guarantee the convergence of the LMS algorithm in the mean square, μ should satisfy the condition $0 < \mu < \frac{2}{\sum_{i=1}^{N} \lambda_i}$. As $\lambda_{max} \leq \sum_{i=1}^{N} \lambda_i$, the first bound imposes a larger upper bound on μ than that of the second one. Therefore, the condition of $0 < \mu < \frac{2}{\sum_{i=1}^{N} \lambda_i}$ is the necessary and sufficient condition for the overall stabililty of the LMS algorithm[9].

The simplicity and the robustess of LMS algorithm make it the predominant learning method used in EC. Leaky LMS algorithm[9][31] is a modified version of the LMS designed to stop parameter growth to excessively large values. It is obtained by minimizing the combination of the mean-squared error(MSE) and the energy in the impulse response of the adaptative filter. In the leaky LMS, the cost function

$$J(k) = E\{e^2(k)\} + \alpha \mathbf{h}^{\mathrm{T}}\mathbf{h}$$

is minimized with respect to the tap-weight vector $\mathbf{h}$, where α is a positive control parameter and $E\{\}$ is an expectation operator.

The minimization yields the following update for the tap-weight:

$$\hat{h}_i(k+1) = (1-\beta)\hat{h}_i(k) + \mu x(k-i+1)e(k) \tag{2.2}$$

where $\beta = \alpha\mu, (0 \leq \beta < 1)$ is the leakage factor which controls the leakage rate. $\beta = 0$ correspondes to the regular LMS algorithm. Leaky LMS reaches the compromise between the minimum of MSE and the optimum of weights power, so it can be used to prevent weights from drifting to large values which eventually leads to bursting. To guarantee that parameter drift is contained in a suitably small region, β is required to be large. However, leaky LMS results in a biased optimum. The closer β is to 1, the larger the bias. Thus, β has to be chosen small. But if β is too small, there will not be enough leakage to control drift and bursting will occur. Therefore , a compromise is required[29][32]. In [30], a relation between step size μ, leakage factor β and the size of the disturbances(usually one has a prior estimate of it) is derived so that the boundary separating the estimated parameter space into stable(non-bursting) and unstable(bursting) regions can be obtained. Bifurcation analysis [33]-[37] was used to establish that within the usual range of values of leakage , step size, and disturbances, the system will contain either a stable fixed point or a stable period two orbit. It was shown that when the adaptive system has a stable fixed point, nearby initial conditions will converge to it, no bursting is present. When

the stable period two orbit is present, nearby initial conditions will spiral into it. This is the case when the system bursts. Thus, the main part of [30] is attempting to derive the exact location of the fixed points and establish bifurcation curves along which the EC adaptive problem changes from the bursting to non-bursting behavior.

Considering the complexity of the derivation , the simplest model shown in Figure 2.2 with single parameter adaptive hybrid at the near-end and a nonadaptive scalar at the far-end was analysed. Since bursting is more likely in short loops, only the worst case of one delay is discussed. Cases when the inputs were not persistent excitations are the only ones considered since they are the only cases that could possibly lead to bursting.

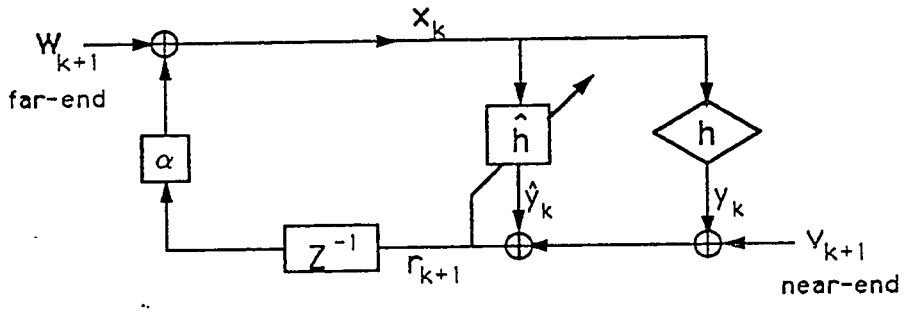

Figure 2.2: Model of single adaptive hybrid system

where h is the first-order near-end echo-path transfer function, $\hat{h}$ is its estimate, and α is echo attenuation factor for far-end echo path. v_{k+1} is the near-end signal and w_{k+1} is the far-end signal. In this case, we assume w_{k+1} to be zero.

The update of parameter $\hat{h}$ is

$$\hat{h}_{k+1} = (1-\beta)\hat{h}_k + \mu x_k r_{k+1} \tag{2.3}$$

The error sequence is given by

$$r_{k+1} = hx_k - \hat{h}x_k + v_{k+1} \tag{2.4}$$

Define $\tilde{h}_k = h - \hat{h}_k$, and rewrite (2.4) as

$$r_{k+1} = \tilde{h}_k x_k + v_{k+1} \tag{2.5}$$

Then, substituting (2.5) into (2.3), we have

$$\tilde{h}_{k+1} = (1 - \beta - \mu x_k^2)\tilde{h}_k - \mu x_k v_{k+1} + \beta h \tag{2.6}$$

As $x_k = \alpha r_k + w_{k+1}$, with $w_{k+1} = 0$, we get

$$x_{k+1} = \alpha r_{k+1} = \alpha \tilde{h}_k x_k + \alpha v_{k+1}, \tag{2.7}$$

Suppose v_{k+1} is a constant, i.e., $v_{k+1} = v$, and define $u = x\sqrt{\mu}$, $v = -\alpha\tilde{h}$, $d = \alpha v\sqrt{\mu}$(also a constant), and $a = -\alpha h$, then (2.6) and (2.7) of the first iterate map can be rewritten as

$$v_{k+1} = v_k(1 - \beta - u_k^2) + u_k d + \beta a. \tag{2.8}$$

$$u_{k+1} = -v_k u_k + d \tag{2.9}$$

The second iterate map is given by

$$\begin{aligned} u_{k+2} &= -(v_k(1 - \beta - u_k^2) + u_k d + \beta a)(d - u_k v_k) + d \\ v_{k+2} &= (v_k(1 - \beta - u_k^2) + u_k d + \beta a) \\ &\quad \times (1 - \beta - (d - u_k v_k^2) + (d - u_k v_k)d + \beta a \end{aligned}$$

Let $u = u_{k+2} = u_k$, $v = v_{k+2} = v_k$, the fixed points of the second iterate map are at

$$u_1 = \frac{d + \sqrt{d^2 - 4\beta(1-a)}}{2}, v_1 = 1$$

$$u_2 = \frac{d - \sqrt{d^2 - 4\beta(1-a)}}{2}, v_2 = 1$$

It is discovered that the curve $4\beta(1 - a) = d^2$, i.e., $4\beta(1 + \alpha h) = d^2$ divides the (d, β) region into stable(P1) and unstable(P2) parts shown in Figure 2.3.

Along the curve $4\beta(1 + \alpha h) = d^2$, the fixed points of the first and the second iterate maps coincide at $(u, v) = (d/2, 1)$, and the Jocabian of the first iterate has an eigenvalue at -1. This is an indication that along this curve the system period doubles. Then if

(d, β) pair lies in region P1, i.e. $4\beta(1 + \alpha h) \geq d^2$, the system will not burst. Otherwise, bursting will definitely happen.

From the definition we made before, it is clear that d is not exactly the near-end input. As $d = \alpha v\sqrt{\mu}$, the boundary $4\beta(1 + \alpha h) = d^2$ changes to

$$4\beta(1 + \alpha h) = \alpha^2 \mu v^2 \tag{2.10}$$

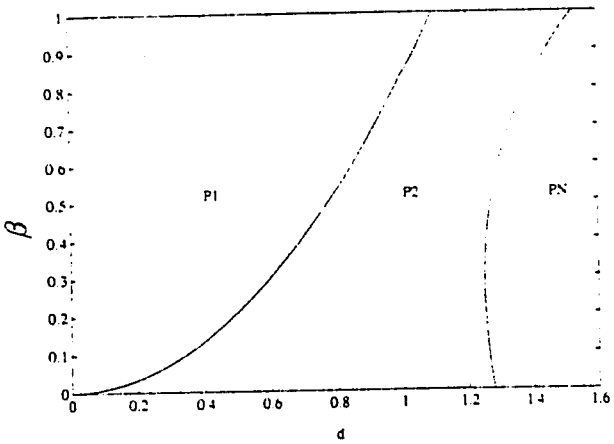

Figure 2.3: Bifurcation lines in (d, β) parameter space

Chapter 3 will provide simulations conducted to verify the accuracy of this boundary. The simulation results show that the derived boundary is quite accurate and suitable leakage factor can be chosen in $P1$ region to avoid bursting. For dc term combined with small-amplitude sinusoid, a similar boundary can be derived. Therefore, following this approach, we can find the proper leakage factor to prevent bursting for a given first-order system. However, the complexity of the analysis makes it inapplicable for practical orders.

2.3 New Double Talk Detector

As explained earlier, bursting results from the high correlation between the "excitation" (input to the near-end EC) and the "disturbance"(near-end signal) when considering the performance of the near-end hybrid . Thus, stopping adaptation based on this correlation would help avoid bursting. In [38], a new test signal which approximately measures this

correlation is proposed for use in the double-talk detector(or near-end speech detector) scheme commonly used to halt updating in the presence of near-end signal.

The basic idea of any Double Talk Detector(DTD)[39][40] is to freeze the parameter adaptation when the ratio of the energy in v_k(near-end input) to the energy in x_k(input to the EC) exceeds a predermined threshold. A too cautious DTD will frequently interrupt the adaption so that the adaptive filter may be unable to achieve good echo attentuation, while a too bold DTD will allow continuous adaptation even when the near-end signal may result in a large parameter estimation error and possibly bursting. The new DTD in [38] is based on the selection of a proper test signal and an associated threshold so as to detect the presence of high correlation between the near-end and far-end signals rather than just their frequencies.

To be consistant with the notations in [38], the block diagram of the system model is repeated in Figure 2.4 here. The model is still the simple first order case discussed earlier.

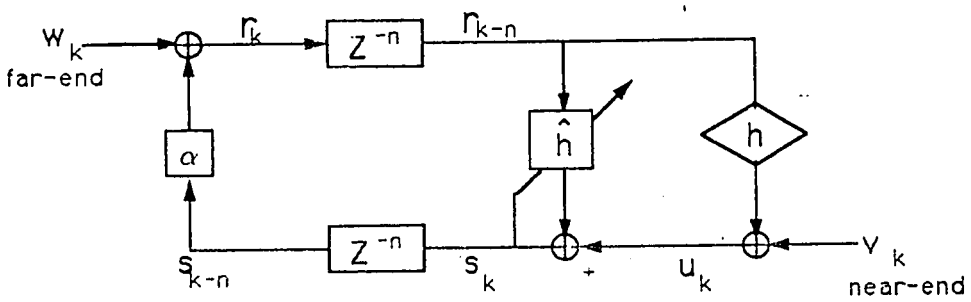

Figure 2.4: Single adaptive hybrid reprinted from [38]

The conventional DTD defines the test signal as

$$Tc = \frac{Average\{u_{k+i}^2\}}{Average\{r_{k+i-1}^2\}}$$

Whenever T_c exceeds a predetermined threshold Θ, adaptation is prohibited. But the differences in signal power, carrier frequency, and bandwidth will all affect the selection of the average threshold Θ. Thus, the optimization of threshold Θ over the set of all

possible inputs is usually accomplished through trial and error in practice. This way is quite inconvenient and it is not guaranteed the threshold can be suitable for all cases.

The proposed DTD is related to the decorrelation degree of v_k and r_{k-n}, where n is the delay in the telephone line. The test signal for the new DTD has an easy-to-select threshold. Its main idea will be briefly reviewed here.

The equilibrium of the adaptive parameter of the average system is reached when

$$Avg\{s_k r_{k-n}\} = 0 \tag{2.11}$$

since

$$\begin{aligned} s_k &= v_k + h r_{k-n} - \hat{h}_{k-1} r_{k-n} \\ &= v_k + \tilde{h}_{k-1} r_{k-n} \end{aligned} \tag{2.12}$$

Eq.(2.11) changes to

$$Avg\{s_k r_{k-n}\} = Avg\{v_k r_{k-n}\} + Avg\{\tilde{h}_{k-1} r_{k-n}^2\} = 0 \tag{2.13}$$

Assuming μ is very small, when Eq.(2.11) is satisfied, the parameter estimate error is effectively invariant, i.e., $\tilde{h}_{k-1} = \tilde{h}$, then (2.11) can be rewritten as:

$$Avg\{s_k r_{k-n}\} \approx Avg\{v_k r_{k-n}\} + \tilde{h} Avg\{r_{k-n}^2\} = 0 \tag{2.14}$$

The average equilibrium is obtained at:

$$\tilde{h}^* = -\frac{Avg\{v_k r_{k-n}\}}{Avg\{r_{k-n}^2\}} \tag{2.15}$$

If we define the test signal as

$$T_1 = \frac{|Avg\{v_k r_{k-n}\}|}{Avg\{r_{k-n}^2\}}$$

then, we can see that the new test signal T_1 has the advantage that an appropriate threshold Θ for T_1 can be easily determined from the allowable parameter error ϵ for $|\tilde{h}|$.

Given a constant $\epsilon > 0$ such that on the average $|\tilde{h}^*| \leq \epsilon$, then $T_1 \leq \Theta = \epsilon$. Thus, whenever T_1 is larger than the allowable Θ, adaptation is stopped.

However, the signal v_k needed to construct T_1 is not accessible in practice, so a new test signal T_n is proposed as:

$$\begin{aligned} T_n &= \frac{|Avg\{u_k r_{k-n}\}|}{Avg\{r_{k-n}^2\}} \\ &= \left| \frac{Avg\{v_k r_{k-n}\}}{Avg\{r_{k-n}^2\}} + h \right| \leq |\tilde{h}^*| + |h| \end{aligned}$$

To achieve $|\tilde{h}^*| \leq \epsilon$, the new DTD halts the adaptation when T_n exceeds a threshold $\Theta \leq |\tilde{h}^*| + |h| \leq \epsilon + |h|$ (guideline for choosing threshold of T_n). Though h is a unknown parameter of the echo path , we can use knowledge of its range to get a reasonable threshold for T_n. The threshold for T_n is used instead of directly using the threshold for $|\tilde{h}|$ since $|\tilde{h}|$ cannot be measured in a real case(h is not known).

Simulation graphs are provided in [38] to verify the effectiveness of this new DTD. The model in Figure 2.4 with both near-end and far-end inputs as sinusoid is analysed. If conventional DTD is used, optimizing the threshold for stopping adaptation must be accomplished experimently. e.g., if the same range of $|\tilde{h}|$ is required, even a simple variation of the input frequency will result in the change in the threshold of T_c. Thus, the final Θ has to be determined through trial over the set of all inputs. However, for the new DTD, the threshold can be directly obtained by guidelines mentioned above. Furthermore, simulations show that the new DTD more accurately indicates the need to halt adaptation and hence exhibits less sensitivity to the initialization of the parameter estimate in comparison with the conventional one. Therefore, the new DTD is better than the conventional one .

In general, for narrowband near-end signals, the adaptive coefficients will drift away from the optimum until bursting occurs. Thus, if we can decide on a reasonable parameter error range ϵ , we will be able to determine the threshold for the test signal T_n. Whenever

T_n exceeds that threshold, adaptation is stopped and bursting can be avoided.

Though this method is successfully applied to the first-order hybrid case, it can not be extented to the general cases as we will show . It is clear that the main idea of this approach is to relate the allowable parameter error $|\tilde{h}|$ to the test signal so that the range for $|\tilde{h}|$ will be useful for determining the threshold for T_n. This works when the number of the coefficients in AF is only one . We will now consider generalizing this approach.

Assume the AF at the near-end has one parameter $\hat{h}$, and the near-end echo path is modeled as an M-order FIR filter. Following the same steps from (2.11-2.15), we have the equilibrium

$$\tilde{h}^* = -\frac{Avg\{v_k r_{k-n}\} + h_2 Avg\{r_{k-n-1} r_{k-n}\} + \ldots + h_M Avg\{r_{k-n-M+1} r_{k-n}\}}{Avg\{r_{k-n}^2\}}$$

Still using the definition of the new test signal,

$$T_n = \frac{|Avg\{u_k r_{k-n}\}|}{Avg\{r_{k-n}^2\}} \tag{2.17}$$

$$= \left| \frac{Avg\{v_k r_{k-n}\} + \ldots + h_M Avg\{r_{k-n} r_{k-n-M+1}\}}{Avg\{r_{k-n}^2\}} + h_1 \right| \tag{2.18}$$

$$\leq |\tilde{h}^*| + |h_1| \tag{2.19}$$

Eqs.(2.17-2.19) clearly show the relationship between the threshold of $|\tilde{h}^*|$ and that of T_n.

However, for the AF which has more than one parameter(a practical case), this method is not suitable any more. For example, if the AF has $N(1 < N \leq M)$ parameters, Eq.(2.11) will be changed to

$$Avg\{v_k r_{k-n}\} + \tilde{h}_1 Avg\{{r_{k-n}}^2\} + \tilde{h}_2 Avg\{r_{k-n} r_{k-n-1}\} + \cdots$$
$$+\tilde{h}_N Avg\{r_{k-n} r_{k-n-N+1}\} + \ldots + h_M Avg\{r_{k-n} r_{k-n-M+1}\} = 0$$

Here there are N undecided variables $\tilde{h}_i (i = 1, \ldots, N)$ in one equation. Given the individual range for $\tilde{h}_i < \epsilon_i (i = 1, \ldots, N)$, we cannot directly determine a threshold for T_n as given by Eq.(2.17).

2.4 Double Adaptive Filters

Thus far, the methods mentioned are those directly designed to ensure the avoidance of bursting. The following approach was implemented in commercial products. Even though it does not seem it was intended to avoid bursting, it results in a bursting free EC.

In[16][18], the echo cancellers with two adaptive filters, known as foreground filter and background filter, are described. The foreground filter performs the real echo cancellation, while the background filter is used in adaptive mode to automatically search for any new coefficients that may improve cancellation by the foreground filter. Whenever this is the case, then the new coefficients are transferred to the foreground filter. The purpose for using two adaptive filters instead of one is to effectively distinguish between the case of double talk and the case of echo path changes. In the first case adaptation is stopped while in the second case adaptation continues. An echo canceller based on a single filter cannot easily distiguish between the two since both result in large errors.

The criteria under which the coefficients are transferred are different for these two products. Plessey's product[16] checks the error from the two filters. If the long term average of the adaptive error(from the background one) is less than 7/8(experimental value) of the fixed error(from the foreground one), then the coefficients are transferred to the foreground filter. Using only this criterion, it cannot be guaranteed that the bursting will be prevented before its occurrence. As mentioned in Chapter 1, the error before bursting is still decreasing and simple observation of the error cannot tell when bursting will happen. Product of M/A-COM uses the echo return loss enhancement(ERLE) as the criterion. Referring to Fig.2.2, the ERLE value is obtained as send-in $(y_k + v_{k+1})$ to send-out(r_{k+1}) signal power ratio[17][40]. If $ERLE$(background)> $ERLE$(foreground)+3 dB consistently, then the coefficients are transferred.

To avoid bursting, signal correlators are included in these two products. If an "improper" input is injected to the system, the danger of bursting will be prevented by these

signal correlators. The possible presence of tones or periodical signals is identified. These inputs are considered as possibly capable of destablizing the system through adaptation to the wrong optimum or bursting. Whenever such a correlated signal is detected, the background filter coefficients, even if deemed to give better cancellation, are not transferred to the foreground. This will stop the drifting phase before it leads to bursting. Furthermore, in these two products, double-talk detectors are also included to prevent adaptation while large near-end signals are present. Through using any of these two products, bursting will not be encountered any more, the complexity of the hardware is their main disadvantage.

2.5 Conclusion

In this chapter, several approaches proposed in the literature to control bursting are reviewed. Leaky LMS and a modified DTD both show satisfactory performance for the simplified model of single adaptive hybrid with one parameter at the near-end and nonadaptive hybrid with one scalar at the far-end. However, for the more complicated(realistic) models, these two methods are not applicable any more. Though the commercial products from Plessey and M/A-COM seem to be effective in avoiding bursting , the complexity of the hardware is a high price to pay.

In Chapter 3 and 4, we will introduce several simple but effective ways to prevent bursting, and computer simulation results are provided as well.

Chapter 3

Proposed Simple Approaches For Controlling Bursting

In Chapter 2, the usage of leaky LMS, double talk detector, and double adaptive filters to avoid bursting were reviewed. The first two approaches are very effective, but they are only suitable for a first-order AF. The third approach is applicable to any order of the AF, but its requiremets for computational and hardware complexity are very high. In this Chapter, we propose some simple approaches for avoiding bursting. Some of the proposed approaches are shown to have restrictions, others are similar to those reviewed in Chapter 2 in being applicable only for low-order hybrid cases.

In this Chapter, parameter drift is detected by monitoring the position of the poles of the overall system. This approach is then combined with leaky LMS to derive a boundary for separating bursting and non-bursting regions for a higher-order case. A second approach based on restricting the coefficients of the adaptive filters is also proposed. Three different ways are applied to the real hybrid cases to verify its validity. Next, an evaluation of all these methods is provided. Finally, the effect of using normalized LMS(NLMS) is discussed. It is found that bursting still occurs even if NLMS is used.

It should be noted that all the simulations in this and the next Chapters are done with the configuration of Fig.2.2. The far-end attenuation is $\alpha = 0.2$, and the structure of the adaptive hybrid(expressed as M/N later) will vary depending on the specific run.

M stands for the order of the echo path model and N represents the number of the AF. The coefficients for the hybrid(69 taps) are provided in Appendix B.

3.1 Pole Position Method

It is well known that when the poles of the system are outside the unit circle, the system is unstable. This is the case we should avoid. It is also observed(Figs.3.1-3.2) that bursting happens as the poles move back into the unit circle from the outside. These two figures illustrate the result of applying $dc = 1$ from near-end to the single parameter adaptive hybrid system with $h = 0.1$ in Fig.2.2. The time evolution of the location of the only pole of the system is shown in Fig.3.2. When bursting happens in the system, it shows up in all the signals .

From this observation , it can be concluded that to avoid bursting, the basic way is to keep the poles of the system inside the unit circle. If there is a trend for a pole to go out of the unit circle , adaptation should be stopped. Adaptation will resume only when the proper input conditions resume.

This approach will then introduce the problem of how to calculate the poles of the system. In the following, the general expression for deriving poles of the system is provided, and a specific example is explained to show its effectiveness.

Considering the diagram of Fig.2.2, we assume the near-end echo path is modelled with parameters $h_1, h_2, \ldots, h_M$, while the AF has N adjustable parameters $\hat{h}_1, \hat{h}_2, \ldots, \hat{h}_N (N \leq M)$. For this case:

$$\begin{aligned} r_{k+1} &= y_k - \hat{y}_k + v_{k+1} \\ &= (h_1 x_k + h_2 x_{k-1} + \ldots + h_M x_{k-M+1}) \\ &\quad -(\hat{h}_{1k} x_k + \ldots + \hat{h}_{Nk} x_{k-N+1}) + v_{k+1} \end{aligned}$$

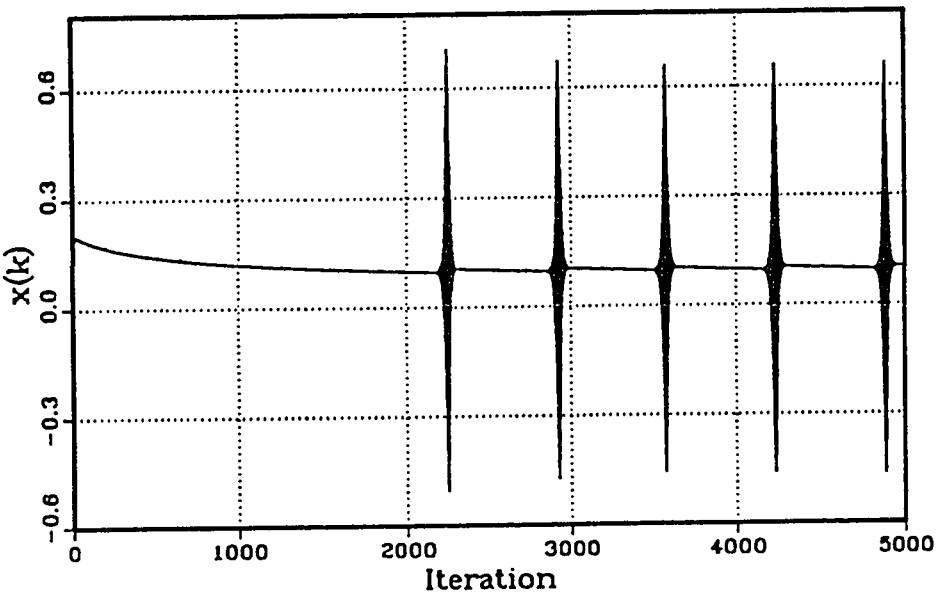

Figure 3.1 Time evolution of x_k illustrating bursting for single end adaptive hybrid (1/1) case. Near-end signal is dc=1.

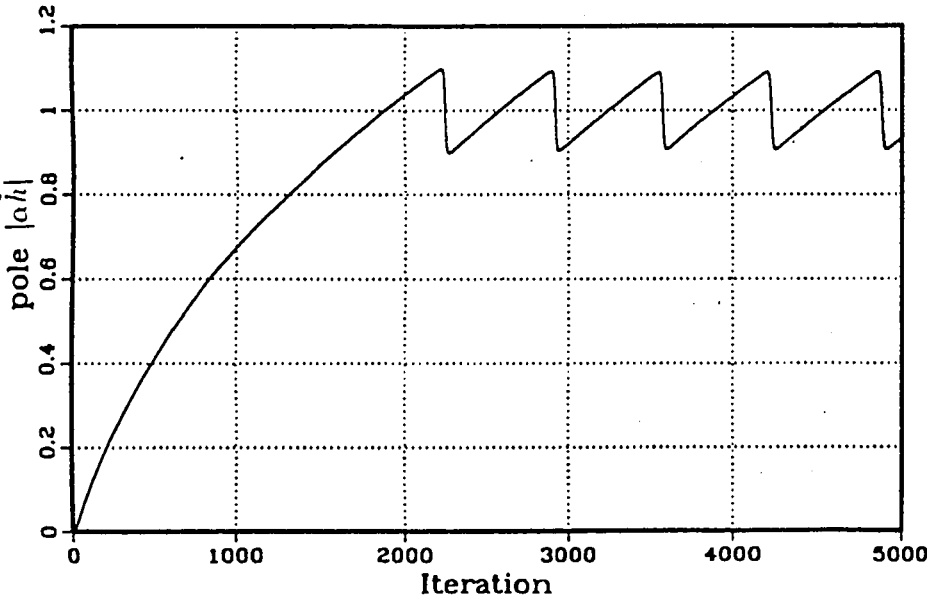

Figure 3.2 Time evolution of pole position illustrating bursting for the same condition as Figure 3.1.

Define $\tilde{h}_{ik} = h_i - \hat{h}_{ik}$, the above equation can be rewritten as

$$\begin{aligned} r_{k+1} &= \tilde{h}_{1k}x_k + \tilde{h}_{2k}x_{k-1} + \ldots + \tilde{h}_{Nk}x_{k-N+1} \\ &\quad + h_{N+1}x_{k-N} + \ldots + h_M x_{k-M+1} + v_{k+1} \end{aligned} \tag{3.1}$$

Taking the Z-transform of both side of (3.1), and defining

$$r_{k+1} \overset{ZT}{\Longrightarrow} R(z), v_{k+1} \overset{ZT}{\Longrightarrow} V(z)$$

we get

$$R(z) = \tilde{h}_{1k}X(z) + \ldots + \tilde{h}_{Nk}X(z)z^{-N+1} + h_{N+1}X(z)z^{-N} + \ldots + h_M X(z)z^{-M+1} + V(z) \tag{3.2}$$

Since

$$x_k = w_{k+1} + \alpha r_k \tag{3.3}$$

The Z-transform of Eq.(3.3) is

$$X(z) = W(z) + \alpha z^{-1} R(z) \tag{3.4}$$

Substituting (3.2) into (3.4), we have

$$\begin{aligned} X(z) &= W(z) + \alpha z^{-1} X(z)(\tilde{h}_{1k} + \ldots + \tilde{h}_{Nk}z^{-N+1} + \\ &\quad h_{N+1}z^{-N} + \ldots + h_M z^{-M+1}) + V(z)\alpha z^{-1}. \end{aligned}$$

Assuming $W(z) = V(z) = 0$, the characteristic equation of this situation is given by

$$1 - \alpha z^{-1}\tilde{h}_1 - \ldots - \alpha z^{-N}\tilde{h}_N - \alpha z^{-N-1}h_{N+1} - \ldots - \alpha z^{-M}h_M. \tag{3.5}$$

Set this expression to zero, the pole positions can be obtained through solving this M-degree polynomial. It is clear in this equation that there is no direct relation between the input, the algorithm used for adaptation, and the cofficients of the polynomial. The characteristic equation is the same irrespective of the inputs. However, the input will

be reflected in the values of x_k and r_{k+1}, thus in the adaptation of $\tilde{h}_i$, and is eventually reflected in the locations of the poles. The fact that the characteristic equation is only related to the configuration of the system(i.e., the order of the echo path and the number of the coefficients for AF for this single adaptive hybrid model) will be quite convenient for us to get the positions of the poles.

Consider the case $M = 2, N = 1$, the characteristic equation is

$$1 - \alpha z^{-1}\tilde{h}_1 - \alpha z^{-2}h_2$$

$$1 - \alpha z^{-1}\tilde{h}_1 - \alpha z^{-2}h_2 = 0 \Longrightarrow z = \frac{\alpha\tilde{h} \pm \sqrt{\alpha^2\tilde{h}^2 + 4\alpha h_2}}{2} \tag{3.6}$$

For constant or sinusoidal inputs, the expression for the two poles is the same. When $|\frac{\alpha\tilde{h}\pm\sqrt{\alpha^2\tilde{h}^2+4\alpha h_2}}{2}| > 1$, i.e. the poles of the closed loop are outside the unit circle, the system will be unstable. It is necessary to check the position of the poles regularly to make sure the poles will not go out of the unit circle. Though this method will be very useful , its complexity is prohibitive for large M. This limits the applicability of this approach to practical cases.

3.2 Pole Position Method Combined with Leaky LMS

Though verifying the stability of poles is computationally expensive, it is the most logical way of avoiding bursting. Any method, as long as it can keep the poles of the system inside the unit circle, is successful in avoiding bursting. The effectiveness of leaky LMS in its prevention of bursting has been discussed[30]. This leads us to consider combining these two approaches. With leaky LMS as the adaptation algorithm, we will determine the pole position as a function of the leakage factor β. Through restricting the poles to be inside the unit circle, we can then get a boundary for the leakage to ensure bursting does not happen .

First, the simplest case which was discussed in [30] is re-derived here based on pole

position to verify the validity of this idea. With Fig.2.2, near-end echo path is a first-order adaptive hybrid. From Eq.(3.5), it is known the characteristic equation is $1-\alpha\tilde{h}z^{-1}$, thus, the only pole of the system is at $\alpha\tilde{h}$. It is required that

$$|\alpha\tilde{h}| < 1 \Longrightarrow |\tilde{h}| < \frac{1}{\alpha}$$

to ensure no bursting presents. For leaky LMS, we have

$$\hat{h}_{k+1} = (1-\beta)\hat{h}_k + \mu x_k r_{k+1} \tag{3.7}$$

Defining $\tilde{h}_k = h - \hat{h}_k$, and considering $r_{k+1} = \tilde{h}_k x_k + v_{k+1}$, (3.7) changes to

$$\tilde{h}_{k+1} = (1-\beta)\tilde{h}_k + \beta h - \mu x_k(\tilde{h}_k x_k + v_{k+1}) \tag{3.8}$$

When the system reaches the steady state, i.e. $\tilde{h}_{k+1} = \tilde{h}_k = \tilde{h}$, Eq.(3.8) changes to

$$\tilde{h}(\beta + \mu x_k^2) = -\mu x_k v_{k+1} + \beta h$$

$$\tilde{h} = \frac{\beta h - \mu x_k v_{k+1}}{\beta + \mu {x_k}^2} \tag{3.9}$$

Extensive simulations show that $\tilde{h}$ is always negative preceding bursting. Thus, $|\tilde{h}| < \frac{1}{\alpha}$ is simplified as $\tilde{h} > -\frac{1}{\alpha}$. Applied Eq.(3.9) to $\tilde{h} > -\frac{1}{\alpha}$, we have

$$\mu {x_k}^2 - \alpha\mu v_{k+1} x_k + \beta + \alpha\beta h > 0$$

Define $\Delta = (\alpha\mu v_{k+1})^2 - 4\mu(\beta + \alpha\beta h)$, then the ranges of x_k for satisfying this inequality depend on different values of Δ. If $\Delta > 0$, as $\mu > 0$, the range for x_k is $x_k > x_1 = \frac{\alpha\mu v_{k+1} + \sqrt{\Delta}}{2\mu}$ or $x_k < x_2 = \frac{\alpha\mu v_{k+1} - \sqrt{\Delta}}{2\mu}$; if $\Delta = 0$, all values of x_k except $x_k = \frac{\alpha\mu v_{k+1}}{2\mu}$ can satisfy the inequality; if $\Delta < 0$, any value of x_k is acceptable. Thus,

$$\alpha^2\mu v_{k+1}^2 = 4(\beta + \alpha\beta h) \tag{3.10}$$

can be considered as the boundary separating the different cases. Compared with Eq.(2.10) , we can see that Eq.(3.10) is exactly the same as that derived from bifurcation analysis of [30] and it separates the bursting and non-bursting regions.

Simulation is done with specifications as following: the echo attenuation is $\alpha = 0.2$, the echo path at the near-end is $h_1 = 0.1$, the estimator was initialized at $\hat{h}_0 = 0$, $v_{k+1} = 1$ for every k, and step size $\mu = 2^{-5}$, the boundary is calculated as

$$\beta = \frac{\alpha^2 \mu v_{k+1}^2}{4(1 + \alpha h)} = \frac{0.2^2 \times 2^{-5} \times 1}{4 \times (1 + 0.2 \times 0.1)} = \frac{1}{3264}$$

From the analysis in Chapter 2, it is concluded bursting is averted when $\beta > \frac{1}{3264}$ and occurs with $\beta < \frac{1}{3264}$. Figs.3.3-3.4 show x_k versus time when $\beta = \frac{1}{3300}$ and $\beta = \frac{1}{3200}$.

From the above derivation and simulation , it is clear that through the way of considering pole position as a criterion to get the proper leakage factor is very effective.

Here, we extend this approach to a higher-order case where the echo path is modelled as a second-order FIR and the AF with one parameter. If the pole position method for a leaky LMS update is applied, a lower bound can be derived for the leakage factor.

From Eq.(3.6), we can see that the poles are at

$$Z_{1,2} = \frac{\alpha \tilde{h}_1 \pm \sqrt{\alpha^2 \tilde{h}_1^2 + 4\alpha h_2}}{2}$$

$$|Z_{1,2}| < 1 \Longrightarrow |\alpha \tilde{h}_1 \pm \sqrt{\alpha^2 \tilde{h}_1^2 + 4\alpha h_2}| < 2 \tag{3.11}$$

Extensive simulations show that it is the pole at $\frac{\alpha \tilde{h}_1 - \sqrt{\alpha^2 \tilde{h}_1^2 + 4\alpha h_2}}{2}$ that moves outside the unit circle during bursting. One example is provided in Figs.3.5 and 3.6 showing the variation of the two poles of this system. System specifications are: $h_1 = 0.7, h_2 = 0.49, v_{k+1} = 1$ for all k, and $\mu = 2^{-5}$.

Since $\alpha \tilde{h}_1 - \sqrt{\alpha^2 \tilde{h}_1^2 + 4\alpha h_2}$ is less than zero for $h_2 > 0$, we need only to consider

$$\alpha \tilde{h}_1 - \sqrt{\alpha^2 \tilde{h}_1^2 + 4\alpha h_2} > -2$$

$$\Longrightarrow \alpha^2 \tilde{h}_1^2 + 4\alpha h_2 < (2 + \alpha \tilde{h}_1)^2$$

$$\tilde{h}_1 > \frac{\alpha h_2 - 1}{\alpha} \tag{3.12}$$

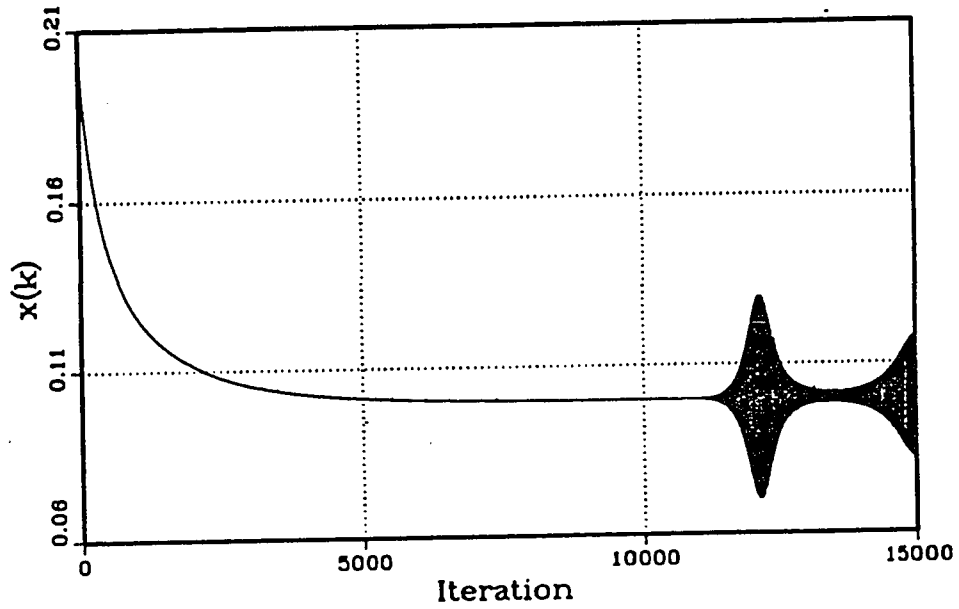

Figure 3.3 Time evolution of x_k with leakage factor $\beta = \frac{1}{3300}(1/1$ case). Near-end signal is dc=1.

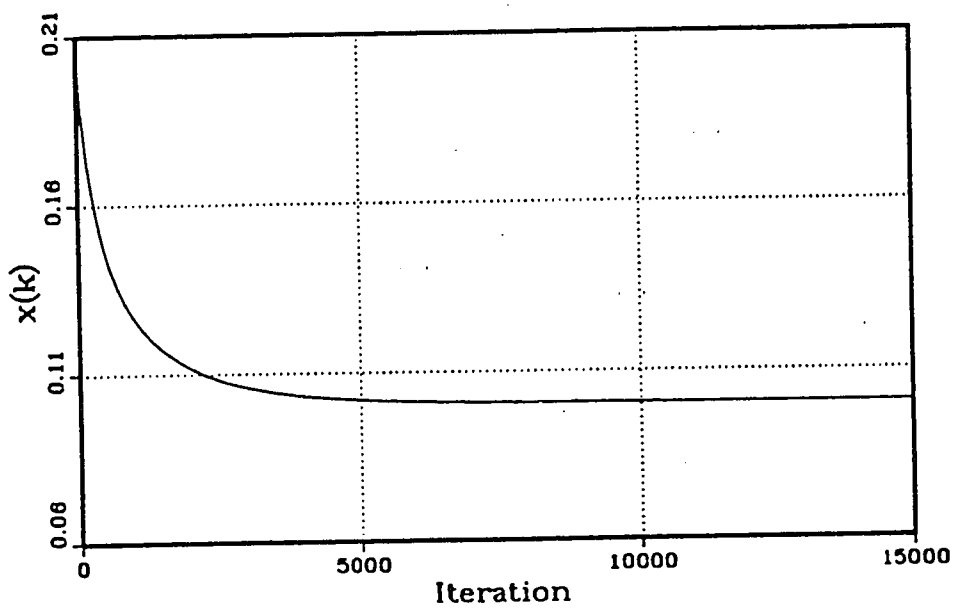

Figure 3.4 Time evolution of x_k with leakage factor $\beta = \frac{1}{3200}(1/1$ case). Near-end signal is dc=1.

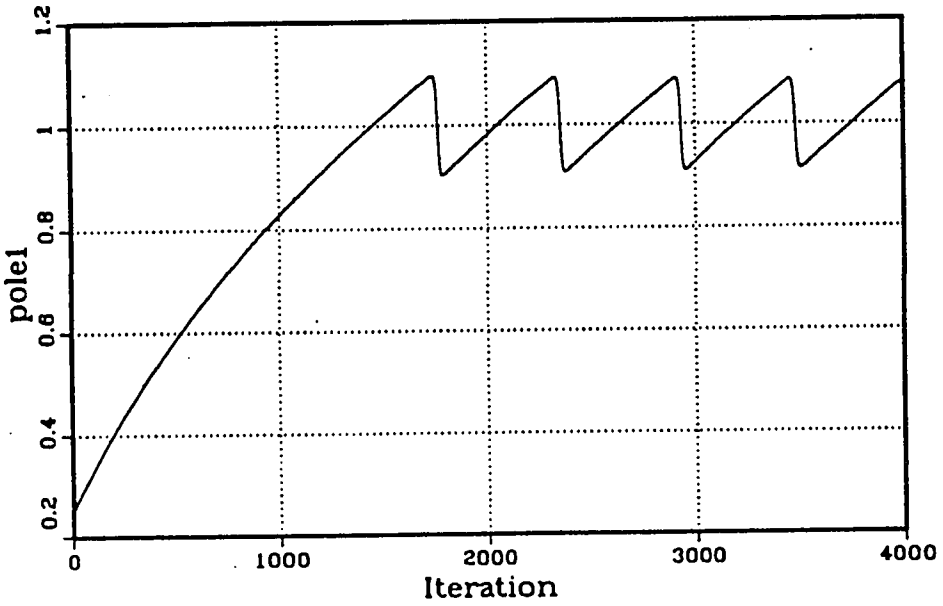

Figure 3.5 Time evolution of the pole at $\frac{\alpha\tilde{h}_1-\sqrt{\alpha^2\tilde{h}_1^2+4\alpha h_2}}{2}$ with dc=1 at near-end(2/1 case).

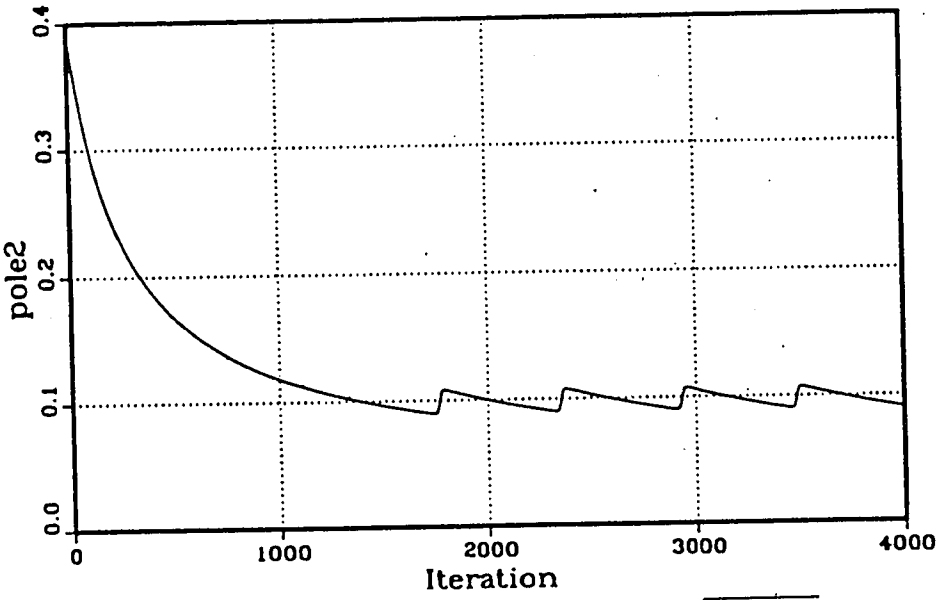

Figure 3.6 Time evolution of the pole at $\frac{\alpha\tilde{h}_1+\sqrt{\alpha^2\tilde{h}_1^2+4\alpha h_2}}{2}$ with dc=1 at near-end(2/1 case).

For the adaptive filter's coefficients,

$$\begin{aligned}\tilde{h}_{1k+1} &= (1-\beta)\tilde{h}_{1k} - \mu x_k r_{k+1} + \beta h_1 \\ &= (1-\beta)\tilde{h}_{1k} + \beta h_1 - \mu x_k(\tilde{h}_{1k}x_k + h_2 x_{k-1} + v_{k+1}) \\ &= (1-\beta-\mu {x_k}^2)\tilde{h}_{1k} - \mu h_2 x_k x_{k-1} - \mu x_k v_{k+1} + \beta h_1 \end{aligned} \tag{3.13}$$

At the steady state, $\tilde{h}_{1k+1} = \tilde{h}_{1k} = \tilde{h}_1$, $x_k = x_{k-1} = x$, Eq.(3.13) changes to

$$\tilde{h}_1(\beta + \mu {x_k}^2) = \beta h_1 - \mu x^2 h_2 - \mu x v_{k+1}$$

$$\tilde{h}_1 = \frac{\beta h_1 - \mu x^2 h_2 - \mu x v_{k+1}}{\beta + \mu x^2} \tag{3.14}$$

Substituting (3.14) into (3.12) , we have

$$\frac{\beta h_1 - \mu x^2 h_2 - \mu x v_{k+1}}{\beta + \mu x^2} > \frac{\alpha h_2 - 1}{\alpha}$$

$$(-\mu + 2\alpha\mu h_2)x^2 + \alpha\mu v_{k+1}x + (-\beta + \alpha\beta h_2 - \alpha\beta h_1) < 0$$

Similar to the argument for Eq.(3.10) , the boundary for leakage factor in this case is

$$\alpha^2\mu^2 v_{k+1}^2 = 4\mu\beta(2\alpha h_2 - 1)(\alpha h_2 - 1 - \alpha h_1)$$

$$\Longrightarrow \beta = \frac{\alpha^2\mu v_{k+1}^2}{4(2\alpha h_2 - 1)(\alpha h_2 - 1 - \alpha h_1)}$$

An example is used to check the accuracy of this boundary. Same conditions as used in Fig.3.5-3.6 are applied. Then

$$\beta = \frac{0.2^2 \times \frac{1}{32} \times 1}{4 \times (2 \times 0.2 \times 0.49 - 1)(0.2 \times 0.49 - 1 - 0.2 \times 0.7)} = 3.73 \times 10^{-4}$$

Thus, theoretically, if $\beta > 3.73 \times 10^{-4}$, no bursting is present. If $\beta < 3.73 \times 10^{-4}$, bursting will occur. Simulation results show the actual boundary is 3.69×10^{-4}, which is quite close to the theoritical one. Figs.3.7-3.8 provide the time evolution of x_k with $\beta = 3.7 \times 10^{-4}$ and $\beta = 3.6 \times 10^{-4}$. The difference between the theoretical analysis and practical result is believed to be due to the quantization and round-off errors.

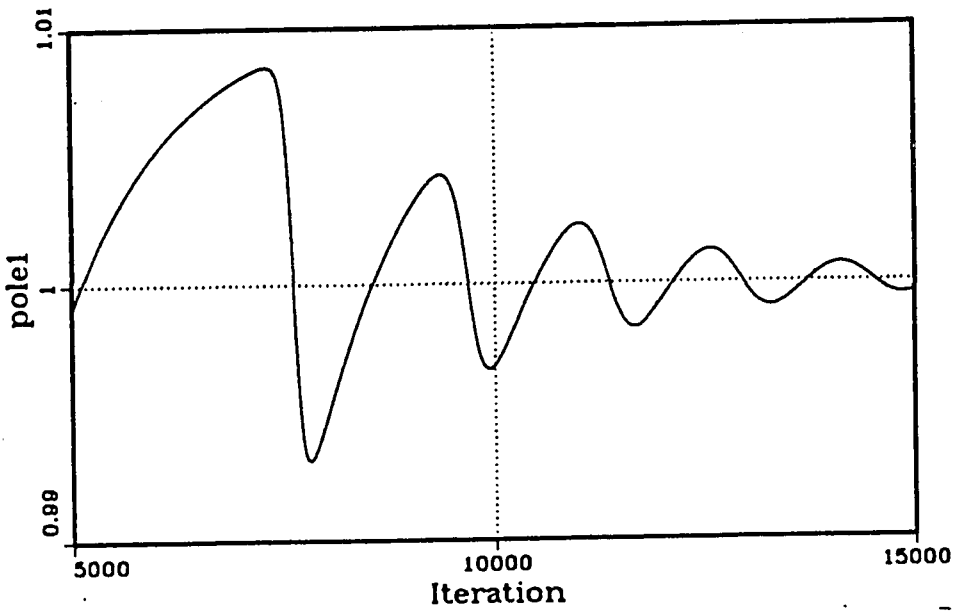

Figure 3.7 Time evolution of the x_k with leakage factor $\beta = 3.6e-4$(2/1 case).

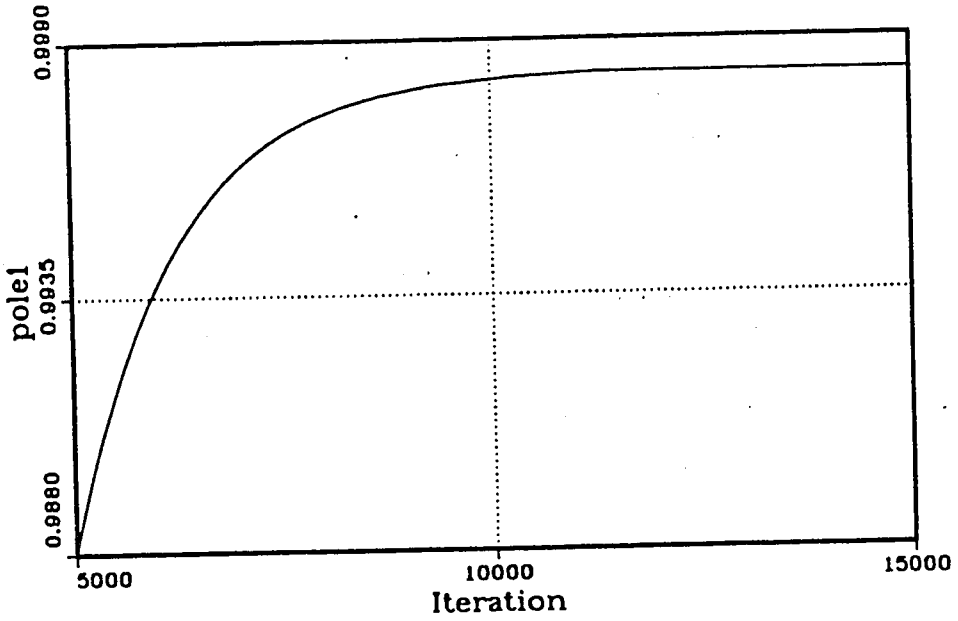

Figure 3.8 Time evolution of the x_k with leakage factor $\beta = 3.7e-4$(2/1 case).

3.3 Discussion

From the above analysis, we can see that checking the system poles regularly or combining pole position idea with leaky LMS to determine an appropriate leakage factor β will work to ensure avoidance of bursting. However , there are drawbacks for these two approaches.

First, determination of the pole locations requires finding the roots of a high-order polynomial. It is quite difficult to solve for the roots of a polynomial whose order is higher than 5 . In reality, finding the roots of such a polynomial is usually done numerically. In this application, it is not practical to expect to perform this operation in real time for every iteration.

It should also be noted that when determining the bound on the leakage , we have to know which pole is likely to move outside of the unit circle . For the second-order system mentioned above , if the pole of $\frac{\alpha\tilde{h}_1+\sqrt{\alpha^2\tilde{h}_1^2+4\alpha h_2}}{2}$ is chosen to be analyzed; then, knowing that $\alpha\tilde{h}_1 + \sqrt{\alpha^2\tilde{h}_1^2 + 4\alpha h_2} > 0$ for $h_2 > 0$, Eq.(3.11) reduces to

$$\alpha\tilde{h}_1 + \sqrt{\alpha^2\tilde{h}_1^2 + 4\alpha h_2} < 2$$

$$\Longrightarrow h_1 < \frac{1-\alpha h_2}{\alpha} \tag{3.15}$$

Combining Eqs.(3.14) and (3.15), a different boundary would be

$$\beta = \frac{\alpha^2\mu v_{k+1}^2}{4(1-\alpha h_1-\alpha h_2)}$$

which is 4.1×10^{-4} if the same values of $\alpha, \mu, v_{k+1}, h_1,$ and h_2 are applied. It has already been verified that this value is not the accurate boundary. Thus, the knowledge of which pole will go out of the unit circle is important. This information is not easily checked on a real time basis.

The third limitation of this approach is that the characteristic equation depends on the prior knowledge of the echo path which is quite difficult to know. Of course, in the theoretical analysis, it can be considered as a known parameter. In practice, both

the order of the echo path and the associated coefficients are not known. This is also a drawback to all the existing methods reviewed in Chapter 2 except the double adaptive filters method[16][18].

The above analysis prompts us to consider the other ways which would be independent of the knowledge of the echo path. In the following section, we discuss a simple method based on restricting the dynamic range of the coefficients to stop the parameters from drifting thus eliminating bursting[43].

3.4 Restricting the Dynamic Range of the Adaptive Filter

As explained earlier, during the time leading up to the actual bursting, the coefficients of the AF consistently drift to significantly large values(much larger than their optimum values) . e.g. in Fig.3.2, the magnitude of the pole , $|\alpha\tilde{h}|$, is provided. It can be seen when $|\tilde{h}|$ reaches and surpasses $\frac{1}{\alpha} = \frac{1}{0.2} = 5$ and comes back inside the unit circle , bursting would happen. But $|\tilde{h}| = |h - \hat{h}| = |0.1 - \hat{h}|$, the estimator $|\hat{h}|$ can reach around 5. Compared with the real value of $h = 0.1$, "5" is much larger than the optimum value for this coefficient. Of course, this is a case which has only one parameter, when the AF has more coefficients, the relationship may not be that obvious . But the fact that the weights will drift to quite large values during the drift phase is true for all orders. This leads to the expectation that limiting the dynamic range of the coefficients may be effective in stopping the drift phase preceding the bursting and thus preventing the bursting from occurring. This idea can be implemented in three different ways.

3.4.1 First Approach: Coefficient Limits Based on Optimum Values

For the first approach, it is proposed to train the echo canceller through the usage of a proper excitation: white noise or speech on the far-end and zero input on the near-end for

training the near-end echo canceller. The system is allowed to converge and the weights finally reach their optimum values on the average. These values are then used to determine the allowable limits on the variation in the coefficients for cases of spectually insufficient inputs as in the single tone case. More specfically, suppose h_i is the optimum value for the *ith* weight , then this weight is only allowed to change in the range of 0 and $2h_i$. The factor of "2" would allow for considerable variation in the echo path. Although the coefficients of the EC will drift away from their optimum values if excitation is not persistent, when any of the weights hits or surpasses its own maximum or minimum allowable value, it is fixed to the boundary value and all the other weights are also temporarily frozen at their own current non-optimum values. The algorithm continues to do the adaptation, but the values will not be used in the cancellation unless they satisfy the above conditions for the weights. As soon as the proper input condition is applied, the coefficients will automatically reflect this change and move back towards the optimum values away from the bounds.

Simulation results prove the effectiveness of this method. With Fig.2.2, modelling the near-end echo path as a 3-tap FIR with coefficients $h_1 = 0.7, h_2 = 0.49$, and $h_3 = 0.3$, the EC has two parameters $\hat{h}_1$ and $\hat{h}_2$ and μ is chosen as 2^{-5}. Figs.3.9 and 3.10 provide the time evolution of the first tap weight of the AF. White noise is applied as far-end input for the first 1000 iterations, this allows the coefficients of the AF on the near-end to reach their optimum values . It can be seen in Fig.3.9 that the coefficient oscillates around an average value. Thus, the optimum is considered to be the average of the last 100 values for a specific weight. Next, a tone(500 Hz) sampled at 8000Hz is injected from the near-end. After 7000 iterations, the tone is replaced by white noise at the far-end again. For this case, during the tone injection, the AF algorithm will consider the input from near-end as a large error, the coefficients will increase in the magnitude to produce high gain in an effort to generate large output to cancel the error, thus, they will start

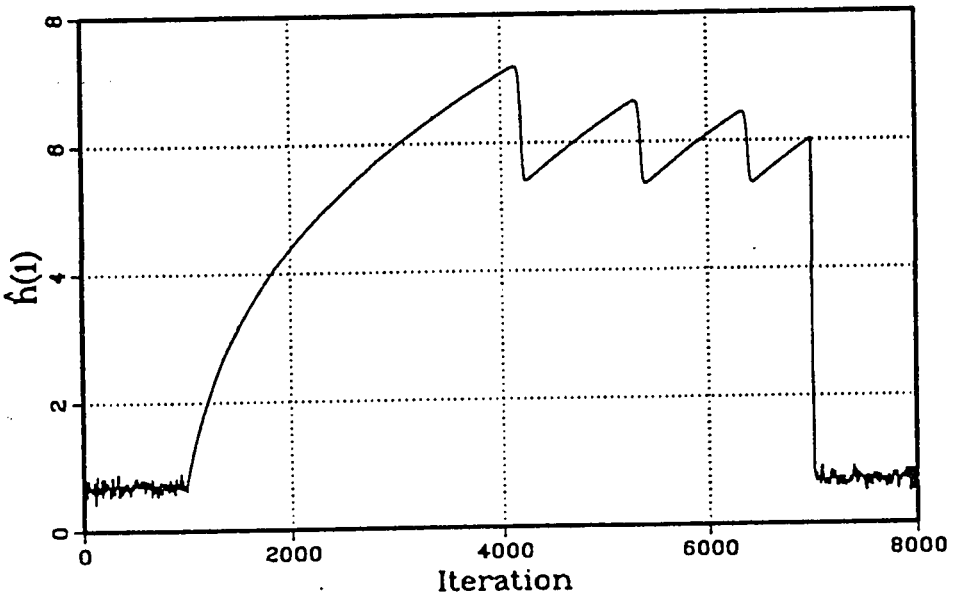

Figure 3.9 Behavior of one adaptive weight(3/2 case) with bursting. Sinusoid and white noise are as input alternately.

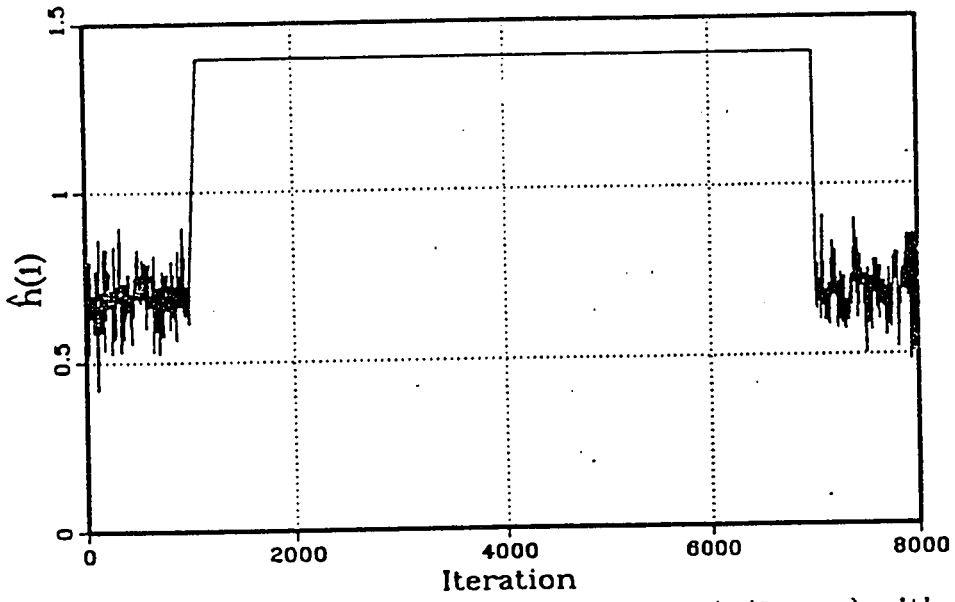

Figure 3.10 Behavior of one adaptive weight(3/2 case) with the first approach applied. Sinusoid and white noise are as input alternately.

to drift away from the optimum eventually leading to bursting. Fig.3.10 shows the same scenarios with the restriction applied on the coefficients : when any weight reaches its own maximum absolute value, it is frozen at that value, and all the other weights are frozen at their present values, too. Here the simple model is used to allow us to follow the changes in the cofficients . A practical hybrid of 69-tap impulse response[25] is also used with an AF employing 16 weights. When 500 Hz sinusoidal signal is injected from near-end from beginning and with step size of $\mu = 1/10$(large step size is to initiate bursting earlier), bursting will occur after 16000 iterations. Fig.3.11 illustrates this residual echo x_k versus time and one adaptive weight is depicted in Fig.3.12. It can be seen how far the weight will drift away from its optimum value when the tone is applied. However, when the weights are restricted to twice the optimum value, bursting will definately not happen.

Even though this approach is likely to avoid bursting with minimal complexity; it does restrict the adaptation of coefficients in normal operation. Figs.3.13 and 3.14 provide evolution of the first and the fifth coefficients of the same 69/16 system as above with near-end white noise input. Roughly seen, the weights change in the range $(-0.6, 0.6)$, but the largest optimum values for weights of this 16-tap AF is below 0.02(see Appendix B). Thus, these weights will frequently hit our range of restriction, and will be forced to stay at the boundary values decided by far-end white-noise case. This can be avoided by careful selection of the allowable range of variation for the coefficients. In any case, it should not present a problem since the instantaneous values of the coefficients is not of crucial importance.

3.4.2 Second Approach: Coefficient Limits Based on Maximum and Minimum Allowable Values

The above approach is fairly simple. However, it assumes an initial trainning period to allow the EC's coefficients to converge to the optimum values. This is not necessarily always possible. Also, changes in the delay of the channel(location of the maximum) may

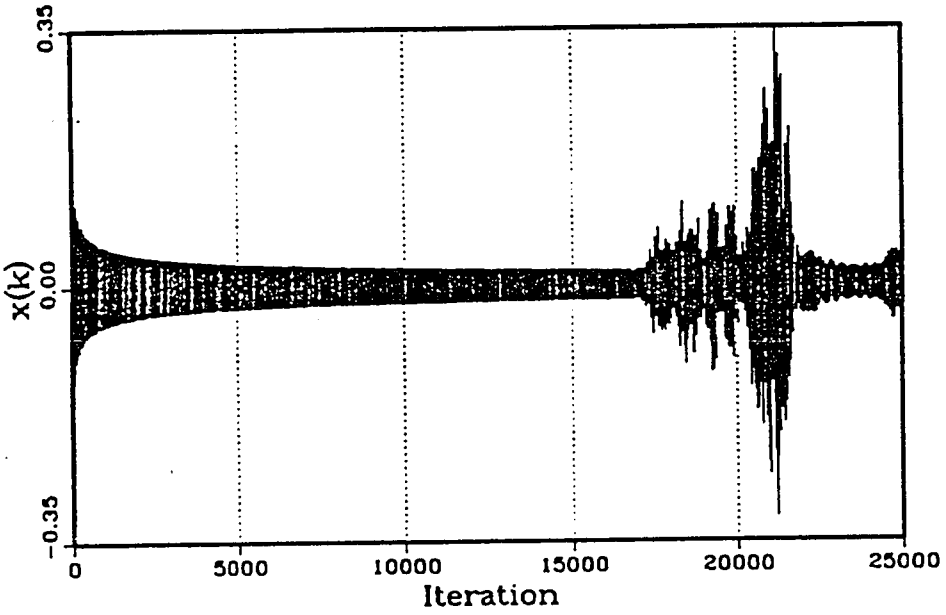

Figure 3.11 Time evolution of x_k in 69/16 hybrid with sinusoid near-end input. $\mu = 1/10$.

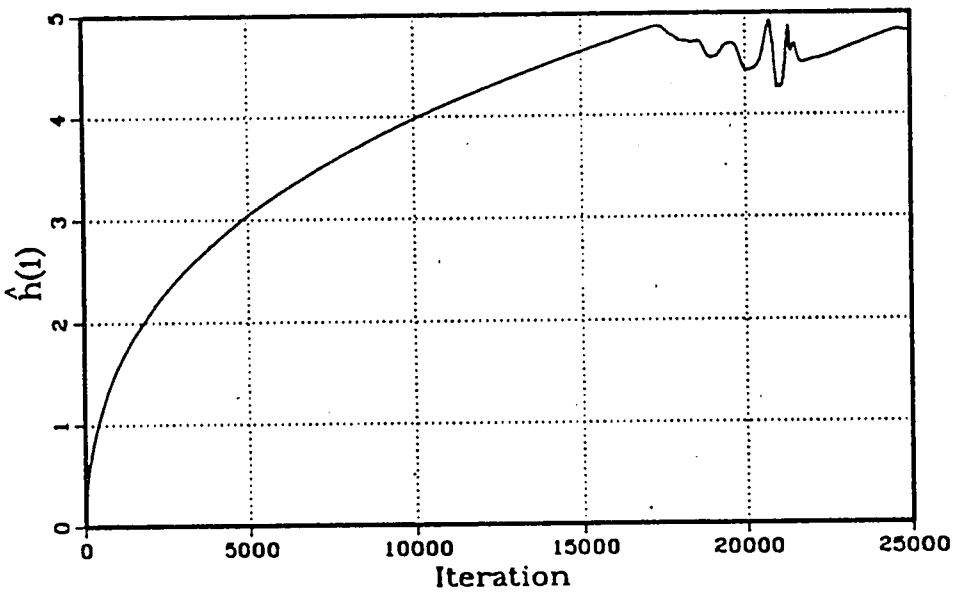

Figure 3.12 Time evolution of one adaptive weight in 69/16 hybrid with sinusoid near-end input. $\mu = 1/10$.

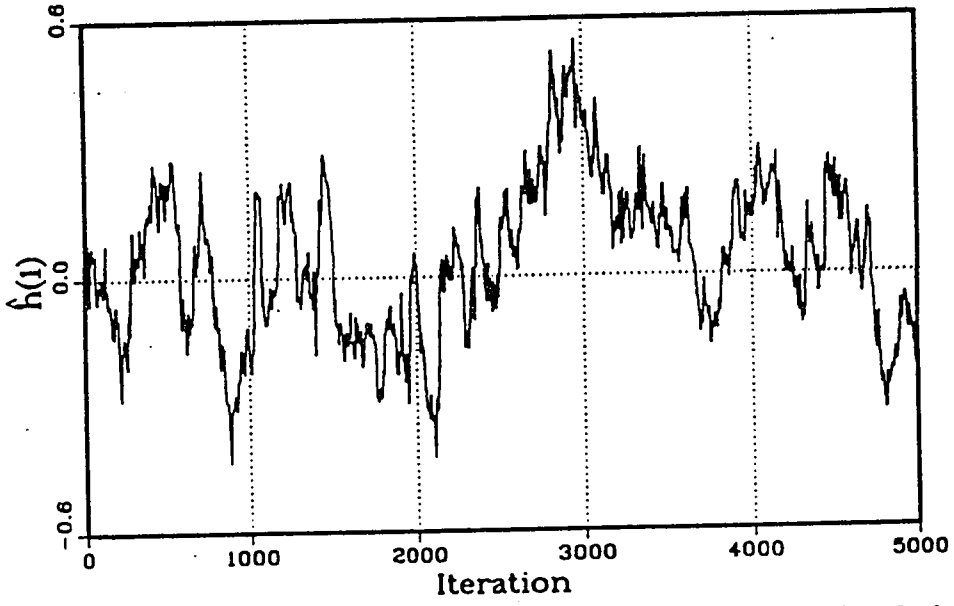

Figure 3.13 Time evolution of the first weight of 69/16 hybrid with white noise from near-end.

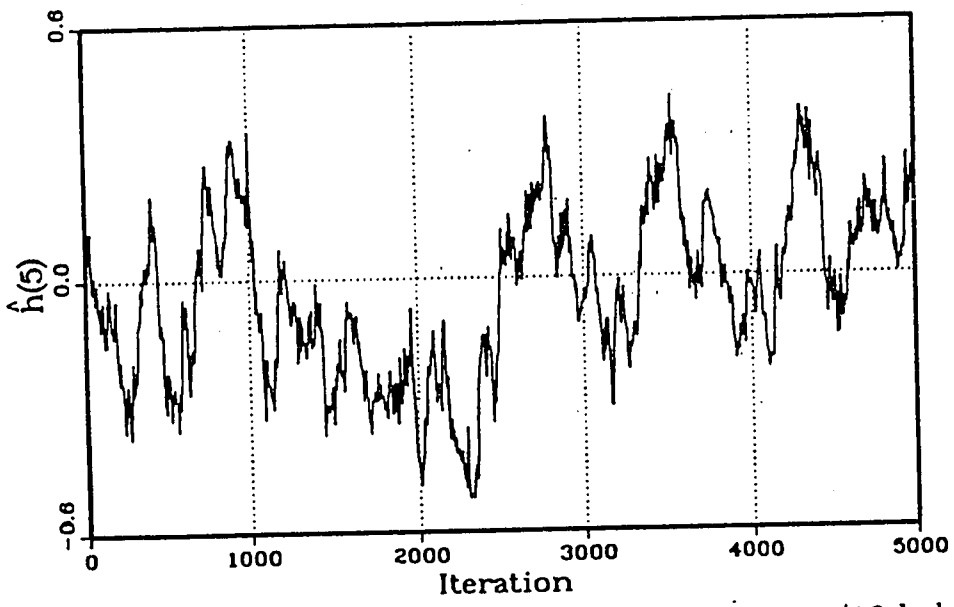

Figure 3.14 Time evolution of the fifth weight of 69/16 hybrid with white noise from near-end.

end up requiring periodical trainning. Thus, an alternate approach which assumes the availability of the knowledge of maximum/minimum allowable values for all the coefficients is proposed. This would be based on statistical studies of the possible range of values for the coefficients. Two contradictory requirements would have to be satisfied. The allowable range has to be wide enough to cover all possibilities for hybrids responses and it also has to be limited enough to stop the coefficients before causing the poles to cross into the unstable region. Here , simulation results using one 69-tap hybrid with 16-tap adaptive filter is already provided in Fig.3.11. The biggest magnitude $|h_{max}|$ of this 69-tap hybrid is considered as the maximum value. And $(-2|h_{max}|, 2|h_{max}|)$ is the dymanic range for all weights. It is assumed this would cover most hybrids. When we use the above dynamic range to restrict the weights, no bursting happens, x_k is just a scaled sine wave. This assumes that an allowable range for all weights of 2 times of $|h_{max}|$ is a reasonable range for most practical loops and allows for unknown delay in response(i.e. unknown location of peak). Depending on the possible range of allowable echo paths, it is conceivable that some combination of coefficients, individually within the allowable range, results in poles outside the unit circle, such a scenario is possible but highly unlikely. From simulation results, we have not encountered this situation at all.

3.4.3 Third Approach: Coefficients Limits Based on Power of Adaptive Filter Response

This approach to stop bursting is based on utilizing leakage concept to limit the growth of the coefficients[2]. As explained earlier, leakage achieves this objective by minimizing

$$J(k) = E\{e^2(k)\} + \alpha \mathbf{h}^{\mathrm{T}}\mathbf{h}$$

where α is the control factor and $\bar{\mathrm{h}}$ is the coefficient vector of AF, $e(k)$ is the error between the real echo and its estimation. Thus, the algorithm converges to a set of coefficients minimizing Mean Square Error(MSE) while having low energy ($\mathbf{h}^{\mathrm{T}}\mathbf{h}$) . The

proposed approach is closely related to this requirement by using the coefficient energy as a constraint. The updating algorithm seeks to minimize

$$J = E\{e^2(k)\}$$

while ensuring $\mathbf{h^T h} < \mathbf{g}$, where $\mathbf{g}$ is some predetermined threshold. It has been shown that in "normal" operation $\mathbf{h^T h}$ has a significantly smaller value than in the stage preceding bursting. $\mathbf{g}$ is determined as a multiple of the average value of $\mathbf{h^T h}$ for the expected range of echo path coefficients. The new value for $\mathbf{h^T h}$ is routinely checked against the constraints. If it hits the constraints, the coefficients are not updated . Again, normal operation is resumed when regular input is received resulting in coefficients moving back the allowable range. The workload of calculating the summation of the power is not tedious. At every iteration, the new coefficients are already obtained , thus, the calculation of their power will be quite easy. The only drawback of this approach is we still need the statistical investigation for all the range of the "normal" cases whose values should be obtained through experiments. However, the allowable range for g is fairly large since for a near-end tone input case, the power of the weights before bursting could reach several orders of that of all other cases(e.g., in 69/16 system, the power is the order of hundreds versus "0.1" for near-end tone versus far-end white noise). Thus, a tight range for g is only required if we want to stop the drifting not just to avoid bursting.

Compared with the leakage approach proposed in [30]; we can see that this proposed approach is directly implementable for realistic higher order while that in [30] was not executable to higher orders. Both approaches seek to limit the growth of coefficients, here by using the energy constraint and in[30] by using leakage. It should be noted that leakage would be applied all the time resulting in a bias in the optimum coefficients under normal operation. By contrast, the current proposed approach would not affect normal operation. It will result in any changes only when drifting starts driving the coefficients to excessively large values. Compared to the approaches proposed in 3.4.1 and 3.4.2; this

current approach is more complex. However, it does not require trainning(as in 3.4.1) and does allow for different delays(different locations of the maximum value of impulse response) unlike that in 3.4.2.

3.5 Effect of Using Normalized LMS

In the papers studying bursting covered in this thesis, only regular LMS was used as simplicity. However, depending on the application, normalized LMS is used to ensure the good performance for inputs with varying power[42] . In this section, we will study the effect of normalization on bursting. The adaptation algorithm for NLMS is

$$\hat{h}_i(k+1) = \hat{h}_i(k) + \frac{\alpha r_{k+1} x_k}{\gamma + X_k^T X_k}, i = 1, \ldots, N$$

Where N is the number of the tap weights for AF, X_k stands for the input vector at time k, i.e. $X = [x_k, x_{k-1}, \ldots, x_{k-N+1}]$, T stands for the transpose of the vector. α is adaptation constant while γ is a small positive term included to ensure that the update term does not become excessively large when $X_k^t X_k$ temporarily becomes small.

It is known the convergence time constant is inversely propotional to the power of the input, and the algorithm will converge slowly for low-power signals[22]. Thus , using normalized input rectifies this situation. Compared with regular LMS, NLMS improves the convergence speed . However, we found that bursting will still happen for the normalized adaptation algorithm . This is because bursting is caused by the high correlation between the input and the error of the EC and since this correlation will always exist no matter which algorithm is used. Different values of α and γ result in different times at which bursting happens, but they will not eliminate it. Figs.3.15-3.17 provide some simulation results showing effect of γ and α on starting time of bursting. All of the three graphs are obtained by using 69/10 system with 1000 Hz sinusoid near-end input. Fig.3.15 and Fig.3.16 use the same α but different γ, while Figs.3.16 and 3.17 use the same γ. As the instantaneous power for the sinusoid input vector is roughly between 0.01 and 0.2(before

realistic hybrids.

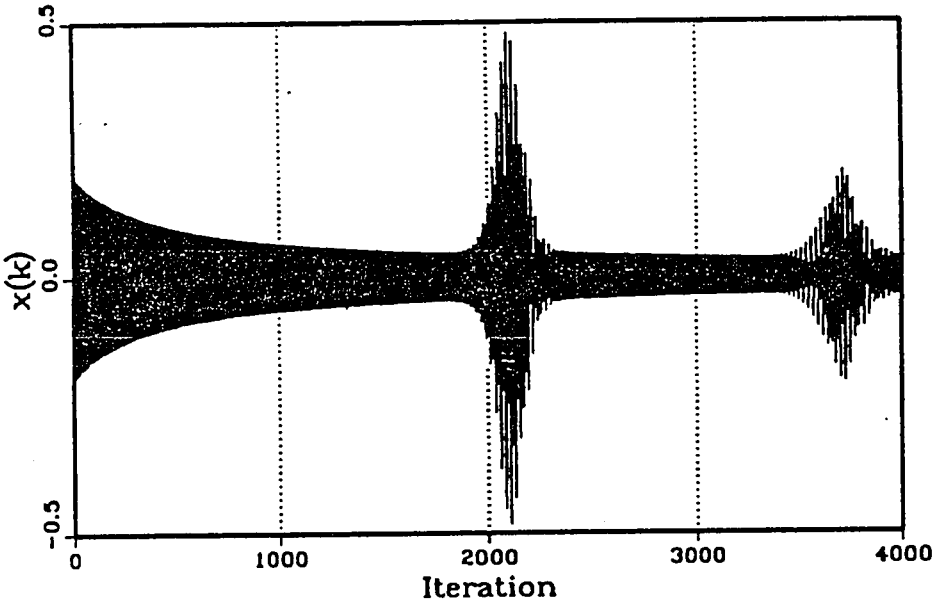

Figure 3.15 Time evolution of $x(k)$ with NLMS applied in the 69/10 system with 1000 Hz near-end input. $\alpha = 0.005$, and $\gamma = 0.01$.

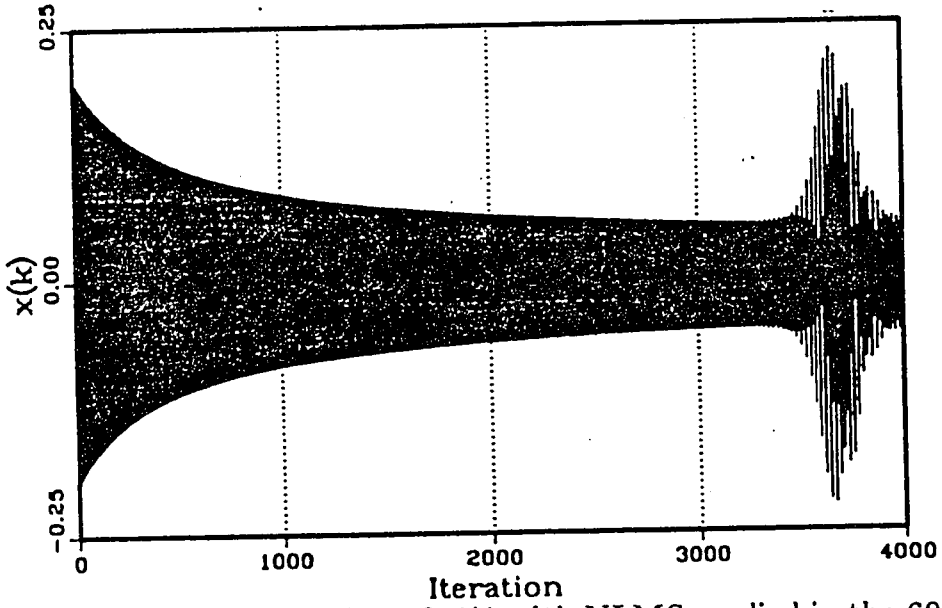

Figure 3.16 Time evolution of $x(k)$ with NLMS applied in the 69/10 system with 1000 Hz near-end input. $\alpha = 0.005$, and $\gamma = 0.05$.

bursting) , α could not be chosen too large, otherwise when the instantaneous input power is too small , instability may be a problem. It is clearly seen no matter which kind of combination for α and γ, bursting will show up all the time. Based on this conclusion , all the following simulations use regular LMS.

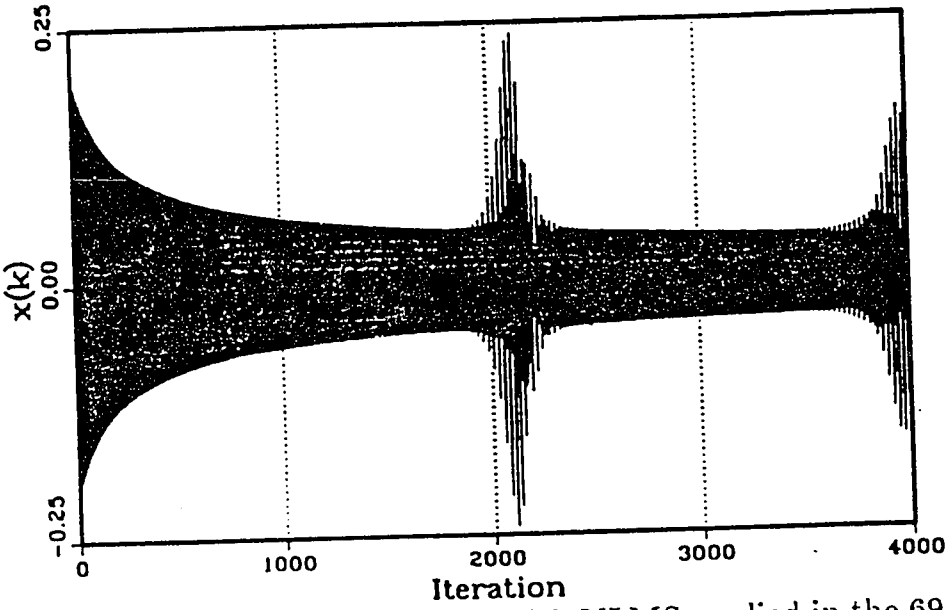

Figure 3.17 Time evolution of $x(k)$ with NLMS applied in the 69/10 system with 1000 Hz near-end input. $\alpha = 0.01$, and $\gamma = 0.05$.

3.6 Conclusion

In this chapter, a method based on controlling the pole position is proposed and its combination with leaky LMS was shown to achieve a good result in eliminating bursting. However, it is only applicable to lower-order hybrid case and cannot easily provide bounds on leakage factor for general cases. The results in [30] were extented to relatively higher order case. However, it was obvious that generalizing this approach to realistic orders is not possible. Next, we presented three approaches restricting the range of the coefficients. These approaches are applicable to any order of the hybrid, therefore, have more practical

significance. Restricting the energy of the coefficients is the best approach but requires computation of $\mathbf{h}^T\mathbf{h}$ routinely. All the methods proposed in this chapter succeed in avoiding bursting with some restrictions very similar to those in other existing methods as reviewed in Chapter 2. In Chapter 4, we will present a more general approach for realistic hybrids.

Chapter 4

Practical Approaches for Bursting Control

4.1 Introduction

In chapter 3, several simple methods to eliminate bursting have been proposed. Because of the shortcomings mentioned in the previous chapter, these methods have obvious limitations. Our objective is to determine an approach that is not mathematically prohibitive(as the method combining pole position calculation with leaky LMS) nor depending on the preknowledge of the range of the coefficients of the AF (as the method restricting the filter weights). In this chapter, a simple and effective approach of using the cross-correlation function as a criterion to detect bursting is proposed and verified through computer simulation in practical hybrids. First, an algorithm presented in [46] for detecting double talk is proposed as a tool to avoid bursting . Its performance is quite satisfactory, but its complexity is significant. Next, a simple approach based on cross-correlation is proposed and its validity is proven by simulation. Finally, an evaluation of these two methods is provided.

4.2 Averaged Cross-Correlation(ACC)

To be consistent with [46], Fig.2.2 is reproduced here as Fig.4.1 with variable r_{k+1} renamed $e(k)$, the error of the EC.

Referring to Fig.4.1, it was shown in Chapter 2 that the basic reason for bursting is the high correlation between the signal $x(k)$ and $v(k)$, since $v(k)$ is a component of the error $e(k)$, it follows that this high correlation also exists in $x(k)$ and $e(k)$.

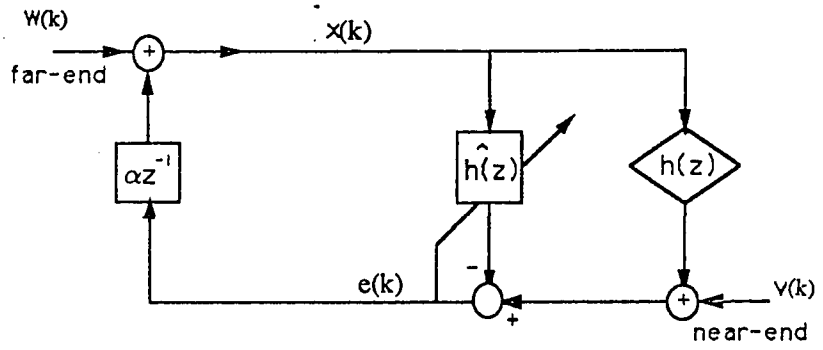

Figure 4.1: Basic structure for single adaptive hybrid

In this section, we will study the property of the correlation between $x(k)$ and $e(k)$. Our objective is to be able to identify any unique characteristics that exist in the phase leading up to bursting. Once such characteristics are identified, they can be used to stop adaptation and thus ensure no bursting happens.

In[46], a new double talk detector(DTD) is proposed based on an averaged cross-correlation (ACC). The main idea in [46] is to use an estimated cross-correlation function – ACC as a criterion to distinguish between the double talk and echo path variation so that adaptation is prohibited during double talk but continuing for echo path change. We will show here that this ACC is also useful for separating tones and white noise as we reported in [44].

The averaged cross-correlation (ACC) is defined in [46][45] as:

$$ACC(k) = \frac{\sum_{i=1}^{N} |C_i(k)|}{N}$$

where $C_i(k)$ is the cross-correlation coefficient between $x(k-i+1)$ and $e(k)$, N is the tap number of the adaptive filter, and k is the iteration number. The update of $C_i(k), i = 1, 2, \ldots, N$ is done using an exponential weighting recursive algorithm as following:

$$P_e^2(k) = \lambda P_e^2(k-1) + (1-\lambda)e^2(k) \tag{4.1}$$

$$P_i^2(k) = \lambda P_i^2(k-1) + (1-\lambda)x^2(k-i+1) \tag{4.2}$$

$$P_{ei}(k) = \lambda P_{ei}(k-1) + (1-\lambda)e(k)x(k-i+1) \tag{4.3}$$

$$C_i(k) = \frac{P_{ei}(k)}{P_e(k)P_i(k)}, i = 1, 2, \ldots, N \tag{4.4}$$

$P_e^2(k)$, $P_i^2(k)$ recursively calculate the estimated power of $e(k)$ and $x(k-i+1)$, $P_{ei}(k)$ is the cross correlation of $x(k-i+1)$ and $e(k)$. λ is the exponential weighting factor which determines the time constant and estimation accuracy of the recursive estimation algorithm. The smaller the λ, the better the time varying signal tracking capability, but the worse the estimating accuracy. Therefore, in practice, for slowly time varying signals, λ is suggested to be in the range of (0.9,1]. In our simulation, for all cases, λ is chosen as 0.95. The following priovides the calculations of ACC for sinusoid and white noise and the characteristics for these signals will be clearly seen.

Unless otherwise specified, configuration of Fig.4.1 is used for all the following simulations, and the step size is set as $\mu = 2^{-5}$.

4.2.1 Characteristics of ACC In Presence of Tones(Near-end or Far-end)

In Fig.4.1, if a tone is inserted from the far-end, no bursting will be present, so the echo canceller performs good cancellation at this frequency. However, tones are not spectrally rich and are not adequate for training echo canceller, thus the coefficients of the AF will not be the optimum ones(See Appendix A). This results from the fact that the coefficients need to cancel the error only at that frequency with no knowledge of the system response at other frequencies. Figs.4.2-4.5 show the averaged cross correlation function for such a case . Note that ACC first converges to some low value, then fluctuates below 0.3(absolute value). Through our simulations, it was shown that the nature of ACC is unaffected by the step size(1/32 or 1/100), the structure of the adaptive hybrid(69/16 or 30/10), or the frequency of the input signal(500 Hz or 100 Hz).

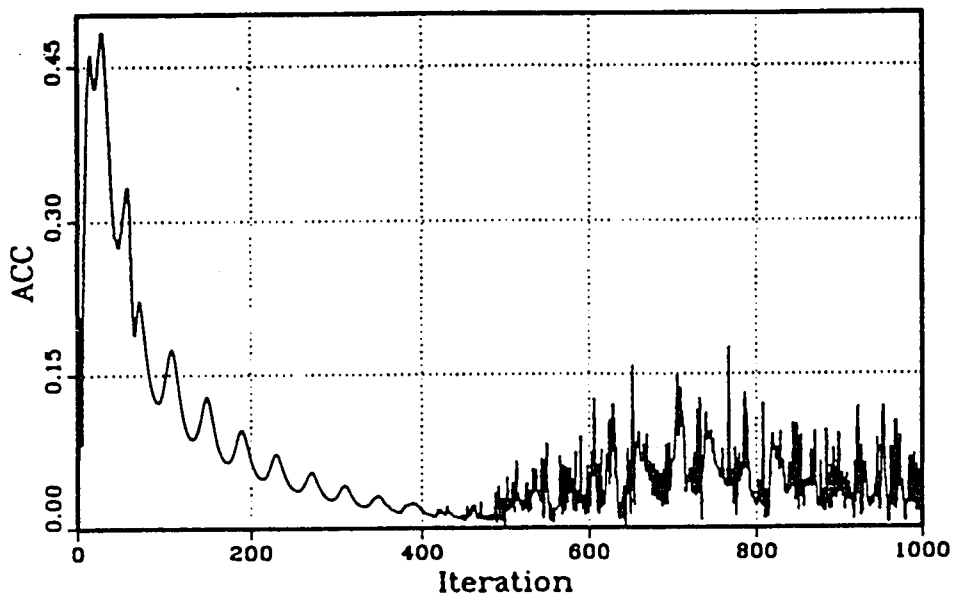

Figure 4.2 ACC of 69/16 single adaptive hybrid with 100Hz sinusoid as far-end input.

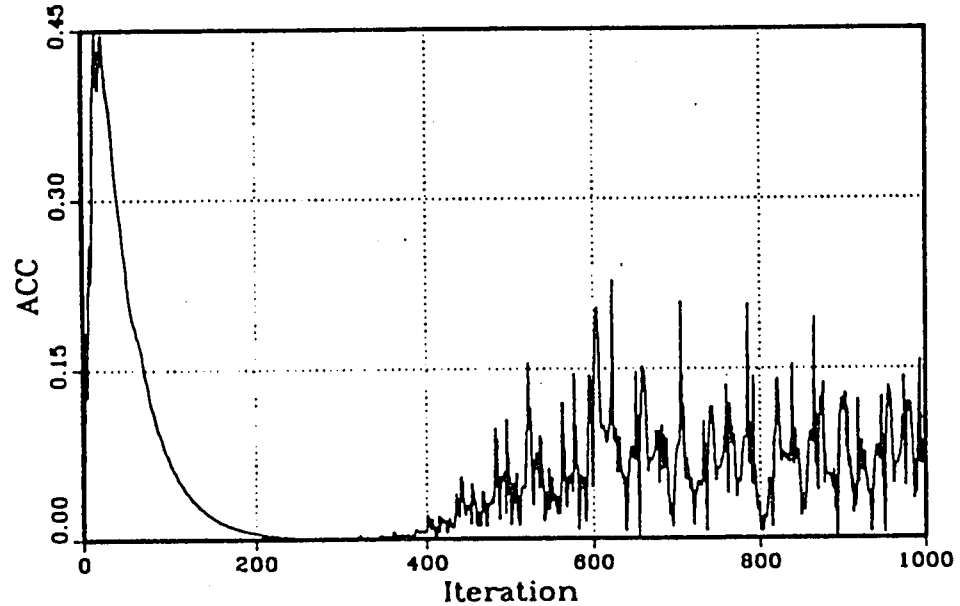

Figure 4.3 ACC of 69/16 single adaptive hybrid with 500Hz sinusoid as far-end input.

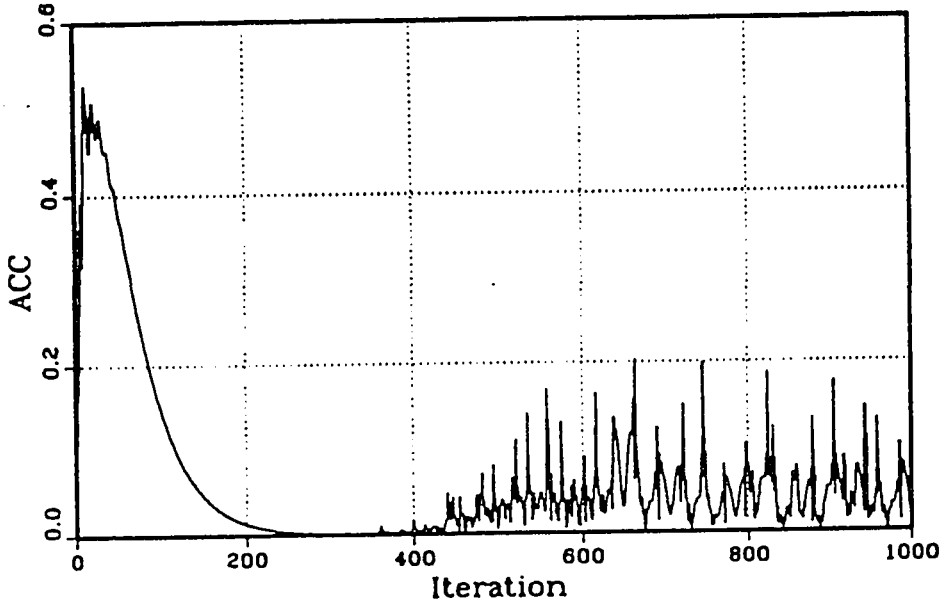

Figure 4.4 ACC of 30/10 single adaptive hybrid with 500Hz sinusoid as far-end input. $\mu = 1/32$.

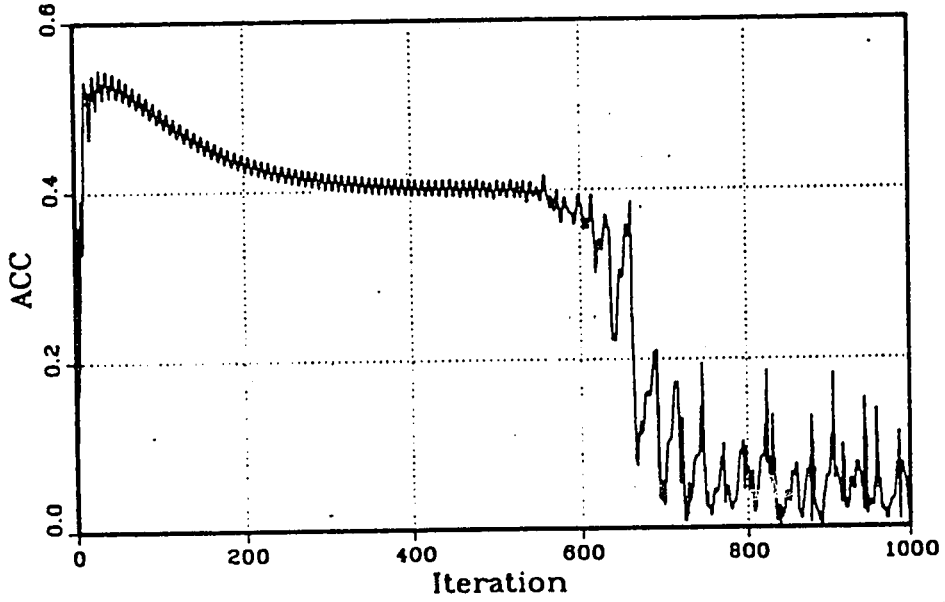

Figure 4.5 ACC of 30/10 single adaptive hybrid with 500Hz sinusoid as far-end input. $\mu = 1/100$.

If the tone is injected from the near-end, this is the case when bursting will happen. For this case, simulations show that ACC is always flat(except for the initial transient) with magnitude above 0.4. Figs.4.6-4.9 provide some examples of using different structure of hybrids(69/16 or 30/10) and tones(500 Hz or 1000 Hz) to check the range of ACC for different cases. However, we can see that though the magnitude range of ACC changes according to different conditions, all retain their flatness and are larger than 0.4. It is worth noting that the absolute value for ACC will not be dependent on the amplitude of the input. This is because ACC is calculated corresponding to the power of $e(k)$ and $x(k-i+1)$. Thus, if the magnitude of the input is increased, it will be reflected in both $P_e(k)P_i(k)$ and $P_{ei}(k)$ which will lead $C_i(k)$ to keep the same range.

4.2.2 Characteristics of ACC for White Noise

If a white gaussian noise is applied to the far-end, ACC has no regularity and looks random . However, it is observed that its magnitude is always below 0.4. Different echo path models are tried to show this characteristic(Figs.4.10-4.11). If the white noise is applied from the near-end, ACC is still below 0.4(Figs.4.12-4.13). Thus, there is not much difference between these two cases(normal operations and double talk). Fortunately, it is not necessary to separate them as neither of which brings bursting problem. Though in the later case, the weights will not converge to the optimum ones, adaptation will be stopped if a double talk detector is used.

4.2.3 Characteristics of ACC for Echo Path Change

Here, we study the nature of ACC in case of a change in the echo path . It has to be ensured that an echo path change will not result in an ACC similar to that observed in cases leading to bursting. Theoretically, it is clear that ACC will only depend on the features of the signals. Of course, in its calculation, the values of $x(k-i+1)$ and $e(k)$ which have relations with the echo path structure will also be included, but they will not

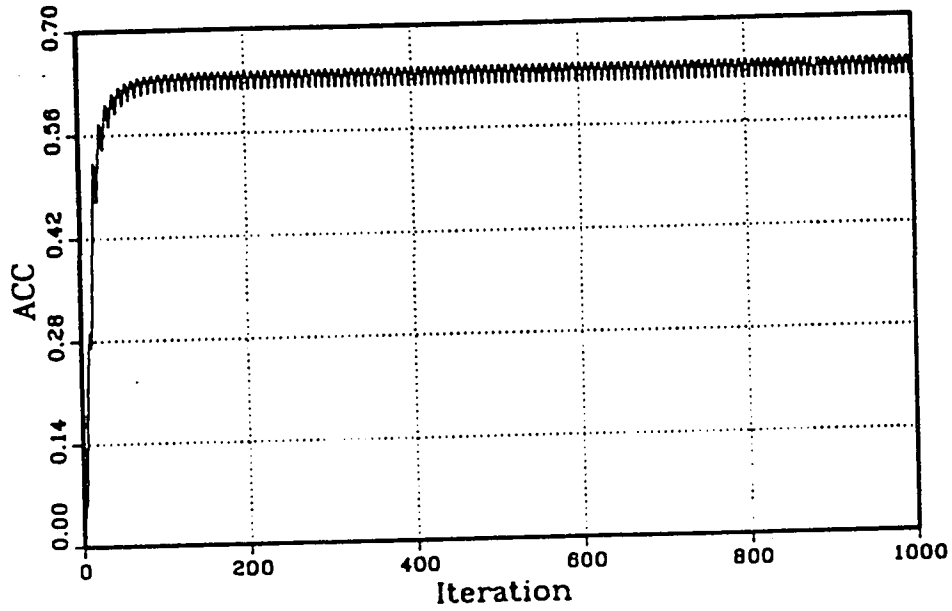

Figure 4.6 ACC of 69/16 single adaptive hybrid with 500Hz sinusoid as near-end input.

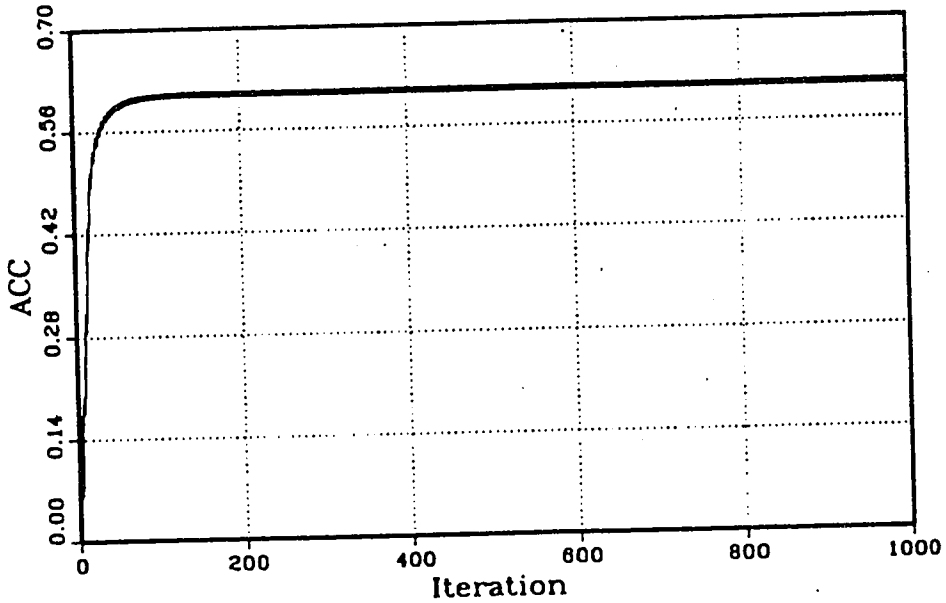

Figure 4.7 ACC of 69/16 single adaptive hybrid with 1000Hz sinusoid as near-end input.

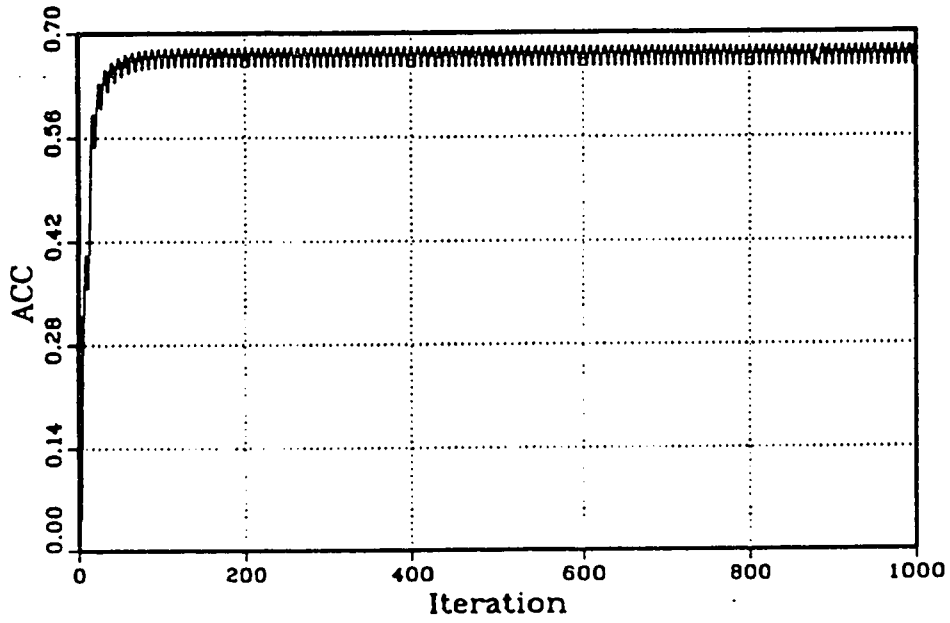

Figure 4.8 ACC of 30/10 single adaptive hybrid with 500Hz sinusoid as near-end input.

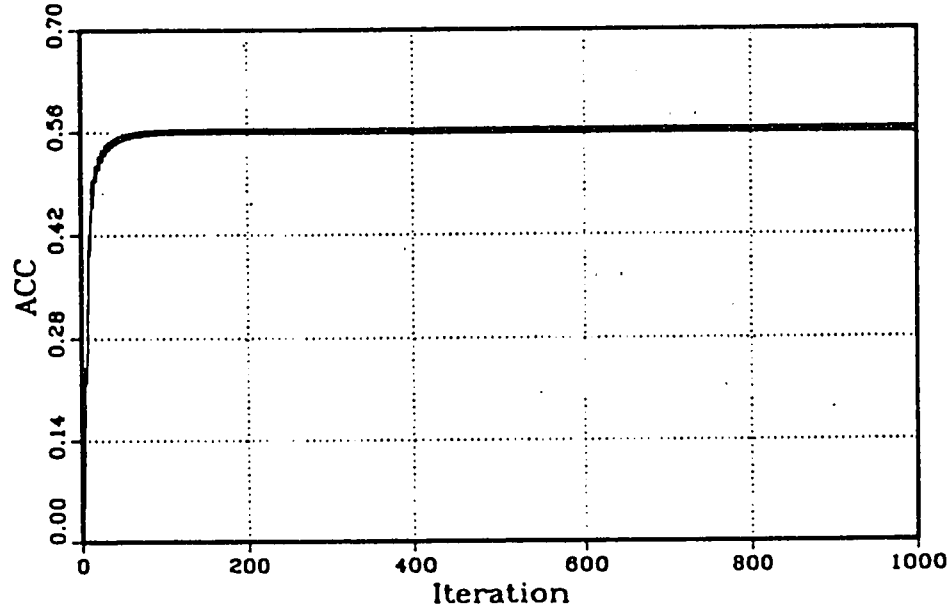

Figure 4.9 ACC of 30/10 single adaptive hybrid with 1000Hz sinusoid as near-end input.

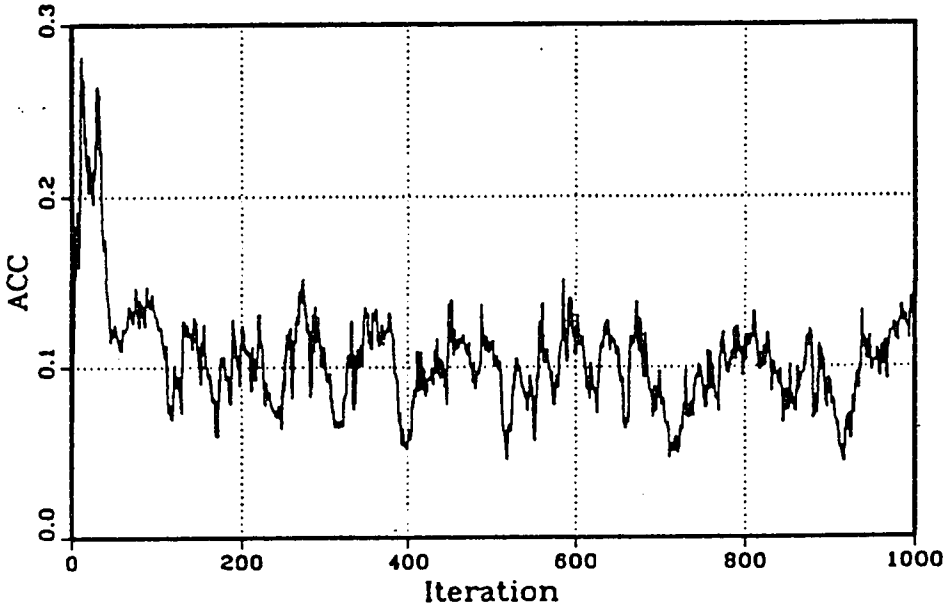

Figure 4.10ACC of 69/16 single adaptive hybrid with white Gaussian noise as far-end input.

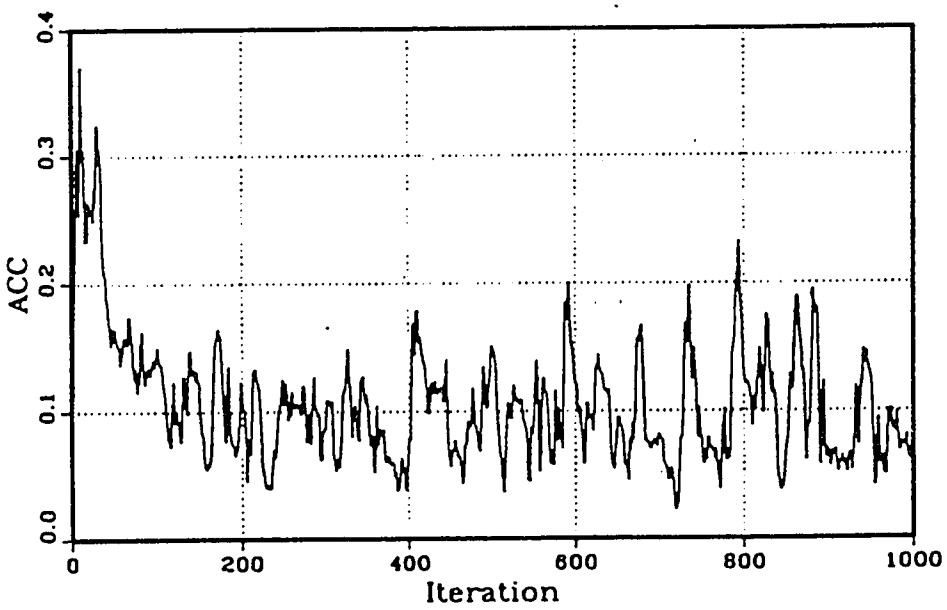

Figure 4.11 ACC of 30/10 single adaptive hybrid with white Gaussian noise as far-end input.

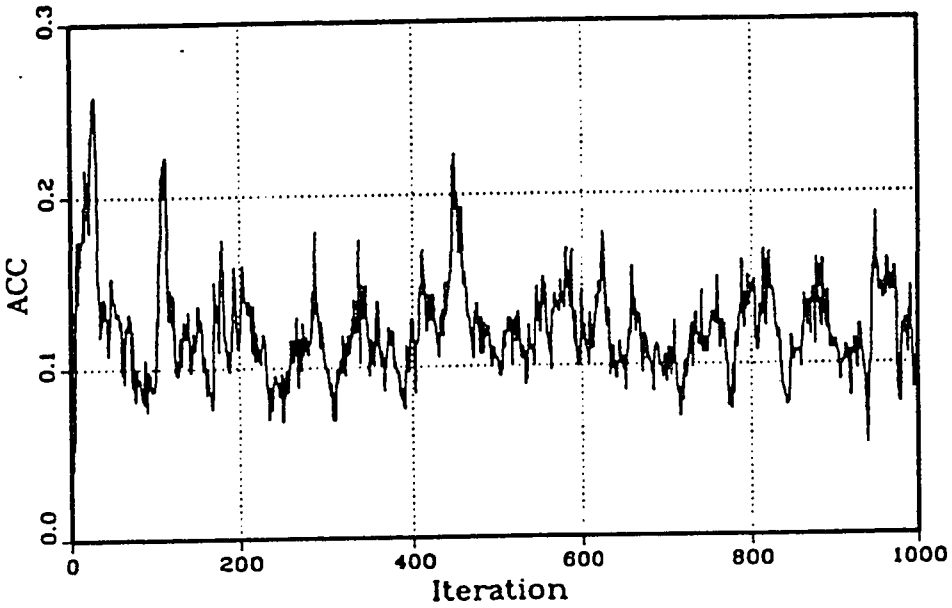

Figure 4.12 ACC of 69/16 single adaptive hybrid with white Gaussian noise as near-end input.

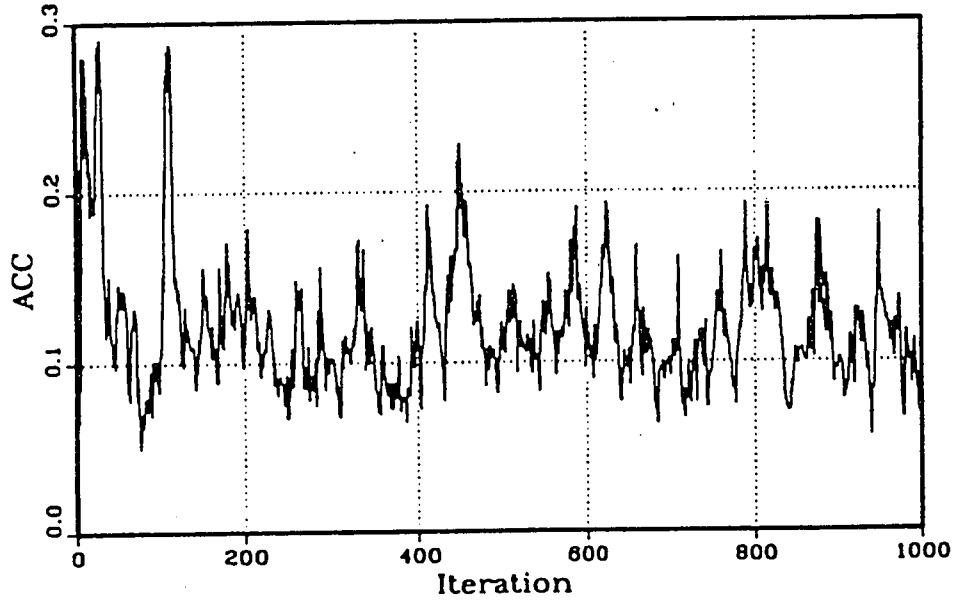

Figure 4.13 ACC of 30/10 single adaptive hybrid with white Gaussian noise as near-end input.

change the nature of signals. Simulation results prove this analysis. In Figs.4.14-4.15, ACCs are calculated for the case of echo path changed 50% after 500 iteration(e.g. all odd number of coefficients are decreased by 50% and all even number of coefficients are increased by 50%, the impulse responses before and after echo path change are provided in Figs.4.16-4.17). Fig.4.14 is obtained for the case of 500 Hz sinusoid injected from the near-end and Fig.4.15 is for far-end white noise case. A little difference can be seen in ACC(Fig.4.15) for white noise case with echo path changed before and after 500 iterations. While for the tone(Fig.4.14) , the difference is so small that it is extremely hard to detect.

4.2.4 Proposed Solution Using ACC to Avoid Bursting

The above simulations illustrated the characteristics of ACC in the parameter drift phase(near-end tone) are unique and obviously different from the normal operation case. This difference can be used as a criterion to easily distinguish whether a tone or white noise is injected. If ACC is found to be larger than 0.4 consecutively for a predetermined number of iterations(e.g., 200 in our simulation), then it is detected that a tone is applied from the near-end and adaptation should be prohibited immediately. But ACC is continuously computed and checked with the criterion. When the input conditions return to "normal", ACC will automatically reflect this change and the weights will be allowed to be adapted again. Of course, with this kind of criterion, we could not distinguish the far-end tone from either near-end white noise as in Figs.4.12-4.13 or far-end white noise as in Figs.4.10-4.11, but none of these conditions will lead the system to burst, so they are allowable conditions and we do not need to identify them individually.

Echo path change is also easily identifiable from the drift case. The algorithm can continue to adapt thus following the variation in the echo path, even cases such as the echo path change occurring at the same time the input is changed from tone to white noise or from white noise to tone. In the first case, echo path change is reflected at the same time adaptation is resumed; in the second one, ACC will be calculated according to

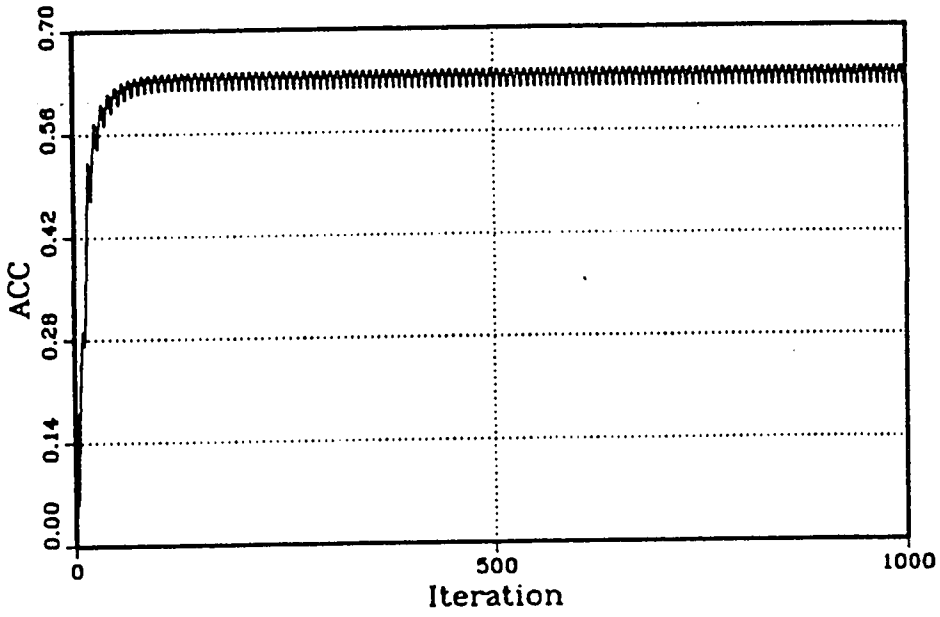

Figure 4.14 ACC of 69/16 single adaptive hybrid with 500 Hz near-end sinusoid and 50% echo path change at 500 iteration.

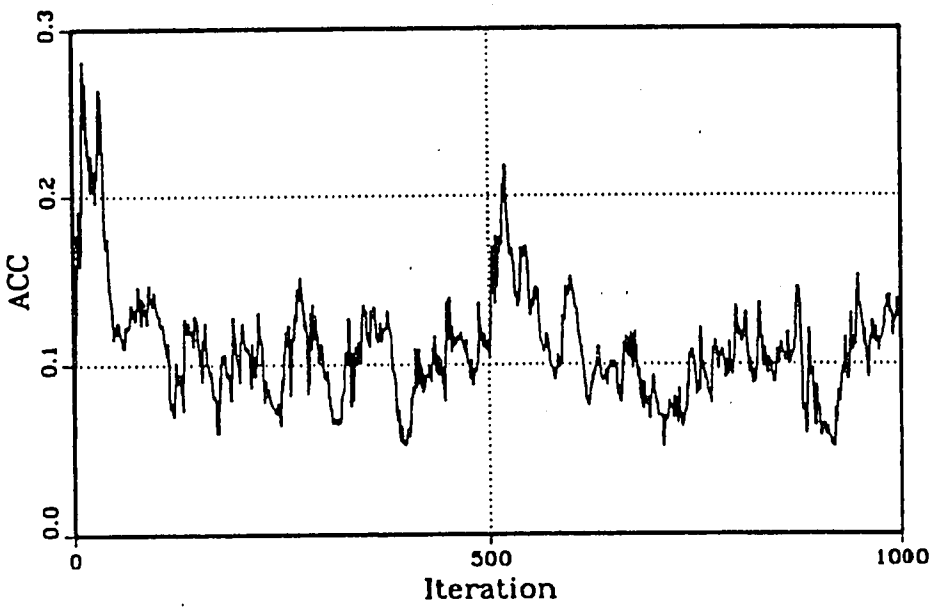

Figure 4.15 ACC of 69/16 single adaptive hybrid with white Gaussian noise as far-end input and 50% echo path change at 500 iteration.

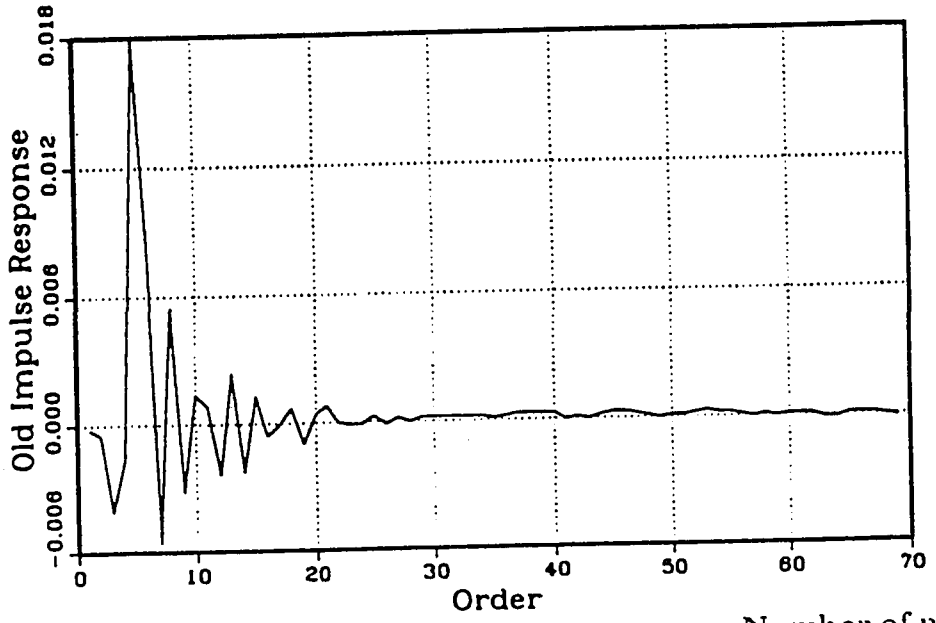

Figure 4.16 Original hybrid impulse response. Number of non-zero taps is 69.

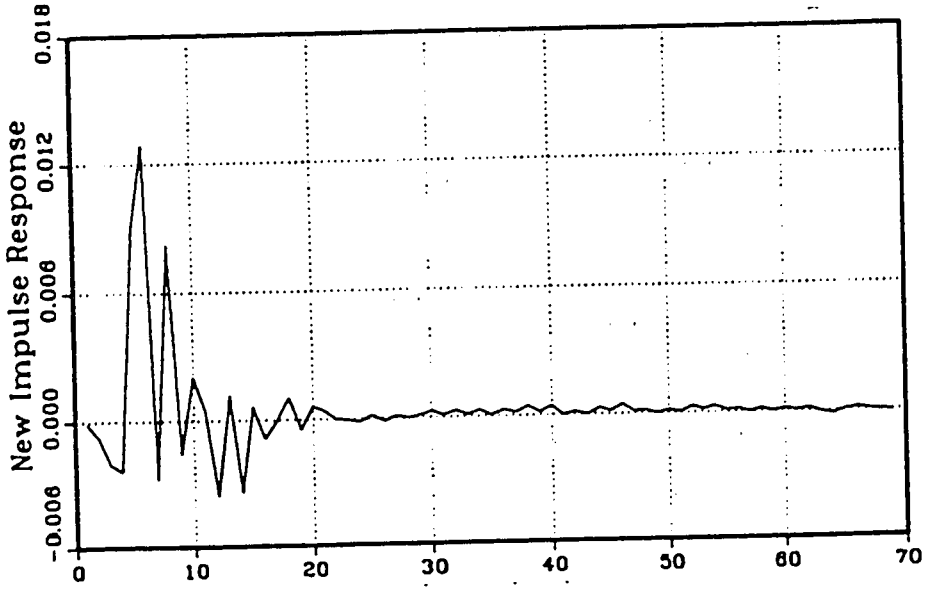

Figure 4.17 Hybrid impulse response after 50% echo path change. Number of non-zero taps is 69.

the new path and checked against the same criterion, if drift case is detected, adaptation will be stopped.

An example is provided to show using ACC as the criterion to detect a near-end tone . A tone(2000 Hz) is first injected from the near-end, after 500 iteration, the tone stops and a white gaussian noise is applied from the far-end, another 500 iteration later, white noise is removed and a tone(1000 Hz) is applied from the near-end again. Curves showing the variation of ACC and one coefficient of the AF, $\hat{h}(6)$, are provided in Figs.4.18-4.19. From Fig.4.19, it is clearly seen after ACC is found to be larger than 0.4 for 200 iterations, weights will be frozen at their current values. When the white noise comes, the weights are automatically allowed to adapt since ACC fails the test. They continue adapting till they converge to their optimum values. e.g., $\hat{h}(6)$ converges to 0.00843(average of the last 100 iterations) which is close to the value of the actual impulse response for the 6th weight 0.0086. When the near-end tone is applied again, ACC will become larger and flat which will be detected by the ACC criterion and the adaptation is then frozen.

Another example given that a 500 Hz near-end tone applied to the 69/16 single adaptive system is illustrated to verify the effectiveness of ACC approach. It is noticed in Fig.4.20 after 16000 iterations, bursting will happen if no restriction is applied to control the drifting of coefficients. However, applying the proposed approach, bursting does not happen as shown in Fig.4.21. We use the criterion that after consecutively 200 iterations of $ACC > 0.4$, the weights will be frozen. While ACC continues to be calculated based on the correlation between the input vector $X(k)$ and the error $e(k)$. Since $X(k)$ changes with time, ACC is not a constant.

Although the usage of ACC is quite useful for preventing bursting, the associated complexity in calculating ACC results in a significant increase in the system's overall complexity. For every iteration, $P_e(k), P_i(k)$, and $P_{ei}(k)$ have to be calculated. The amount of computation of P_{ei} and P_i depends on the number of weights of the adaptive

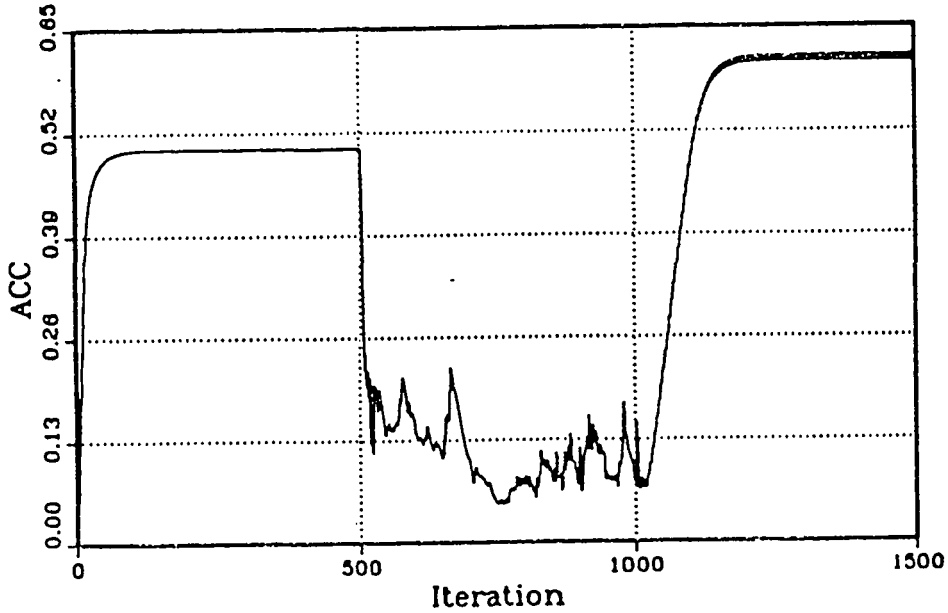

Figure 4.18 ACC of 69/16 single adaptive hybrid with 2000 Hz sinusoid at the near-end first, white Gaussian noise at the far-end from 500 iteration, and 1000 Hz sinusoid again at the near-end from 1000 iteration .

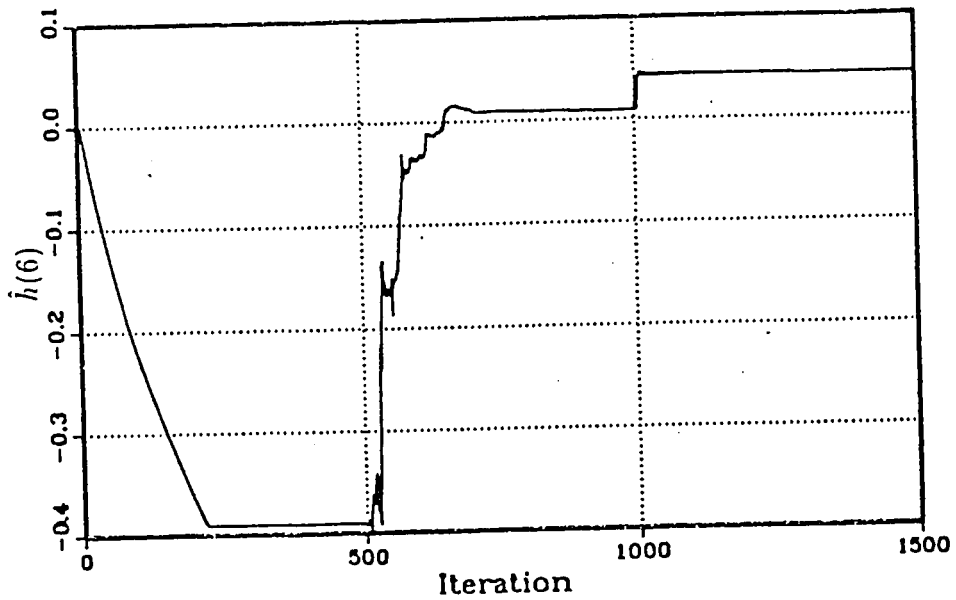

Figure 4.19 Variation of the 6th weight of the adaptive filter with the same conditions as in Figure 4.18.

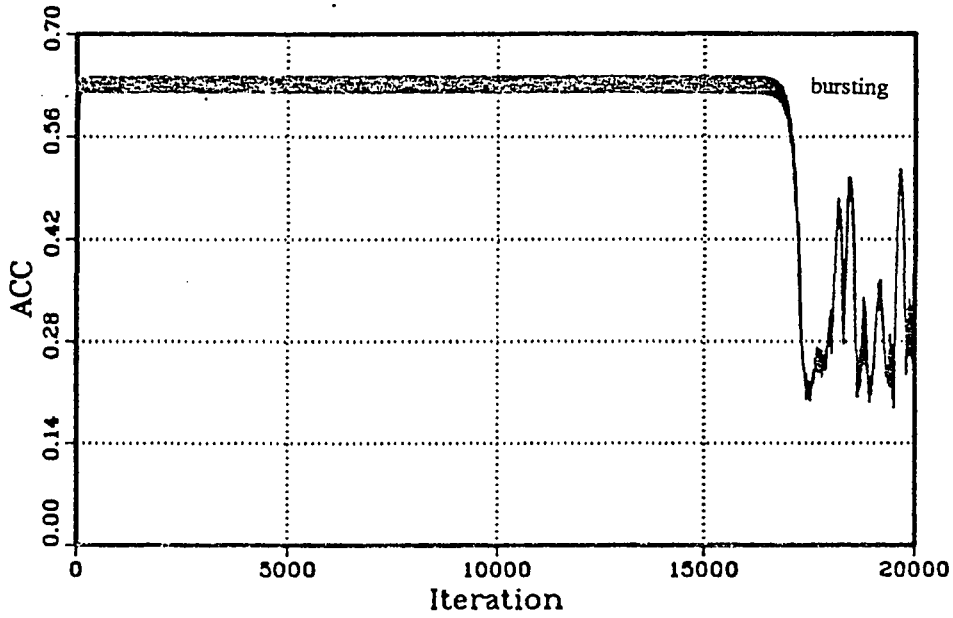

Figure 4.20 ACC of 69/16 single adptive hybrid with 500 Hz sinusoid at the near-end with bursting. $\mu = 1/10$.

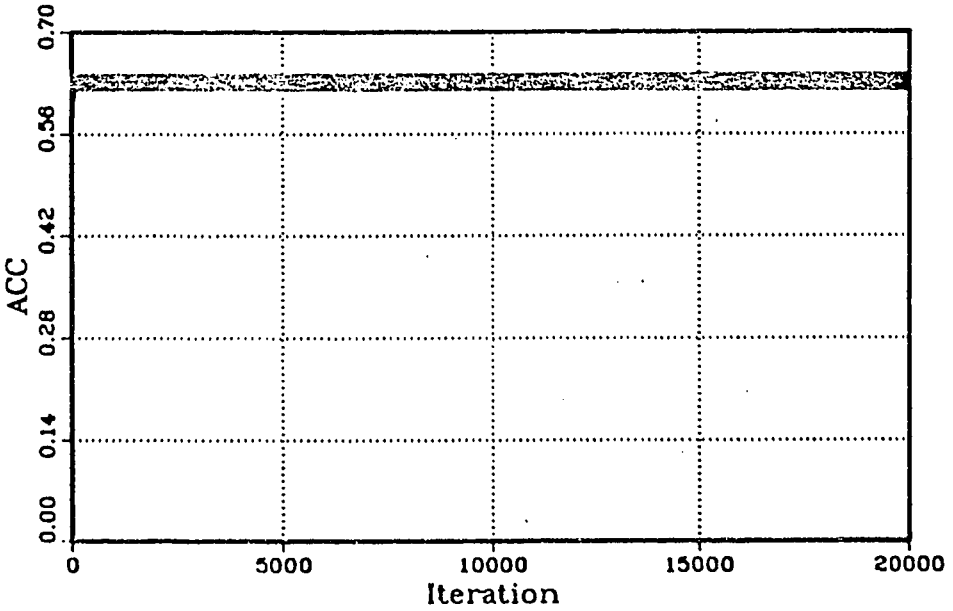

Figure 4.21 ACC criterion is applied to the same conditions as Figure 4.20 to avert bursting.

filter. The more weights chosen, the more computation involved. The total amount of multiplication is 6N+3, addition is 3N, and division is N+1 for every iteration. This can be very significant for large N. This is also a major drawback for the originally intended application of ACC as double talk detector[46]. Thus, simplifying the computional requirements while giving the same performance is the main objective of the next step. In the next section, we will propose a simplification to this algorithm that allows us to stop bursting while requiring significantly less computation.

4.3 Direct Calculation of the Cross-Correlation

P_{ei} is the parameter which relates $x(k-i+1)$ and $e(k)$. It is the most important component of ACC and its normalization relative to the power $P_e(k)$ and $P_i(k)$ leads to the normalized coefficient $C_i(k)$. The normalization procedure makes the values of ACC indepedent of the magnitude of the input signal. e.g. Variation of ACC for unit variance white noise will be exactly the same as that of the white noise with a different variance .

As a result of the complexity of the calculation for ACC in each iteration, the logical question becomes whether it is possible to use only P_{ei} as the criterion because it calculates the cross correlation between $x(k-i+1)$ and $e(k)$, though not normalized. Furthermore, in Eq.(4.3), the recursive algorithm computing P_{ei} for different i is the same except for using a different $x(k-i+1)$. Thus, it is expected that basic features of $P_{e1}(k)$ and $P_{ei}(k)(i \neq 1)$ will not be very different. If that is true, then using one or two specific P_{ei} may provide us with the same information. Based on this analysis, the following part will study the special features of P_{ei}.

4.3.1 Characteristic of P_{ei} and its Usage for Bursting Control

First, we will consider P_{e1}, i.e. the correlation between the current $x(k)$ and $e(k)$. For the system in Fig.4.1, if a tone is injected from the far-end, P_{e1} will eventually decay to

zero and fluctuate with a very small magnitude(Figs.4.22-4.23). A separate window on the graph shows $P_{e1}(k)$ after convergence on a different scale to see the details. However, if the tone is inserted from the near-end, for most of the frequencies, $P_{e1}(k)$ will always keep the same sign and converge to the zero line, i.e., its magnitude continually decreases. This can be seen in Figs.4.24-4.25. 500 Hz and 3000 Hz sinusoids are inserted from the near-end, $P_{e1}(k)$ for the first case is always positive and $P_{e1}(k)$ for the second one is always negative. Through simulation, it is found the crossover point from positive to negative happens when the tone frequency is around 2000 Hz (approximate 1970-2030Hz) . Figs.4.26-27 provide the ACC when 1990 Hz and 2010 Hz sinusoidal signals are applied to the near-end respectively. The fluctuation of ACC around zero line is clearly observed.

When the input is white noise, applied at either the far-end or the near-end, $P_{e1}(k)$ will always be fluctuating around zero(Figs.4.28-29). This will make it difficult to find a criterion to judge whether a tone or white noise is injected, since $P_{e1}(k)$'s keeping the same sign can not be a feature of near-end tones due to the exception around 2000 Hz. Thus introducing the calculation of another parameter $P_{ei}(k)(i \neq 1)$ is considered. Suppose $i = N$ is used, the characteristic of $P_{eN}(k)$ will be similar to that of $P_{e1}(k)$, the only difference is the frequency at which $P_{eN}(k)$ crosses the zero line will be different from that of $P_{e1}(k)$.

With the above analysis, a criterion using P_{ei} to detect bursting is proposed: $P_{ei}(k)$ is computed for two values of i. Whenever at least one of the two $P_{ei}(k)$s keeps the same sign for a predermined number of iterations, it is determined that there is a tone inserted from the near-end, then adaptation should be stopped . Since the two P_{ei}s are regularly calculated and checked, when normal conditions return, adaptation is resumed. As a far-end tone or near-end white noise will make the $P_{ei}(k)$ fluctuate around zero, the detection algorithm may assume the presence of far-end white noise and continue to do the adaptation. This is acceptable since neither of these two cases will lead to bursting.

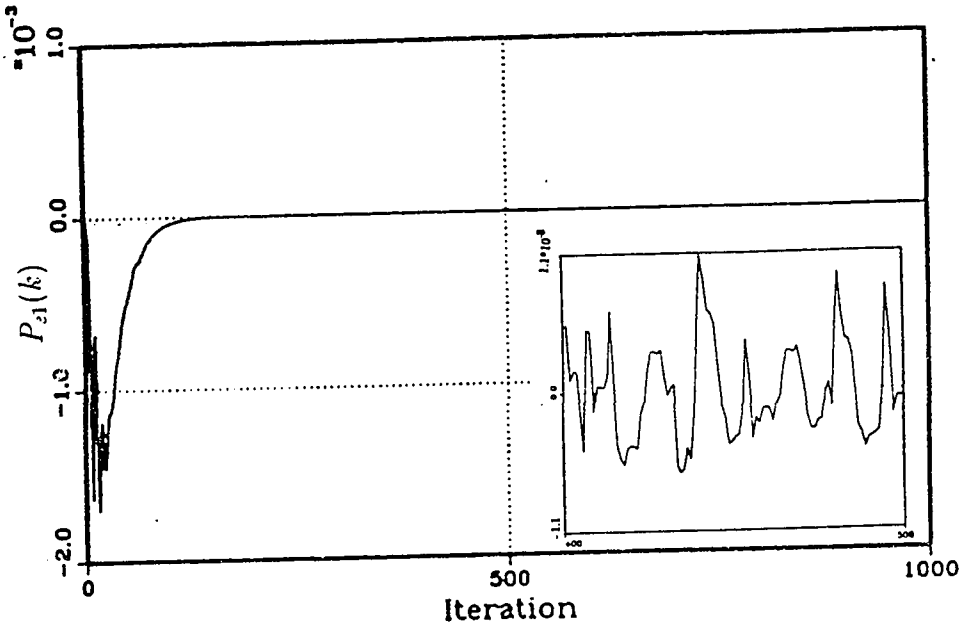

Figure 4.22 P_{e1} of 69/16 single adaptive hybrid with 500 Hz sinusoid at the far-end.

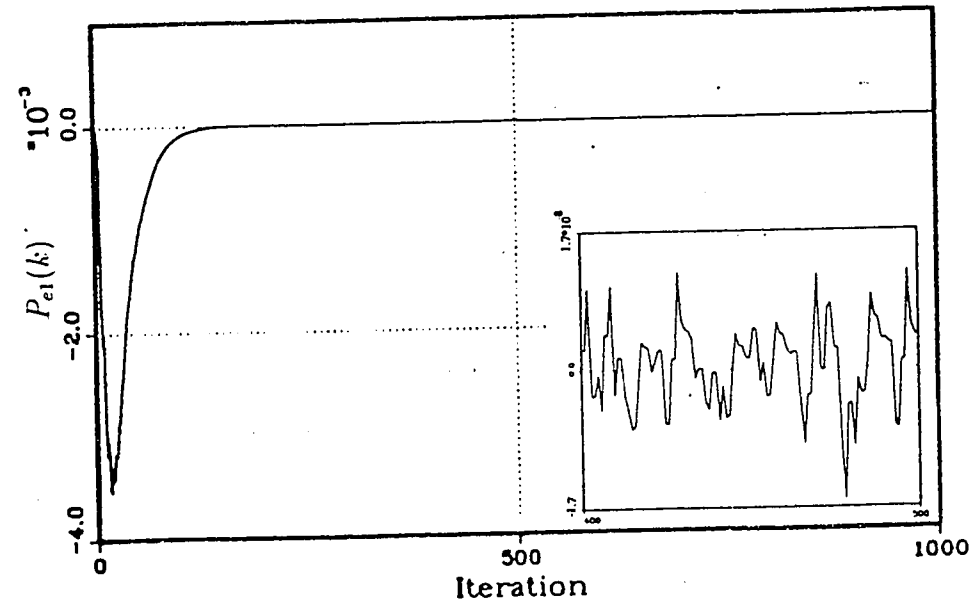

Figure 4.23 P_{e1} of 69/16 single adaptive hybrid with 1000 Hz sinusoid at the far-end.

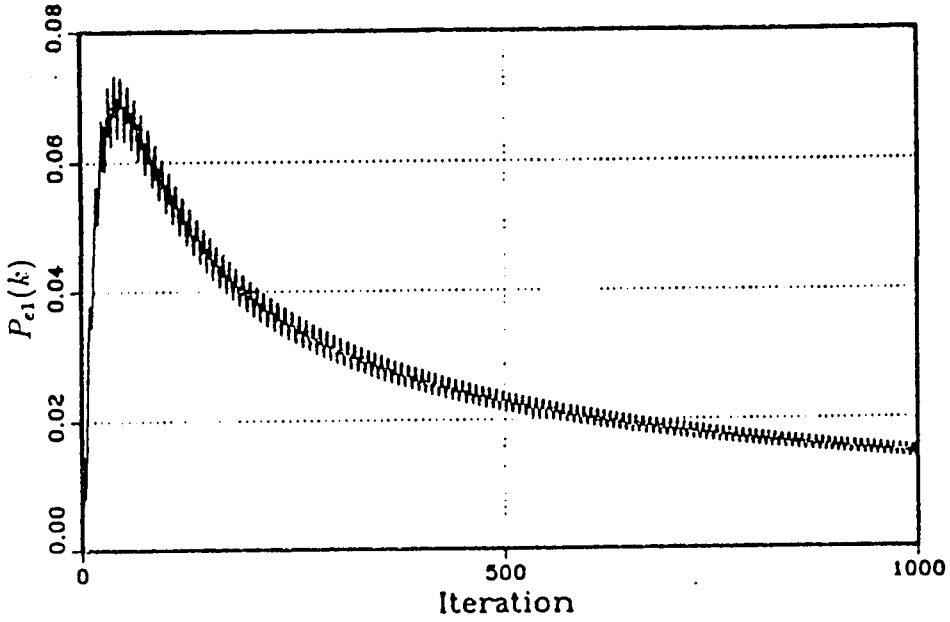

Figure 4.24 P_{e1} of 69/16 single adaptive hybrid with 500 Hz sinusoid at the near-end.

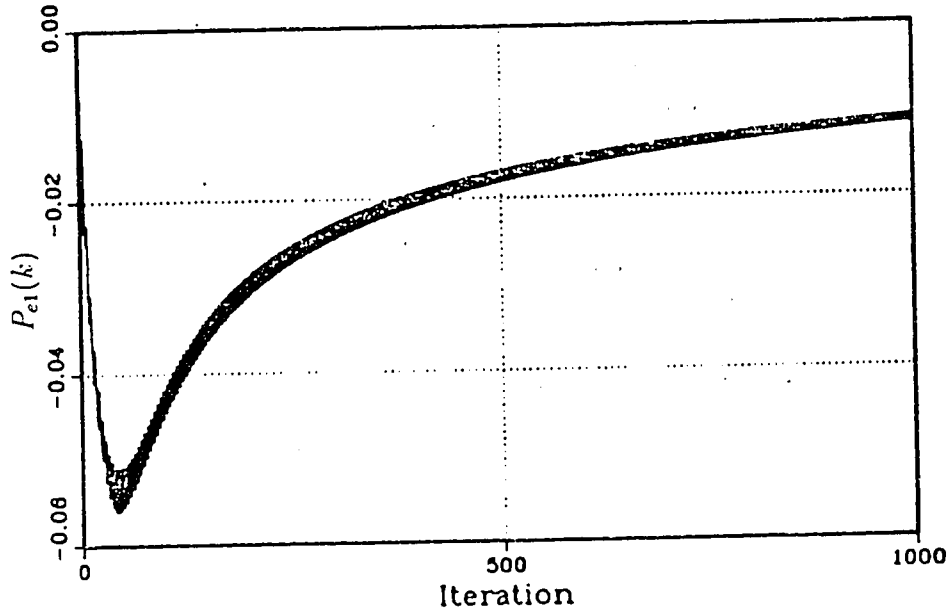

Figure 4.25 P_{e1} of 69/16 single adaptive hybrid with 3000 Hz sinusoid at the near-end.

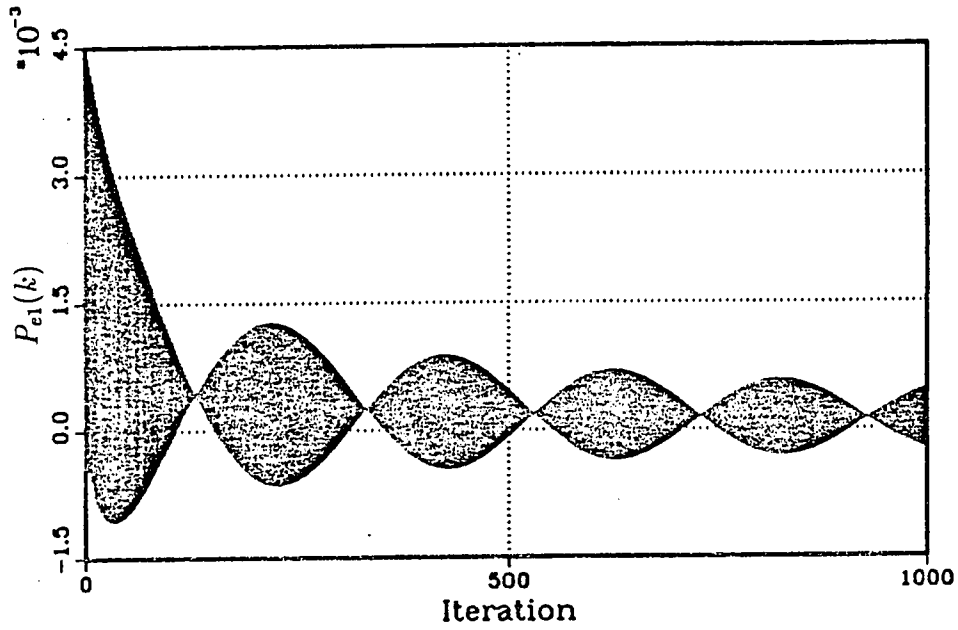

Figure 4.26 P_{e1} of 69/16 single adaptive hybrid with 1990 Hz sinusoid at the near-end.

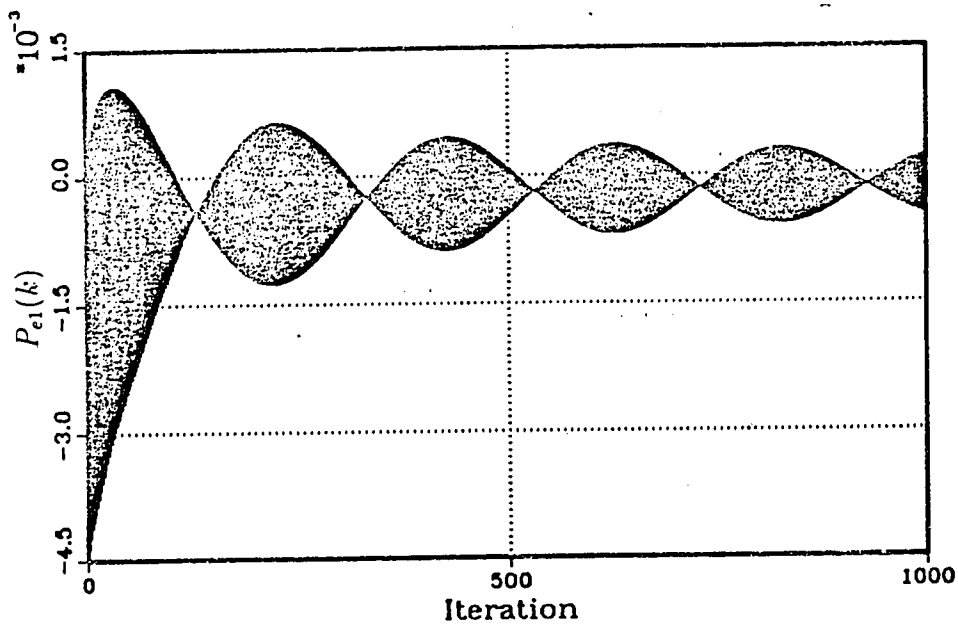

Figure 4.27 P_{e1} of 69/16 single adaptive hybrid with 2010 Hz sinusoid at the near-end.

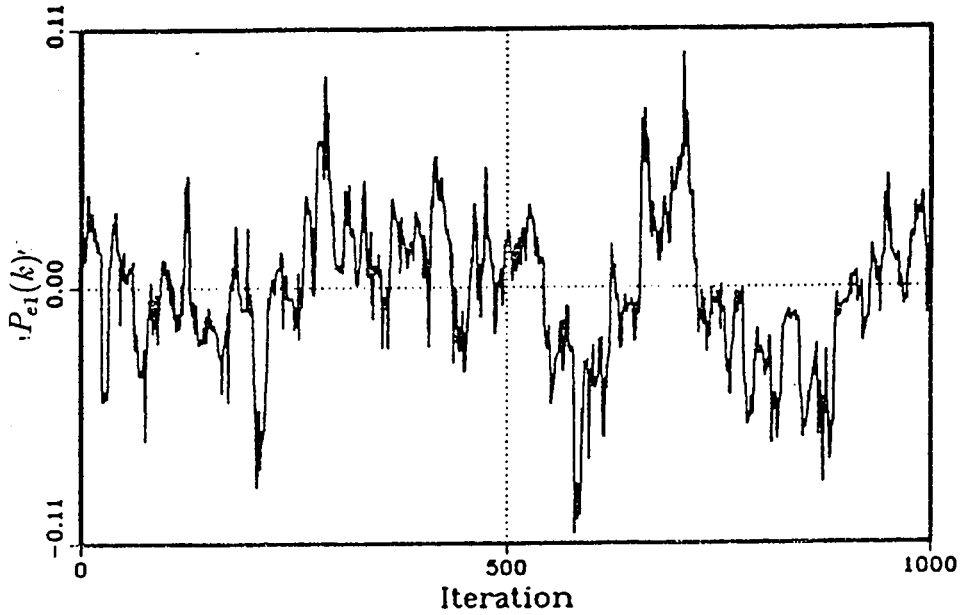

Figure 4.28 P_{e1} of 69/16 single adaptive hybrid with white Gaussian noise at the near-end.

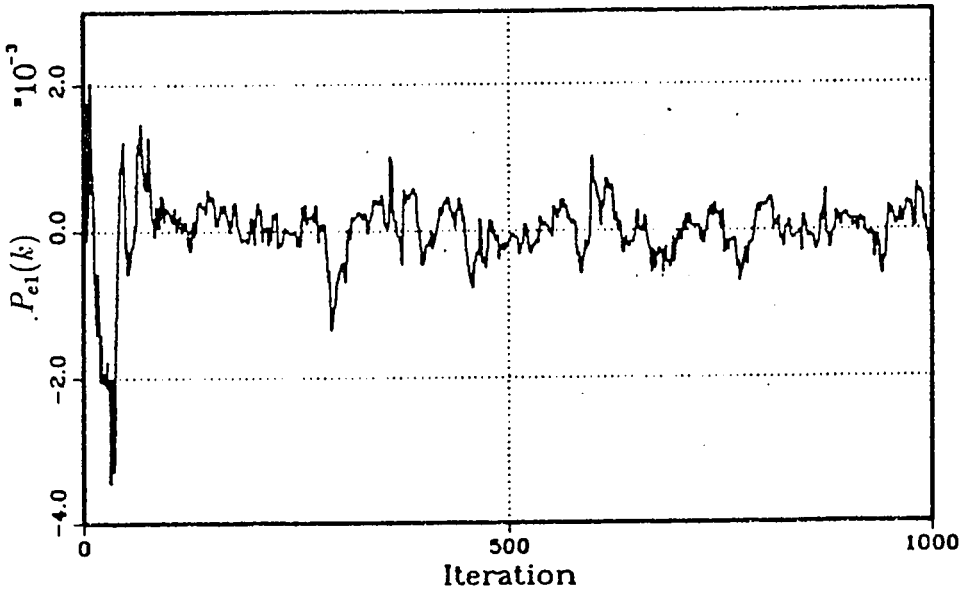

Figure 4.29 P_{e1} of 69/16 single adaptive hybrid with white Gaussian noise at the far-end.

If the processor used in echo canceller could not detect the sign change for the case far-end tone due to limited accuracy, the adaptation will continue but will not lead to bursting. The selection of the P_{ei} terms to be calculated has to be done carefully. Extensive simulations were carried out to ensure that for the selected pair, there will always one P_{ei} that will remain the same sign. Table 4.1 summarizes these results. Based on Table 4.1, it is suggested to choose one even order and the other of odd order. It can be seen from the Table 4.1 if $P_{e1}(k)$ and $P_{e15}(k)$ are used for analysis, there will be some confusion for the frequencies around 2000 Hz because both of them are changing signs . However, the combination of $P_{e2}(k)$ and $P_{e15}(k)$ will work well. This was also verified for other combinations.

Figs.4.30-4.31 illustrate using $P_{e1}(k)$ and $P_{e16}(k)$ as the couple with the criterion mentioned above to avoid bursting. The input conditions are exactly the same as those used for Fig.4.18 and 4.19. It can be seen during the tone input period, $P_{e1}(k)$ will cross the zero line(a detailed description of $P_{e1}(k)$ before 400 iteration is provided in the window), fortunately, $P_{e16}(k)$ still keeps the same sign. When this situation stays unchanged for 200 iterations, the weights are frozen, and bursting is prohibited. When white noise comes or later another tone is applied, the performance of $P_{e1}(k)$ and $P_{e16}(k)$ are just what we expect. Figs.4.32-4.33 show the variations of the 5th and 6th weights of the AF. The simplified method proposed here enables us to detect and stop bursting before it happens in the same way as the averaged method using ACC (section 4.2) did. However, there exist differences in details. Comparing Fig.4.19 with Fig.4.32, it is noticed for the first tone input part, the values at which $\hat{h}(6)$ is frozen are different. This is reasonable since the instantaneous value after consecutive 200 iterations of $ACC > 0.4$ is not identical to that after consecutive 200 iterations of $P_{e1}(k)$ or $P_{e16}(k)$ keeping the same sign. This frozen value will be the initial one for the white noise input part. Although this far-end white noise will allow the coefficients to converge to the same averaged optimum values,

freq.(Hz)	Pe1	Pe2	Pe3	Pe4	Pe5	Pe6	Pe7	Pe8	Pe9	Pe10	Pe11	Pe12	Pe13	Pe14	Pe15	Pe16
300	+	+	+	+	+	+	alter	-	-	-	-	-	-	-	-	-
500	+	+	+	alter	-	-	-	-	-	-	-	alter	+	+	+	+
700	+	+	alter	-	-	-	-	-	+	+	+	+	+	+	alter	+
1000	+	alter	-	-	-	alter	+	+	+	alter	-	-	-	alter	+	-
1200	+	-	-	-	alter	+	+	+	-	-	-	+	+	+	alter	+
1500	+	-	-	alter	+	+	-	-	-	+	+	alter	-	-	+	+
1950	+	-	-	+	+	-	-	+	+	-	-	+	+	-	-	+
2000	alter	-	alter	+	alter	-	alter	+	alter	-	alter	+	alter	-	alter	+
2050	-	-	+	+	-	-	+	+	-	-	+	+	-	-	+	+
2100	-	-	+	+	-	-	+	+	-	-	+	+	-	-	+	+
2500	-	-	+	alter	-	+	+	-	+	+	-	alter	+	-	-	+
3000	-	alter	+	-	+	alter	-	+	-	alter	+	-	+	alter	-	+

Table 4.1 Behaviors of P_{ei} for different frequencies of near-end input.

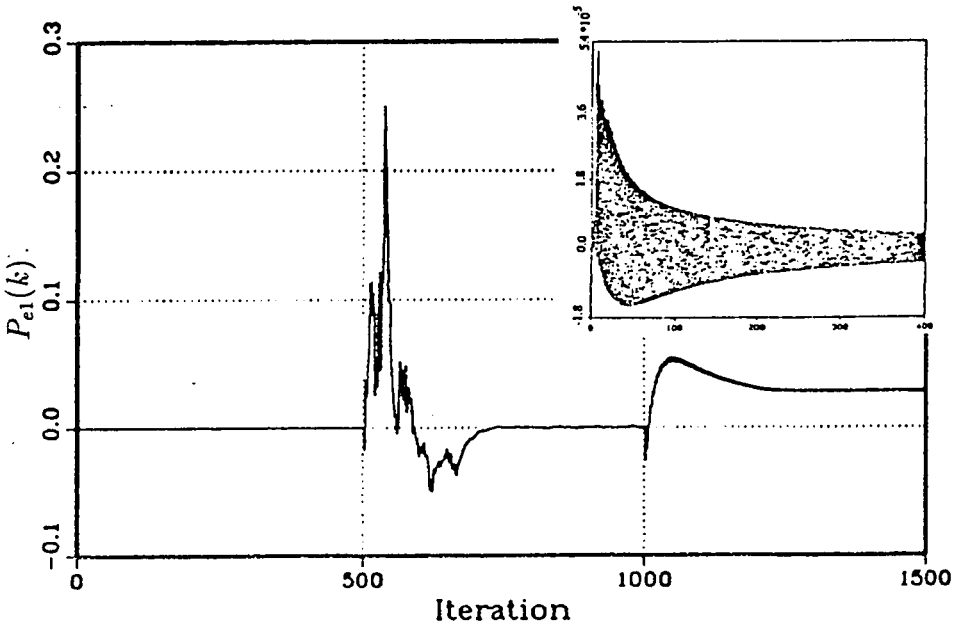

Figure 4.30 P_{e1} of 69/16 single adaptive hybrid with 2000 Hz sinusoid at the near-end first, white Gaussian noise at the far-end from 500 iteration, and 1000 Hz sinusoid again at the near-end from 1000 iteration .

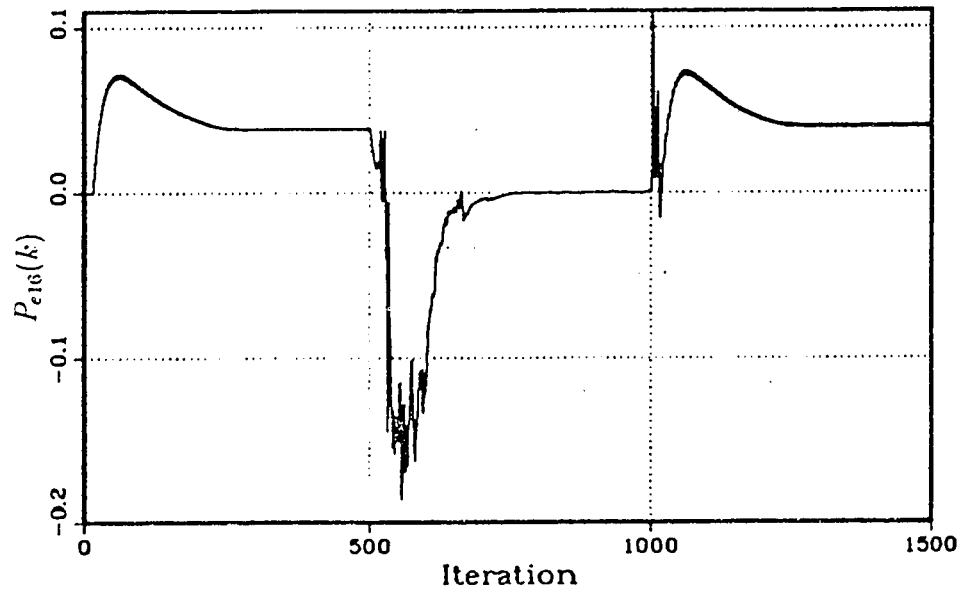

Figure 4.31 P_{e16} of 69/16 single adaptive hybrid with the same conditions as above.

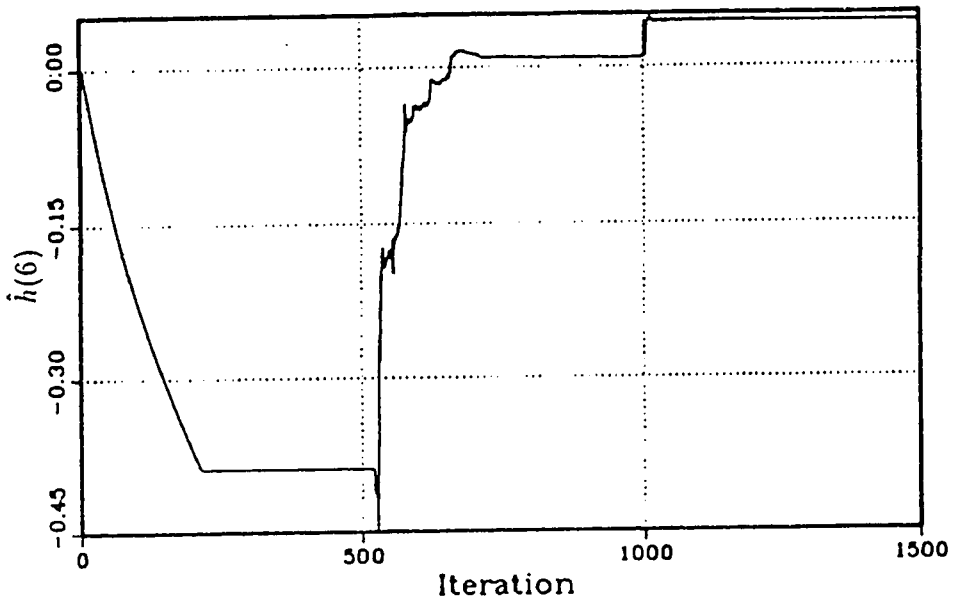

Figure 4.32 Variation of the 6th weight of the adaptive filter with the same conditions as in Figure 4.30.

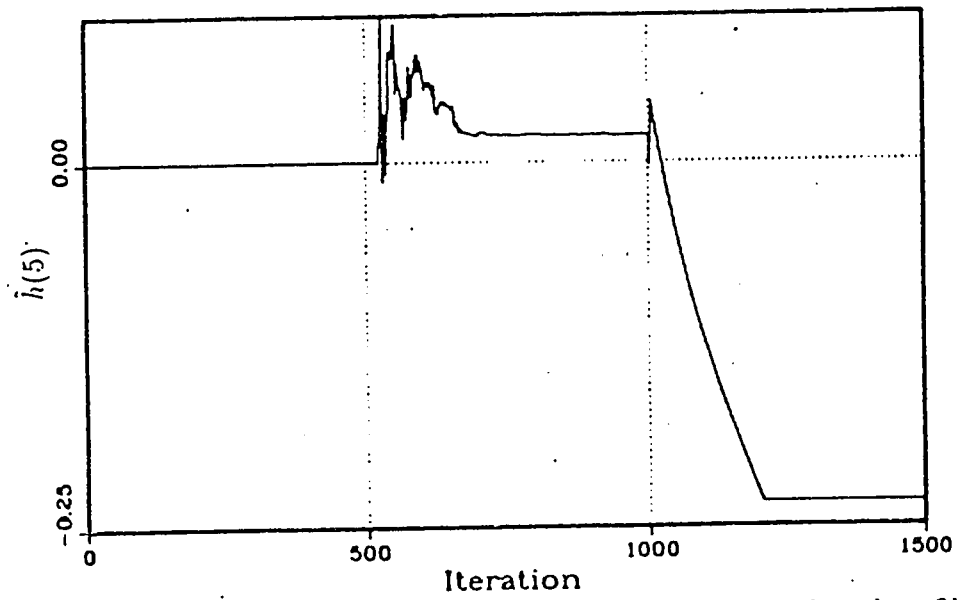

Figure 4.33 Variation of the 5th weight of the adaptive filter with the same conditions as in Figure 4.32.

the instantaneous values for the $1000th$ iteration will be a little different. It is recorded that the instantaneous value for $1000th$ iteration in Fig.4.19 is 8.4802695e-3, and in Fig.4.32, the value is 8.4802667e-3. These values will be the initial values for the next single-frequency tone. As these two are so close, the final value the weights frozen at will be very close.

Another example given earlier for testing of the validity of ACC is used again here. In Fig.4.34, $P_{e1(k)}$ is plotted to show how the near-end tone evokes bursting. For Fig.4.35, the P_{ei} approach is applied and bursting is averted.

4.4 Conclusion

In this Chapter, we proposed two correlation-based approaches to enable us to detect and stop bursting before it happens. The first approach uses the averaged cross correlation (ACC) while the second uses cross correlation of the error with two of the input vector components. Both are successful and feasible for practical hybrids. However, using the second approach based on evaluating only two cross correlation P_{ei}s will save a lot of computation. For every iteration, ACC approach will require 6N+3 of multiplications, 3N of additions, and N+1 of divisions. While P_{ei} method only needs to calculate two $P_{ei}(k)$s which will include 4 multiplications and 2 additions. Thus, P_{ei} approach is quite significantly less complex.

Although ACC is considered complicated compared with P_{ei}, it is still superior to all other methods dicussed in Chapter 2 and 3. It was also suggested for use as a double talk detector[46]. For the two approaches proposed in this Chapter, two adavantages are worth highlighting. Firstly, they are practical. They do not require restricting the order of the hybrid to very low values, like leaky LMS method or pole position method, also they do not need the preknowledge of the range of the echo path coefficients to set a criterion or the exact order to derive an expression of the characteristic equation for the

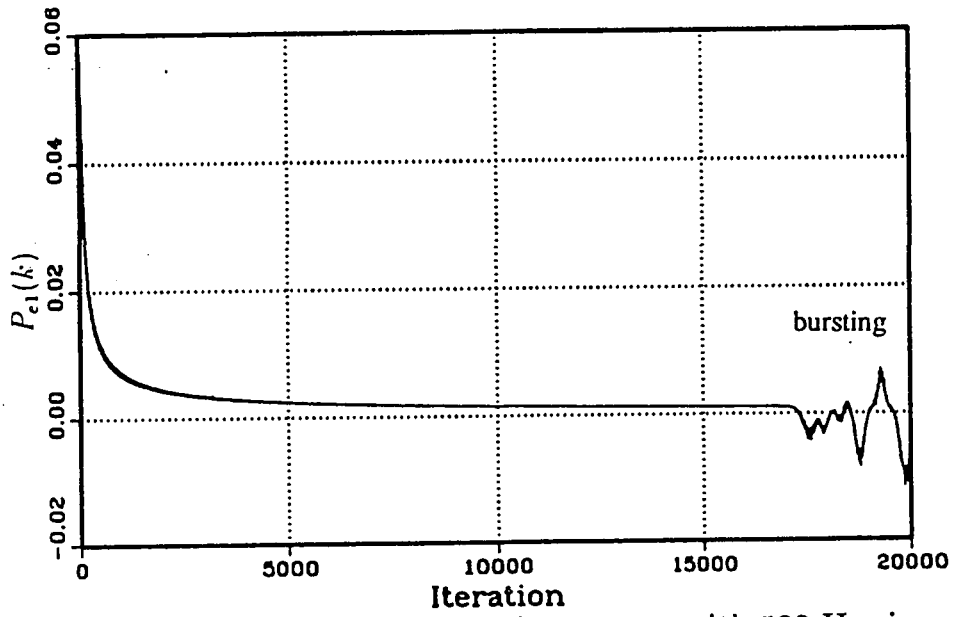

Figure 4.34 P_{e1} of 69/16 single adptive system with 500 Hz sinusoid at the near-end with bursting. $\mu = 1/10$.

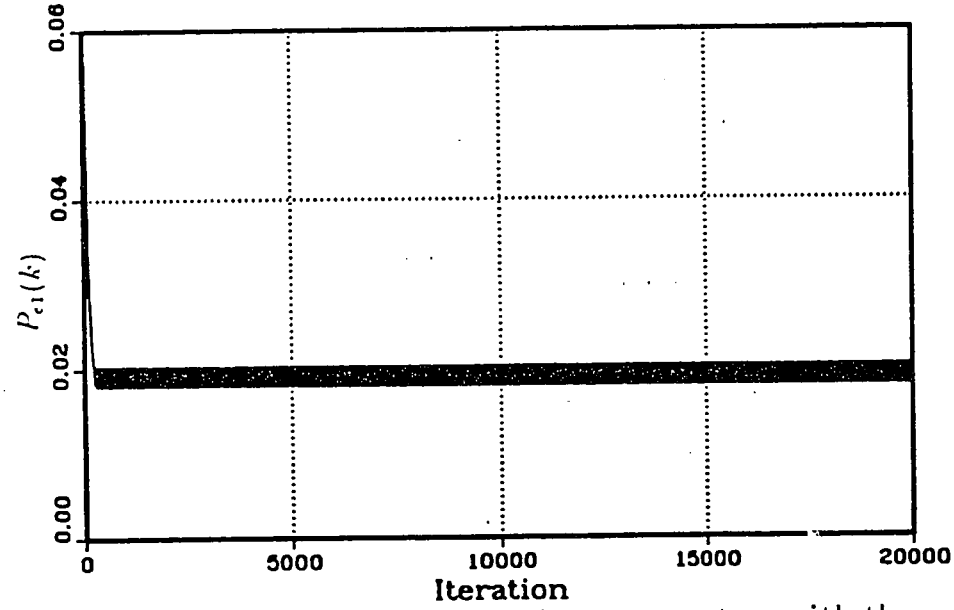

Figure 4.35 P_{e1} criterion applied to the same system with the same input condition as Figure 4.34.

system. Secondly, they are robust. The criterion will not be affected by the order of the adaptive hybrid , by the input conditions or by the echo path change, while the methods such as leaky LMS whose derivations need the exact information of echo path model are more restricted. In this sense, ACC and P_{ei} are quite effective and practical.

Finally, recall that all of the above discussions considered the case of single adaptive hybrid case with a scalar feedback at the far-end. It has not been tested the case of far-end hybrid with AF since the presence of the far-end adaptive filter results in minimum feedback; effectively opening up the feedback path. In this case, even if bursting happens, it is of extremely low magnitude that it can be effectively ignored. Fig.4.36 shows such a case.

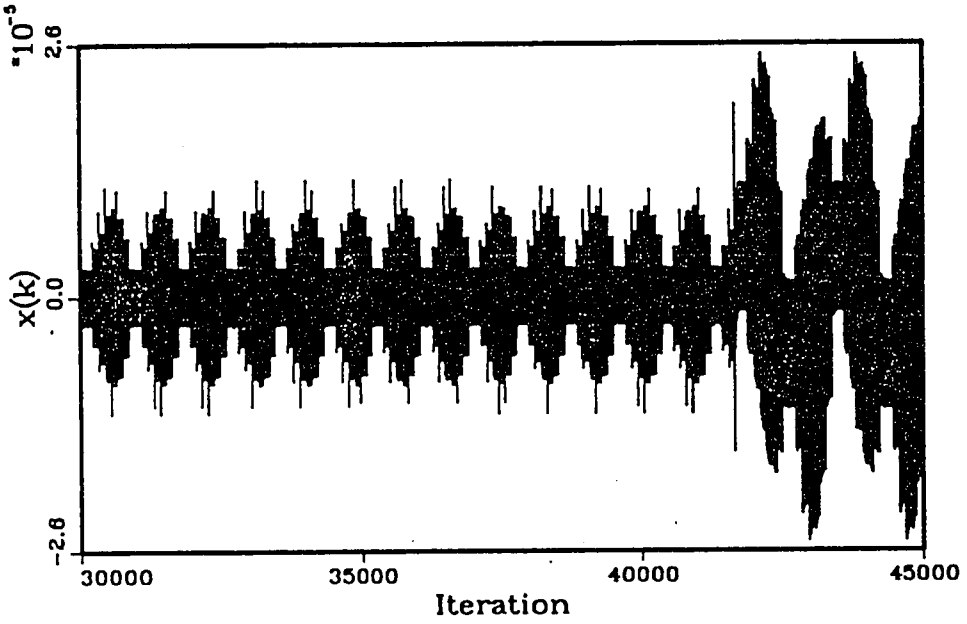

Figure 4.36 Bursting in the double adptive hybrid(69/16) system with 500 Hz sinusoid at the near-end. $\mu = 1/10$.

To conclude, we have proposed two methods to detect and stop bursting and illustrated their performance through extensive simulations. These algorithms work well even when the echo path suddenly changes. However, they are not intended to detect double talk. One would have to use a regular double talk detector as well. It is worth noting that even though the ACC was proposed in [46] as a way to detect double talk as opposed to echo path change, we have not been able to verify its use for such an objective. Only minor

differences exist between the two and they are very dependant on the input. Fig.4.37 provides what the ACC looks like during double talk. First white noise with variance of one is inserted from far-end, after 500 iteration, another white noise with the same variance is applied from near-end. It can be seen there is not much difference for ACC between double talk and single talk cases. Though the ACC approach does not seem to work well as a DTD as originally intented in [46], it has provided the foundation for this current approach to stop bursting on a practical hybrid.

However, P_{ei} seems to have the ability to detect double talk as the magnitude of P_{ei} for double talk is obviously larger than that of the single talk case(Fig.4.38). Though this difference is easily observed by eye, it is not easy to choose some value as threshold to separate these two cases. Since the magnitude of P_{ei} might change according to the magnitude of the input. Thus it is suggested to continue to use a conventional DTD to detect double talk.

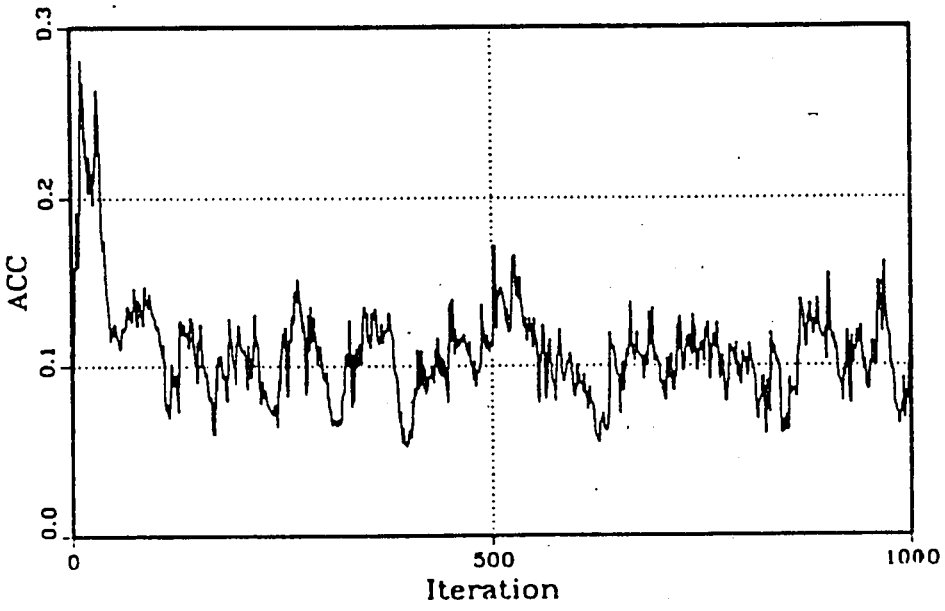

Figure 4.37 ACC of 69/16 single adaptive hybrid with white gaussian noise from the far-end first and double talk beginning at 500 iteration. $\mu = 1/32$.

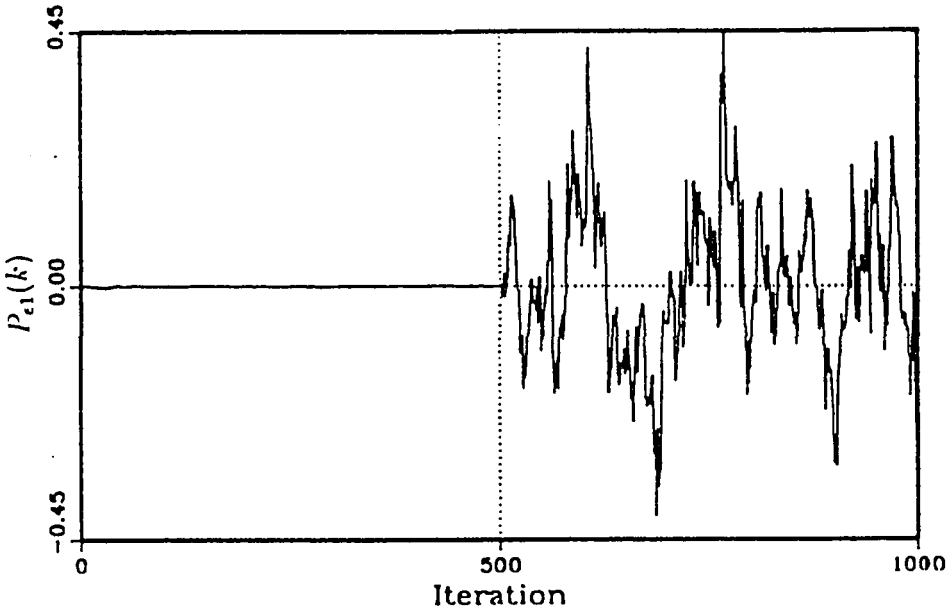

Figure 4.38 P_{e1} of 69/16 single adaptive hybrid with white Gaussian noise from the far-end first and double talk beginning at 500 iteration.

Chapter 5

Conclusion

This thesis has presented several effective and simple approaches to avoid bursting in adaptive hybrid setups. These methods provide different levels of advantages over the current available solutions mentioned in Chapter 2. In Chapter 3, a new approach, using the combination of the leaky LMS and a pole position method to choose the proper leakage factor necessary to avoid bursting, proved to be very effective. Though it is still only applicable to low-order hybrid cases, it already extended the work of [30] to a relatively higher order. The drawback of this method is that a general expression for the boundary of separation of bursting and non-bursting regions, is not available for arbitrary orders. Thus, it is difficult to apply to realistic hybrids. This is the same drawback as for the new double-talk detector suggested in [38]. Generally speaking, none of the published papers discussing bursting control provides a solution to cases when the adaptive filter has more than one coefficient. However, some commercial products with double adaptive filters in parallel can avoid bursting, by employing an extra signal correlator to eliminate the possibility of bursting. However, this approach has double the complexity of the regular system in addition to an unspecified complexity for the signal correlator.

First, approaches based on restricting the dynamic range of the coefficients for the adaptive filter are proposed and verified. They are simple, effective, and superior to available solutions, since they can be used for any combination of hybrid/EC cases. Their drawback is that they require some knowledge of the echo path. However, their require-

ment for knowledge of the echo path is still less crucial than that required for the leaky LMS approach or for the new double-talk detector. The latter approaches need to know the exact order of the echo path and the range of the parameters of the echo path, which is usually not available. However, our approaches only require some basic knowledge of a loose range of possible values for the weights or energy in the weights, which is not as strict as the previous requirements.

Considering these drawbacks, in chapter 4 , we proposed two more practical and effective approaches based on the cross-correlation between the input and the error of the echo canceller to detect and stop bursting. These approaches are the best among all methods suggested and reviewed in this thesis. They both achieve the objective of stopping bursting with different levels of complexity . Compared with the approach with double adaptive filters[16][17][18], the advantage of the simplified crosscorrelation approach is that it significantly reduces the complexity of the hardware . Though, we still need to employ a conventional DTD to detect double talk, this DTD is also necessary in the above products.

The effectiveness of the simplified approach is verified by computer simulation. The next step is to verify the performance on a real time system for a variety of practical hybrids.

In this work, we investigated approaches to control bursting in the single adaptive hybrid system. Such a system is an accurate reflection of practical cases. However, there are cases where the system has double adaptive hybrids. We need to verify the performance of the proposed algorithms for this double hybrid set up.

Appendix A

LMS Solution for Far-end Input with White Noise and Sinusoid

To illustrate the theory of LMS used for the echo cancellation problem, Fig.A.1 is provided here. It is known that the single far-end talker situation is the best configuration for trainning the EC on the near-end. As the near-end is silent, the leaked signal $e(k)$ only contains components of the far-end input, thus ,the echo canceller can make a good estimate of the leaked signal based on the far-end signal so that the squared error converges to a small value.

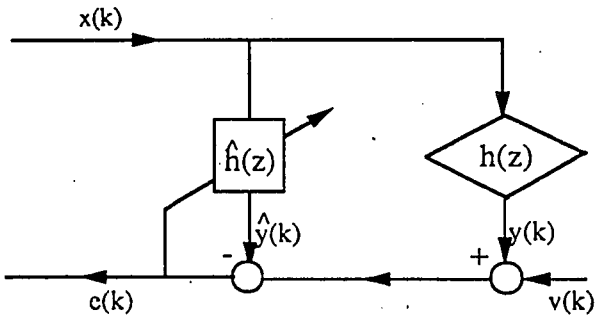

Figure A.1: Model for Single Adaptive Hybrid

Wiener filter theory is based on minimizing the mean-squared error to make the "estimate" as close as possible to the desired one in the MSE sense. It is generally applied in echo cancellation problem.

Wiener filter theory states that the optimum set of tap-weight vector $\mathbf{h_0}$ is given by

the solution to the normal equation

$$\mathbf{R}\mathbf{h_0} = \mathbf{p}$$

where $\mathbf{R}$ is the autocorrelation matrix of the tap-input vector $\mathbf{X(k)}$ and $\mathbf{p}$ is the cross-correlation vector between the tap-input $\mathbf{X(k)}$ and the desired response $y(k)$.

If $\mathbf{R}$ and $\mathbf{p}$ are known exactly, $\mathbf{h_0}$ can be obtained as

$$\mathbf{h_0} = \mathbf{R}^{-1}\mathbf{p}$$

Assuming a stationary process, $\mathbf{R}$ is given as

$$\begin{aligned}\mathbf{R} &= E\{\mathbf{X(k)X^T(k)}\} \\ &= \begin{bmatrix} r(0) & r(1) & r(2) & \dots & r(N-1) \\ r(-1) & r(0) & r(1) & \dots & r(N-2) \\ r(-2) & r(-1) & r(0) & \dots & r(N-3) \\ \vdots & \vdots & \vdots & & \vdots \\ r(-N+1) & r(-N+2) & r(-N+3) & \dots & r(0) \end{bmatrix}\end{aligned}$$

where N stands for the number of the tap-weights in the adaptive filter, E represents the expectation operator, superscript T denotes transpose and $r()$ is the autocorrelation function of the input signal. For a white noise signal, the autocorrelation fuction is zero for all values except $r(0)$. Thus, $\mathbf{R}$ reduces to a diagonal matrix whose diagonal elements are all equal to $r(0)$, i.e. the variance of the white noise input σ^2. $\mathbf{R}$ is rewritten as:

$$\mathbf{R} = \begin{bmatrix} r(0) & 0 & \dots & 0 \\ 0 & r(0) & \dots & 0 \\ \vdots & & & \\ 0 & 0 & \dots & r(0) \end{bmatrix} \tag{A.1}$$

The cross-correlation $\mathbf{p}$ is defined as:

$$\begin{aligned}\mathbf{p} &= E\{y(k)\mathbf{X(k)}\} \\ &= \begin{bmatrix} E\{(\sum_{i=0}^{M-1} h_i x(k-i))x(k)\} \\ E\{(\sum_{i=0}^{M-1} h_i x(k-i))x(k-1)\} \\ E\{(\sum_{i=0}^{M-1} h_i x(k-i))x(k-2)\} \\ \vdots \\ E\{(\sum_{i=0}^{M-1} h_i x(k-i))x(k-N+1)\} \end{bmatrix}.\end{aligned}$$

$$= \begin{bmatrix} \sum_{i=0}^{M-1} h_i r(i) \\ \sum_{i=0}^{M-1} h_i r(i-1) \\ \sum_{i=0}^{M-1} h_i r(i-2) \\ \vdots \\ \sum_{i=0}^{M-1} h_i r(i-N+1) \end{bmatrix}$$

where $y(k)$ is the desired response in Fig.A.1, and $h_i (i = 1, \ldots, M)$ is the echo path impulse response.

For a white noise input, only $r(0)$ is nonzero, thus,

$$\mathbf{p} = \begin{bmatrix} h_0 r(0) \\ h_1 r(0) \\ \vdots \\ h_{N-1} r(0) \end{bmatrix} \tag{A.2}$$

So

$$\mathbf{h_0} = \mathbf{R^{-1}p} = \begin{bmatrix} \frac{1}{r(0)} & 0 & \ldots & 0 \\ 0 & \frac{1}{r(0)} & \ldots & 0 \\ \vdots & & & \\ 0 & 0 & \ldots & \frac{1}{r(0)} \end{bmatrix} \begin{bmatrix} h_0 r(0) \\ h_1 r(0) \\ \vdots \\ h_{N-1} r(0) \end{bmatrix} = \begin{bmatrix} h_0 \\ h_1 \\ \vdots \\ h_{N-1} \end{bmatrix} \tag{A.3}$$

i.e., the solution $\mathbf{h_0}$ will be equal to the truncated impulse response of the echo path. In a practical system, the exact measurement of $\mathbf{R}$ and $\mathbf{p}$ is not available, thus other approximate methods, such as the LMS algorithm, are used to solve for $\mathbf{h_0}$. The LMS algorithm was shown to converge to the Wiener solutions. Simulations provided in the previous chapters show that the weights will be nearly equal to the optimum response of the echo path. Figs.4.19 and 4.32 are examples.

When a single tone is applied to the system, the solution to the normal equation will be different from the previous discussion with white noise input.

For example, for sinusoidal signal $x(k) = Asin(wk)$, the autocorrelation function is given as

$$\begin{aligned} r(n) &= E\{Asin(wk)Asin(w(k-n))\} \\ &= E\{-\frac{A^2}{2}(cos(2wk - wn) - cos(wn))\} \end{aligned}$$

$$= \frac{A^2}{2} cos(wn)$$

Then the correlation matrix changes to:

$$\mathbf{R} = \begin{bmatrix} \frac{A^2}{2}cosw(0) & \frac{A^2}{2}cosw(1) & \dots & \frac{A^2}{2}cos(w(N-1)) \\ \frac{A^2}{2}cosw(-1) & \frac{A^2}{2}cosw(0) & \dots & \frac{A^2}{2}cos(w(N-2)) \\ \vdots & & & \\ \frac{A^2}{2}cosw(-N+1) & \frac{A^2}{2}cosw(-N+2) & \dots & \frac{A^2}{2}cos(w(0)) \end{bmatrix} \quad \text{(A.4)}$$

Since the autocorrelation function $r(n)$ is non-zero for $n \neq 0$, $\mathbf{p}$ changes to

$$\mathbf{p} = \begin{bmatrix} \sum_{i=0}^{M-1} h_i \frac{A^2}{2} cosw(i) \\ \sum_{i=0}^{M-1} h_i \frac{A^2}{2} cosw(i-1) \\ \vdots \\ \sum_{i=0}^{M-1} h_i \frac{A^2}{2} cosw(i-N+1) \end{bmatrix} \quad \text{(A.5)}$$

Though $\mathbf{R}$ and $\mathbf{p}$ exist, the Nth order matrix $\mathbf{R}$ does not contain N independent rows(for a single sinusoid) and thus specifies an under-determined system . Therefore, there are an infinite number of solutions to the normal equation for this situation. That is why the far-end tone will lead the weights of the near-end AF to converge to a different set of values depending on the initial value of the coefficients. Figs.A.2 and A.3 show the tap weight values when a 500 Hz sinusoid is applied from the far-end of the 69/16 single adaptive system after 1000 iterations of adaptation. Fig.A.2 and A.3 are obtained by initially setting all the 16 taps of the AF to be zero or one respectively. It is clearly seen the final weights are different for different initial values.

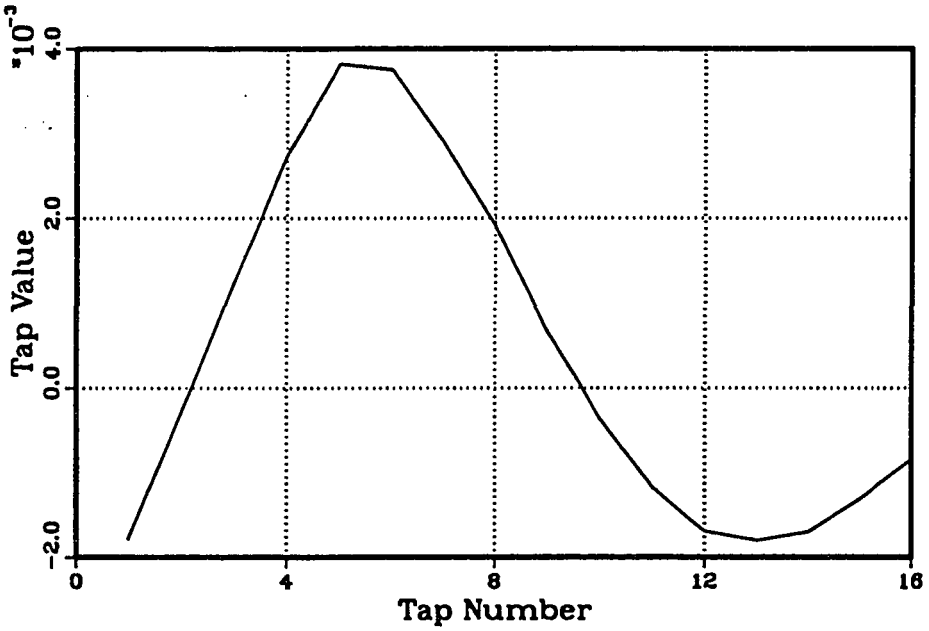

Fig.A.2 Tap values after 1000 iterations of adaption with far-end 500 Hz sinuso id input. Weights are initilized as zeroes. $\mu = 1/32$.

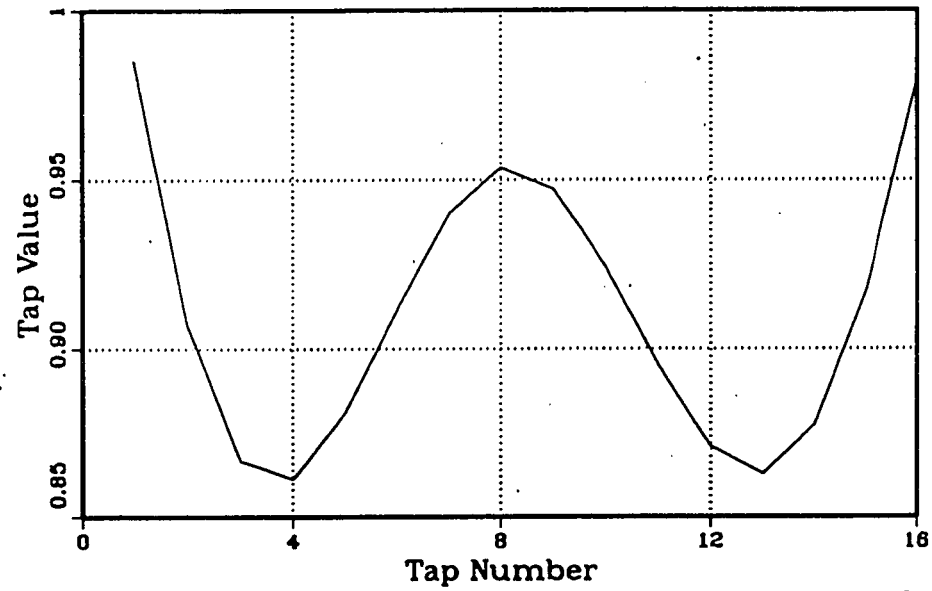

Fig.A.3 Tap values after 1000 iterations of adaption with far-end 500 Hz sinusoid input. Weights are initilized as ones. $\mu = 1/32$.

Appendix B

Coefficients of the 69-tap Hybrid

The coefficents are listed by row.

−0.0002	−0.0005	−0.0041	−0.0016	0.0179	0.0086	−0.0056
0.0055	−0.0032	0.0014	0.0008	−0.0024	0.0024	−0.0023
0.0013	−0.0006	−0.0001	0.0007	−0.0010	0.0004	0.0008
0.0000	−0.0001	−0.0001	0.0003	−0.0001	0.0002	−0.0000
0.0002	0.0002	0.0002	0.0002	0.0002	0.0002	0.0001
0.0002	0.0003	0.0003	0.0003	0.0003	0.0000	0.0001
0.0000	0.0002	0.0003	0.0003	0.0002	0.0001	0.000
0.0001	0.0001	0.0002	0.0003	0.0002	0.0002	0.0001
0.0000	0.0001	0.0000	0.0001	0.0001	0.0001	−0.0001
−0.0001	0.0001	0.0001	0.0001	0.0000	−0.0001	

Bibliography

[1] A.Miura, et al. "A Blockless Echo Suppressor", IEEE *Trans. on Communications*, Com-17, No.4, pp487-495, Aug.,1969.

[2] F.P.Duffy, et al. "Echo Peformance of Toll Telephone Connections in the United States", The Bell Syst. Tech. J., vol.54, pp209-244, Feb.,1975.

[3] Stephen B.Weinstein "Echo Cancellation in the Telephone Network", IEEE Communication Society Magazine, vol.15, no.1,pp-15, January, 1977.

[4] Sondhi, M.M. and A.J. Presti, "A Self-Adaptive Echo Canceller ", The Bell Syst. Tech. J., 45, pp1851-1854, 1966.

[5] M.M.Sondhi, "An Adaptive Echo Canceller", Bell Syst. Tech. J., 46, No.3, pp497-511, March, 1967.

[6] M.M.Sondhi and David A. Berkley, "Silencing Echoes on the Telephone Network", Proceedings of the IEEE, Vol.68,No.8, August 1980.

[7] C.W.K.Gritton. "Echo Cancellation Algorithms". IEEE ASSP Magazine, April,1984.

[8] D.L.Duttweiler and Y.S.Chen "A Single-chip VLSI Echo-Canceler", The Bell System Technical Journal, Vol.59, No.2, February 1980.

[9] Simon Haykin. *Adaptive Filter Theory*. Prentice Hall,1986, 1991.

[10] Johnson, C.R., Jr., "Lectures on Adaptive Parameter Estimation", Prentice-Hall, Englewood Cliffs, NJ, 1988, pp8-21, 126-134.

[11] B.Widrow, et al., "Stationary and Nonstationary Learning Characteristics of the LMS Adaptive filter", Proc. IEEE, vol.64, pp 1151-1162, Aug.1976.

[12] M.L.Honig and D.G.Messerschmit, "Adaptive Filters:Structures, Algorithms, and Applications", New York:Academic,1984.

[13] B.Widrow et al. *Adaptive Signal Processing.* Prentice Hall,1985.

[14] Edward A. Lee , "Digital Communication", Boston:Klumer Academic Publisher, 1988.

[15] Roger L.Freeman "Telecommunication System Engineering", John Wiley Sons, 1989.

[16] "MV3010 Subscriber Line Audio Circuit", PLESSey Semiconductors, May 1990.

[17] Kazuo Ochiai, et al. "Echo Canceller with Two Echo Path Models", IEEE *Transactions on Communications*, vol.Comm-25, No.6, June,1977.

[18] Hyokang Chang and B.P.Agrawal, "A DSP-based Echo-canceller with Two Adaptive Filters", IEEE GLOBECOM'86, vol.3, pp46.8.1-46.8.5.

[19] Weiss, A. and Mitra, D., " Digital Adaptive Filters:Conditions for Convergence, Rates of Convergence, Effects of Noise and Errors Arising From the Implementation", IEEE *Trans. on Information Theory*, vol.IT-25, No.6, pp637-652, Nov.1979.

[20] Sondhi, M. and Motra, D., "New Results on the Performance of a well-known Class of Adaptive Filters ", Proc. IEEE, vol.64, No.11, pp1583-1597, 1976.

[21] Donald l.Duttweiler, "A Twelve-channel Digital Echo Canceller", *IEEE Tranactions on Communications*, May,1978.

[22] D.G.Messerschmit, "Echo Cancellation in Speech and Data Transmission", IEEE *J.Select. Areas Commun.*, SAC-2, pp. 283-303, Mar.,1984.

[23] William A.Sethares et al. "Bursting in Adaptive Hybrids". IEEE *Transactions on Communications*, pp791-799, August,1989.

[24] W.A.Sethares and C.R.Johnson, Jr., " Bursting Discovered in Signal Processing: Feedback to Blame", Proc. 1988 IFAC workshop Robust Adaptive Control, Aug.,1988.

[25] James Ryan et al. "Final Report of Adaptive Echo Cancellers for Telephony".

[26] William A. Sethares, et al. "Parameter Drift in LMS Adaptive Filters", IEEE *Transactions on Acoustics, Speech, and Signal Processing*, vol.ASSP-34, No.4, August, 1986.

[27] Robert R.Bitmead, "Persistence of Excitation Conditions and the Convergence of Adaptive Schemes ", IEEE *Transactions on Information Theory*, vol.IT-30, No.2, March 1984.

[28] Brian D.O.Anderson "Adaptive System, Lack of Persistency of Excitation and Bursting Phenomena", Automatica, Vol.21,pp247-258,1985.

[29] L.Hsu and R.Costa, "Bursting Phenomenon in Continuous Time Adaptive Systems with σ-Modification", IEEE *Trans. on Automat. Control*, vol.32, pp84-86, Jan.1987.

[30] Gonzalo J.Rey et al. "The Dynamics of Bursting in Simple Adaptive Feedback Systems with Leakage". IEEE *Transactions on Circuits and Systems*. pp476-488,May,1991.

[31] John M. Cioffi, "Limited-Precision Effects in Adaptive Filtering ", IEEE *Trans. on Circuits and Systems*, vol.CAS-34, No.7, July, 1987.

[32] Gonzalo J.Rey , C.Richard Johnson, JR., et al. "On Tuning Leakage for Performance-Robust Adaptive Control", IEEE *Trans. on Automatic Control*, vol.34, No.10, Oct.1989.

[33] William A.Sethares et al. "Dynamics of an adaptive hybrid." *IEEE Transaction on Circuits and systems.* pp1-11,January,1991.

[34] J.Guckenheimer and P.Holmes, "Nonlinear Oscillations, Dynamical systems and Bifurcations of Vector Fields", New York:Springer Verlag, 1983.

[35] Golubitsky and Schaeffer, "Singularities and Groups in Bifurcation Theory", New York:Springer-Verlag, 1985.

[36] B.A.Huberman and E.Lumer, " Dynamics of Adaptive Systems", IEEE *Trans. on Circuits and Systems*, vol.37, pp547-550, Apr.1990.

[37] S.Sastry and M.Bodson, " Adaptive Control, Stability, Convergence and Robustness", Englewood Cliffs, NJ:Prentice Hall, 1989.

[38] Z.Ding et al. "Frequency-dependent bursting in adaptive echo cancellation and its prevention using double-talk Detectors." *International Journal of Adaptive Control and Signal Processing.* pp219-236,1990.

[39] S.Minami and T.Kawasaki, "A Double-talk Detection Method For An Echo Canceller." 1985 IEEE International Conference on Communications, pp.1492-1497.

[40] Tatsuki Hayashi, et al. "Echo Canceller with Effective Double-talk Control", ICC, pp40.6.1-40.6.5, 1983.

[41] I.M.Y. Mareels and R.K.Boel " A Performance Oriented Analysis of a Double Hybrid Adaptive Echo Cancelling System", *Journal of Mathematical System, Estimation, and Control*, vol.2, No.1, 1992, pp71-94.

[42] "Digital Signal Processing Applications with the TMS320 Family", Texas Instruments, 1989.

[43] T.Aboulnasr and L.Wang "Elimination of Bursting in Adaptive Hybrids", 16th Biennial Symposium on Communications, Kingston, Ontario, May 27-29, 1992.

[44] L.Wang and T.Aboulnasr "Practical Adaptive Hybrids with no Bursting ", ICASSP-93, Minneapolis, Minnesota, April 27-30, 1993.

[45] B.Porat "Second-order Equivalence of Rectangular and Exponential Windows in Least-Squares Estimation of Autogressive Processed", IEEE *Trans. Acoustics, Speech, and Signal Processing*, vol.ASSP-33, No.4, Oct. 1985.

[46] Hua Ye and Bo-xiu Wu "A new Double-talk Detection Algorithm Based on the Orthogonality Theorem", IEEE *Transactions on Communications*, pp1542-1545, Nov.,1991.